AMERICAN
FERN JOURNAL

QUARTERLY JOURNAL OF THE AMERICAN FERN SOCIETY

VOLUME 111 NUMBER 2 APRIL-JUNE 2021

THE AMERICAN FERN SOCIETY

Council for 2020

AMERICAN FERN JOURNAL

EDITOR

MANAGING EDITOR

ASSOCIATE EDITORS

American Fern Journal 111(2):63–67 (2021)
Published on 7 June 2021

A New Record of the Fern Genus *Cornopteris* (Athyriaceae) From Peninsular Malaysia.

Haja Maideen*, Nur Aliah and Nurul Nadhirah
Faculty of Science and Technology, Universiti Kebangsaan Malaysia, 43600 Bangi, Malaysia

Abstract.—A new record of the fern genus *Cornopteris* Nakai from Peninsular Malaysia is presented. The species, *C. opaca* (D. Don) Tagawa was encountered during recent fieldwork in Mount Berinchang, Cameron Highlands. Previously, it has only been recorded from Mount Kinabalu in Sabah, East Malaysia. A description, photographs, and a distribution map of known occurences in Malaysia have been provided.

Key Words.—Athyriaceae, *Cornopteris*, ferns, morphology, new records

The genus *Cornopteris* was established by Nakai (1930) for *C. decurrenti-alanta* based on morphological characters which could also be described as exindusiate and the horn-like appendages known as "cornua" which plants with them can be described as corniculate (Sano *et al.,* 2000; Kurita 1964). This genus is mainly distributed in tropical and subtropical Asia comprising about sixteen species (Zhaorong & Kato 2013).

Previously, several authors referred close relationship of the genus to *Diplazium*. Ching (1945) considered *Cornopteris* to be an exindusiate derivative of *Diplazium* while Kato (1977, 1979) presumed the genus *Cornopteris* having closer relationship to *Athyrium* based on the same basic number of chromosome, x=40 compared to *Diplazium* where number of chromosome, x=41. Detailed morphological study on *Cornopteris* by Tagawa and Iwatsuki (1972) and Kato (1977) also demonstrated the genus to be distinct from *Diplazium*, and in fact more closely related to *Athyrium* based on stipe base, color and spine.

Both *Cornopteris* and *Athyrium* have the same petiolar anatomy which is 'V'-shaped and having spine on the upper surface of the lamina at the junction of upper costae, costules and mid-veins (Kato 1977). Statement made by Ching (1945) regarding *Cornopteris* derived from *Diplazium* based on evaluation of elongated sori is insufficient. This is because Kato (1977) pointed out there are several species of *Cornopteris* having J-shaped sori as in *Athyrium* and he assumed the ancestral sorus of *Cornopteris* may be the horseshoe or J-shaped sorus.

The close relationship between *Athyrium* and *Cornopteris* are well supported in previous molecular analyses on Athyriaceae (Sano *et al.,* 2000; Adjie *et al.,* 2008; Wang *et al.,* 2003; Liu *et al., 2011*). Sano *et al.,* (2000) proposed *Cornopteris* was monophyletic based on two *Cornopteris* species (*C.*

* Corresponding author: deen@ukm.edu.my

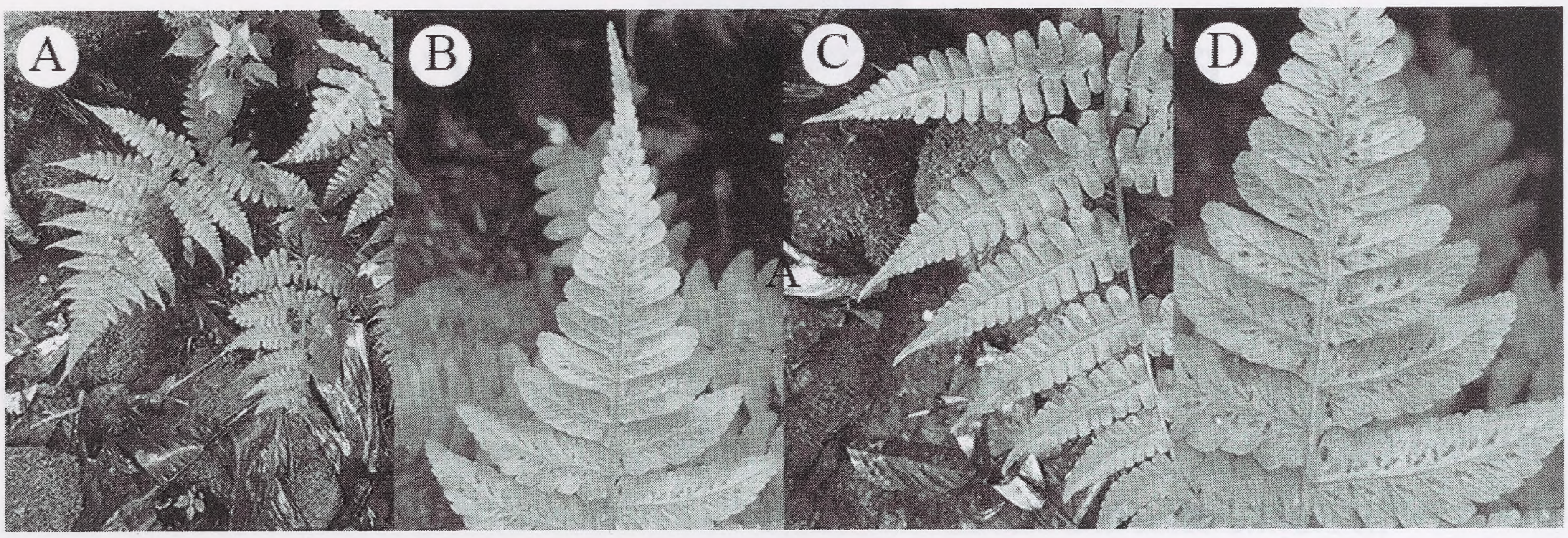

FIG. 1. **A** *Cornopteris opaca* (D. Don) Tagawa **B** lamina bipinnate **C** apex pinnae acuminate **D** exindusiate linear sori.

crenulatoserrulata and *C. decurrenti-alanta*) based on *rbcL* gene sequences. In a later study, Adjie *et al.,* (2008) investigated the intergeneric relationship between *Athyrium* and *Cornopteris* and demonstrated that *Athyrium* was paraphyletic with *Cornopteris* nested within the *Athyrium* clade which was also shown in Sano *et al.,* (2000) and Wang *et al.,* (2003). Recently, Wei *et al.,* (2017) attempted to resolve the infrageneric relationships of *Athyrium* based on comprehensive sampling and using combined molecular and morphological data. Based on their study, *Cornopteris* is treated as separate genus from *Athyrium* in Athyriaceae. Instead, they discovered that *Pseudoathyrium* which is a monotypic genus, have a sister relationship with *Cornopteris*. However, due to difference in several morphological characteristics such as surface of leaf axes and presence of indusia, both genera are then treated as two independent genera in Athyriaceae.

Although many new taxa have been recorded recently, the fern diversity in Peninsular Malaysia is still unclear as checklist of ferns in Malaysia (Parris & Latiff 1997) has not yet been revised up to date following latest classification. A new record of *C. opaca* (D. Don) Tagawa was discovered during recent fieldwork trip to Mount Berinchang, Cameron Highlands. There has been no other publication cited and no thorough fieldwork has been done in the Uda and Dara waterfall where this species has been found as this site is not accessible to the public. This work is a contribution to the knowledge of fern flora in Peninsular Malaysia.

MATERIALS AND METHODS

During field trips in Mount Berinchang, the second author collected specimens of Athyriaceae for her PhD study. Following a careful examination the specimen, *C. opaca* (Fig. 1) was identified as a new record of occurrence on Peninsular Malaysia. The specimens was deposited in Universiti Kebangsaan Malaysia Herbarium (UKMB). Further materials were examined including type specimens in the National Herbarium of the Netherlands (NHN), specimen in

TABLE 1. Specimens of *Cornopteris opaca* examined.

Species	Vouchers
Cornopteris opaca (D. Don) Tagawa	Type:— Indonesia. Java. anon. L 0051168 [image seen NHN!] NMNH 01531502 [image seen NMNH!] NA2019-79 [UKMB], NAGN-41103 [UKMB], NAGN-41105 [UKMB] Dr. Jermy SNP. No. J 15050 [SNP]

National Museum of Natural History (NMNH) and Sabah National Park Herbarium (SNP) (Table 1).

RESULTS AND DISCUSSIONS

In this study, we report *Cornopteris opaca* (Athyriaceae) from Mount Berinchang for the first time in Peninsular Malaysia. Previously, *C. opaca* has only been recorded in Borneo (Mount Kinabalu) East Malaysia (Fig. 2).

Type: Indonesia. Java. anon. (holotype: NHN image seen!). Additional Specimens Examined. Philippines. Mindanao: Mt. Tulad, 6°05′16″N, 125°40′53″E, 21 Mar 1993, Elev. 850m, *J. F. Barcelona & D. T. Busemeyer 693* NMNH 01531502 (NMNH image seen!). Peninsular Malaysia. Pahang:

Mount Berinchang, Uda and Dara Waterfall, 4°31′27″N, 101°23′20″E, 5 Oct 2019, Elev. 1687m, *N. Aliah & N. Nadirah NA2019-79* (UKMB).

Borneo. Sabah: Mount Kinabalu, 6°1′51″N, 116°32′53″E, Elev. 1595m, 14 Sep 2018, *N. Aliah NAGN-41103* (UKMB), Elev. 1557m, 14 Sep 2018, *N. Aliah NAGN-41105* (UKMB), Oct 1980, *Dr. Jermy SNP. No. J 15050* (SNP).

TAXONOMIC NOTES.—Rhizome erect; stipe to 80 cm or more long, scaly at base, scales light brown, lanceolate, margin entire, to 6 mm long and 2 mm wide; lamina bipinnate to tripinnatifid, lanceolate, 25–55 cm or more long, 23–45 cm or more wide, pinnae to 9 pairs below deltoid and acuminate apical lamina, herbaceous, glabrous or rachis or costa and costules with short multicellular

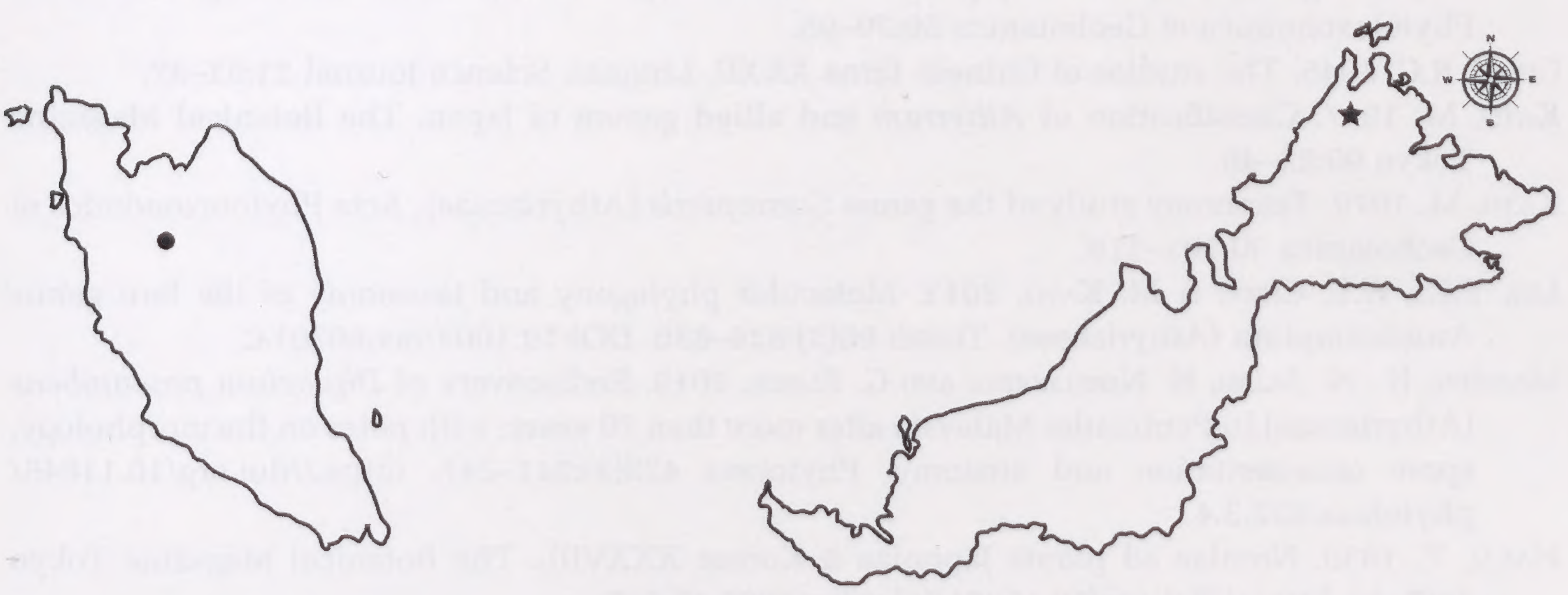

FIG. 2. Distribution of *C. opaca* in Mount Berinchang, Peninsular Malaysia (dot), Mahua field station, Sabah, Borneo (triangle) and Mount Kinabalu, Sabah, Borneo (star) in Malaysia.

hairs and sparsely scaly, scales linear and brown; pinnae 8–11.5 cm long, 2–4 cm wide, base of pinnae equally truncate, apex acuminate, margin lobed ½ or almost to costa into 10–13 segments below the apex, sessile or shortly petiolulate, segments almost at right angle to costa, usually denticulate with few teeth; veins 4–6 pairs in segment, veinlets simple or forked; sori linear, up to 3 mm long, Y-shaped on basal forked veinlets, median or near costule.

Distribution and Habitat.—This species has the widest-ranged distribution compared to other *Cornopteris* species. *Cornopteris opaca* is distributed in Himalaya, Burma to southern China, Taiwan, southern Japan, Indo-China, northern Thailand, Philippines, Peninsular Malaysia (new record), Borneo (Mt. Kinabalu, southern Kalimantan), Java, Bali and Sulawesi. This species usually grows in mountain, evergreen broad-leaved forest at altitude ca. 1500–2300m.

At first glance, the lamina of this species resembles *Diplazium procumbens* (Maideen *et al.,* 2019) and as seen on digitalized *C. opaca* specimens in database of National Museum of Natural History founded in Mindanao, Philippines. Characters such as indusiate sori and creeping rhizome in *D. procumbens* differentiated it from *C. opaca.* Other than that, this is the only genus in Athyriaceae with base of costa and costules corniculate on adaxial sides as well as bearing exindusiate sori which separated this genus from other genera in Athyriaceae.

Acknowledgements

This study was financially supported by Universiti Kebangsaan Malaysia UKM Grantt (UKMGUP2017-025). We are grateful to curators of NHN, NMNH, SNP and UKMB herbarium for providing access to the materials in their care. We would like to thank both reviewers for their insightful comments on the paper to improve our work.—H. Maideen, N. Aliah and N. Nadhirah.

References

Adjie, B., M. Takamiya, M. Ohta, T.A. Ohsawa and Y. Watano. 2008. Molecular phylogeny of the lady fern genus *Athyrium* in Japan based on chloroplast *rbcL* and *trnL-trnF* sequences. Acta Phytotaxonomica et Geobotanica 59:79–95.

Ching, R.C. 1945. The studies of Chinese ferns XXXII. Lingnan Science Journal 21:31–37.

Kato, M. 1977. Classification of *Athyrium* and allied genera of Japan. The Botanical Magazine Tokyo 90:23–40.

Kato, M. 1979. Taxonomy study of the genus *Cornopteris* (Athyriaceae). Acta Phytotaxonomica et Geobotanica 30:101–118.

Liu, Y.C., W.L. Chiou & M. Kato. 2011. Molecular phylogeny and taxonomy of the fern genus Anisocampium (Athyriaceae). Taxon 60(3):824–830. DOI:10.1002/tax.603014.

Maideen, H., N. Aliah, N. Norhazrina and G. Rusea. 2019. Rediscovery of *Diplazium procumbens* (Athyriaceae) in Peninsular Malaysia after more than 70 years, with notes on the morphology, spore ornamentation and anatomy. Phytotaxa 422(3):241–247. https://doi.org/10.11646/phytotaxa.422.3.4.

Nakai, T. 1930. Notulae ad planta Japoniae & Koreae XXXVIII. The Botanical Magazine Tokyo 44:7–40. https://doi.org/10.15281/jplantres1887.47.235.

Parris, B. and A. Latiff. 1997. Towards a pteridophyte flora of Malaysia: A provisional checklist of taxa. Malayan Nature Journal 50:235–280.

SANO, R., M. TAKAMIYA, M. ITO, S. KURITA AND M. HASEBE. 2000. Phylogeny of the lady fern group, tribe Physematieae (Dryopteridaceae), based on chloroplast *rbcL* gene sequences. Molecular Phylogenetics and Evolution 15:403–413.

TAGAWA, M. AND K. IWATSUKI. 1972. Families and Genera of the Pteridophytes Known from Thailand. Memoirs of the Faculty of Science, Kyoto University, Series of Biology 5:67–88.

WANG, M.L., Z.D. CHEN, X.C. ZHANG, S.G. LU AND G.F. ZHAO. 2003. Phylogeny of the Athyriaceae: Evidence from chloroplast *trnL-F* region sequences. Acta Phytotaxonomica Sinica 41:416–426.

WEI, R., A. EBIHARA, Y.M. ZHU, C.F. ZHAO, S. HENNEQUIN AND X.C. ZHANG. 2017. A total-evidence phylogeny of the lady fern genus *Athyrium* Roth (Athyriaceae) with a new infrageneric classification. Molecular Phylogenetics and Evolution 119:25–36. https://doi.org/10.1016/j.ympev.2017.10.019.

ZHAORONG, H. AND M. KATO. 2013. *Cornopteris*. Pp. 443–447, *in* Z.Y. Wu, P.H. Raven and D.Y. Hong (eds.), Flora of China. Volume 2–3. Science Press, Beijing, Missouri Botanical Garden Press, St. Louis.

American Fern Journal 111(2):68–85 (2021)
Published on 7 June 2021

A New *Serpocaulon* (Polypodiaceae) from Northern South America and a Reinterpretation of *S. caceresii*

David Sanín

Herbário BHCB, Instituto de Ciências Biológicas, Departamento de Botânica, Universidade Federal de Minas Gerais, CEP 486, 30123-970, Belo Horizonte, Minas Gerais, Brasil. Current address: Herbario FAUC, Universidad de Caldas, Manizales, Caldas, Colombia, AA 275, e-mail: dav.sanin@gmail.com

Julián Mostacero

Herbario Nacional de Venezuela, Instituto Jardín Botánico Dr. Tobías Lasser, Universidad Central de Venezuela, Apartado 2156, Caracas 1010-A, Venezuela, e-mail: jmosta@gmail.com

Alan R. Smith

University Herbarium, University of California, 1001 Valley Life Sciences Bldg. # 2465, Berkeley, CA 94720-2465, U.S.A., e-mail: arsmith@berkeley.edu

Abstract.—We describe *Serpocaulon psychotrium*, a new species from northern South America, and provide for it a discussion of similar species, line drawings, field photographs, and a distribution map. It is often confused with, and probably related to, the species commonly called *S. caceresii*, also widespread in South America. We reinterpret *S. caceresii* as a heterotypic synonym of *S. articulatum*, an older name, and review the nomenclature of that species. Also, we provide a list of representative specimens for both species and a key to all pinnate species of *Serpocaulon*.

Key Words.—Colombia, Ferns, Polypodiaceae, taxonomy, Venezuela

During a study of *Serpocaulon* A.R. Sm. (Smith *et al.*, 2006; Kreier *et al.*, 2008) with emphasis on South American species (Schwartsburd and Smith, 2013; Smith *et al.*, 2018), it became evident that an undescribed species occurred in Venezuela and probably adjacent countries. Further study revealed that this new species is more widely distributed and is similar to, and sometimes confused with, *S. caceresii* (Sodiro) A.R. Sm. (Sanín, 2018). Examination of type material of that species suggests it is conspecific with *S. articulatum* (C. Presl) Schwartsb. & A.R. Sm., which is also widely distributed in South America (Schwartsburd and Smith, 2013; Sanín, 2018). We here confirm that these two names are synonymous.

Below, we describe the new species, distinguish it from *Serpocaulon articulatum*, select a lectotype for *Polypodium caceresii*, and review the typification of that species. We also provide a key to the once-pinnate species of *Serpocaulon* and cite specimens for both taxa.

Materials and Methods

We studied herbarium specimens and digital databases from B, BM, BR, CAY, COAH, COL, COR, FMB, HUA, JAUM, M, MEDEL, MERF, MO, MY, NY, PORT, Q, QCA, QCNE, QLPS, SI, UC, UCOB, UPTC, US, and VEN herbaria

(Thiers, 2020). In total, we examined 226 specimens, 63 of which were *S. articulatum*, and 163 were *Serpocaulon psychotrium*) (see Appendix 1). Observations of species in the field were made in Colombia (by DS) and Venezuela (by AS and JM). In the type information paragraphs, "bc" in parentheses means "barcode." We follow terminology presented by Tsutsumi and Kato (2006) for the secondary hemiepiphytic habit, Rödl-Linder (1990) for rhizome scales, Moran (1995) for the laminar dissection, Lellinger (2002) for the laminar indument, specifically the hairs, and Sanín (2018) for the spores. In total, 78 morphological characters, shown to be useful in the recognition of species in the group, were selected and examined (Sanín, 2018).

We obtained scanning electron microscope (SEM) images of the spores following the methods used by Ramírez-Valencia, Sanín, and Pardo (2013) and Ramírez-Valencia and Sanín (2016). This was accomplished using a FEI Quanta 200 SEM, with accelerating voltage of 20 kV, in the Centre for Microscopy at the Universidade Federal de Minas Gerais.

The distribution map was created using ArcGIS® v. 10.5 (ESRI, 2016).

Taxonomic Treatment

1. ***Serpocaulon psychotrium*** Mostacero, D. Sanín & A.R. Sm., **sp. nov.** TYPE.—VENEZUELA. Táchira: Distr. Uribante, Potosí at mouth of the río Puya (formerly río Puyita) at W end of Embalse La Honda, 07°57′N, 71°42′W, 1140 m, 20 Jun 1990, *L.J. Dorr et al. 7102* (holotype: NY [bc] none!; isotypes: COL [bc] 336478!, MER [bc] 046202!, MO [bc] 4381972, 4895044, 4895151!, MY [bc] 109654!, PORT [bc] 23036!, VEN [bc] 296654!). (Figs. 1, 2, 3, 4B, 5B).

Diagnosis.—*Serpocaulon psychotrium* is similar to *S. articulatum* and *S. richardii* (Klotzsch) A.R. Sm. in having long-creeping rhizomes, patent rhizomes scales, and pinnate lamina. However, *S. psychotrium* differs from *S. articulatum* by its subulate rhizome scales, prominent impressed veins and sori, and adnate pinnae at the laminar apex (vs. lanceolate rhizome scales, not impressed veins and sori, and free pinnae at the laminar apex). From *S. richardii*, *S. psychotrium* is distinguished by its dark brown rhizome scales and glabrous lamina (vs. whitish to reddish rhizome scales and densely pubescent laminae).

Plants epiphytic, secondarily hemiepiphytic, occasionally terrestrial. **Rhizomes** long-creeping, ca. 5–10 mm in diameter, surfaces not pruinose, black (dried), dull greenish gray (living), densely scaly, the scales spreading, subulate, clathrate, (3–)7–12 × 1–2 mm, ovate, proximally with erose margins, distally entire to subentire laterally, abruptly reduced to a long narrow tip ca. 0.1–0.3 mm wide, acicular in much of its length, curving, basally bicolorous, the central area and apex dark brown to black with elongate cells 2–6 times longer than wide, the margins pale with nonclathrate, indistinct cells, phyllopodia 1–4.5 cm apart, same color as the rhizome, 3–5 × 4–7 mm diameter. **Petioles** about 1/5 to 1/4 the frond length, (8–)17–50(–70) cm × 2–5

mm, usually stramineous, adaxially sulcate, with sparse, appressed, septate hairs. **Laminae** 20–80 × (15–)20–50 cm, 1-pinnate, chartaceous, ovate-lanceolate to oblong-lanceolate, broadest proximally, abruptly tapering to a subconform or conform adnate apical pinna; **pinnae** (3–)6–12(–13) pairs, proximal pinnae (7–)9–20(–23) cm × 1.5–4.5 cm, 2–6 cm apart, free, the distal ones adnate, subfalcate to straight, subentire to entire, acute to short-caudate at the apices, mostly departing at 55–70(–80)° from rachises, apical pinna 8–18 × 1.5–4 cm, rachises usually stramineous, nearly glabrous or with scattered patent, septate, terete, reddish or hyaline hairs mostly 0.1–0.2 mm long, costae not sulcate adaxially, raised on both sides, abaxially with scattered, appressed, subclathrate to clathrate, dark brown, mostly ovate-lanceolate scales 1.5–4 × 0.2–0.5 mm, with long, flexuous apices 7–23 cells wide; **areoles** forming 3–6 rows between costae and pinna margins, blade tissue and margins nearly glabrous to sparsely hairy, the hairs appressed, septate, 2-celled, pale reddish, ca. 0.1 mm. **Sori** borne on the apices of the included veinlets, in 3–4(–5) rows between the costae and pinna margins; **spores** monolete, 42–50 × 24–30 μm, ellipsoid to subellipsoid, irregularly verrucate, verrucae flat to rounded at the apex.

Etymology.—The specific epithet combines the Latin words *psycho* = mind, and *aíthrion*, or *atrium* = hall lit from above, referring metaphorically to the light that clarifies its confused taxonomy. Bruno Manara (1939–2018), botanist, plant illustrator from Flora of Venezuela, and Latin professor, suggested this epithet to JM. It is not related to any known ethnobotanical use of this fern (see Pinkley, 1969).

Indigenous Name.—*Uap-hia* in Venezuela (*F. Matos & S. Arias 1270*, CAR).

Distribution, Habitat, and Phenology.—Colombia, Venezuela; premontane forests, cloud forests; (150–)800–1200(–2000) m (Fig. 3).

Hensen (1990) and Smith *et al.* (2018) mentioned that *Serpocaulon psychotrium* (as *S. caceresii*) occurred from Panama to Bolivia; however, our records now suggest that the species is absent from this range, except for Colombia. Schwartsburd and Smith (2013) also listed *S. psychotrium* (as *S. caceresii*) from Ceará State in Brazil but did not cite a specimen. Specimens exhibit fertile leaves year around.

Similar Species.—Most specimens of *Serpocaulon psychotrium* have been previously identified as *S. fraxinifolium* (Jacq.) A.R. Sm., and to a lesser extent as *S. articulatum* and *S. richardii.* All three species are alike in having long-creeping rhizomes and pinnate laminae. These last two species are most similar in having patent, lanceolate (in *S. articulatum*) or subulate (in *S. psychotrium* and *S. richardii*) rhizome scales (Fig. 4), and 1-pinnate laminae (Table 1). Also, all of these species possess prominent verrucae on the spores (except *S. richardii,* which exhibits gemmulate spores (see Fig. 5). *Serpocaulon psychotrium* differs from *S. articulatum* by having subulate rhizome scales (Fig. 4), prominent veins and sori, and adnate distal pinnae (versus lanceolate rhizome scales, not impressed veins and sori, and conform apical pinna). From

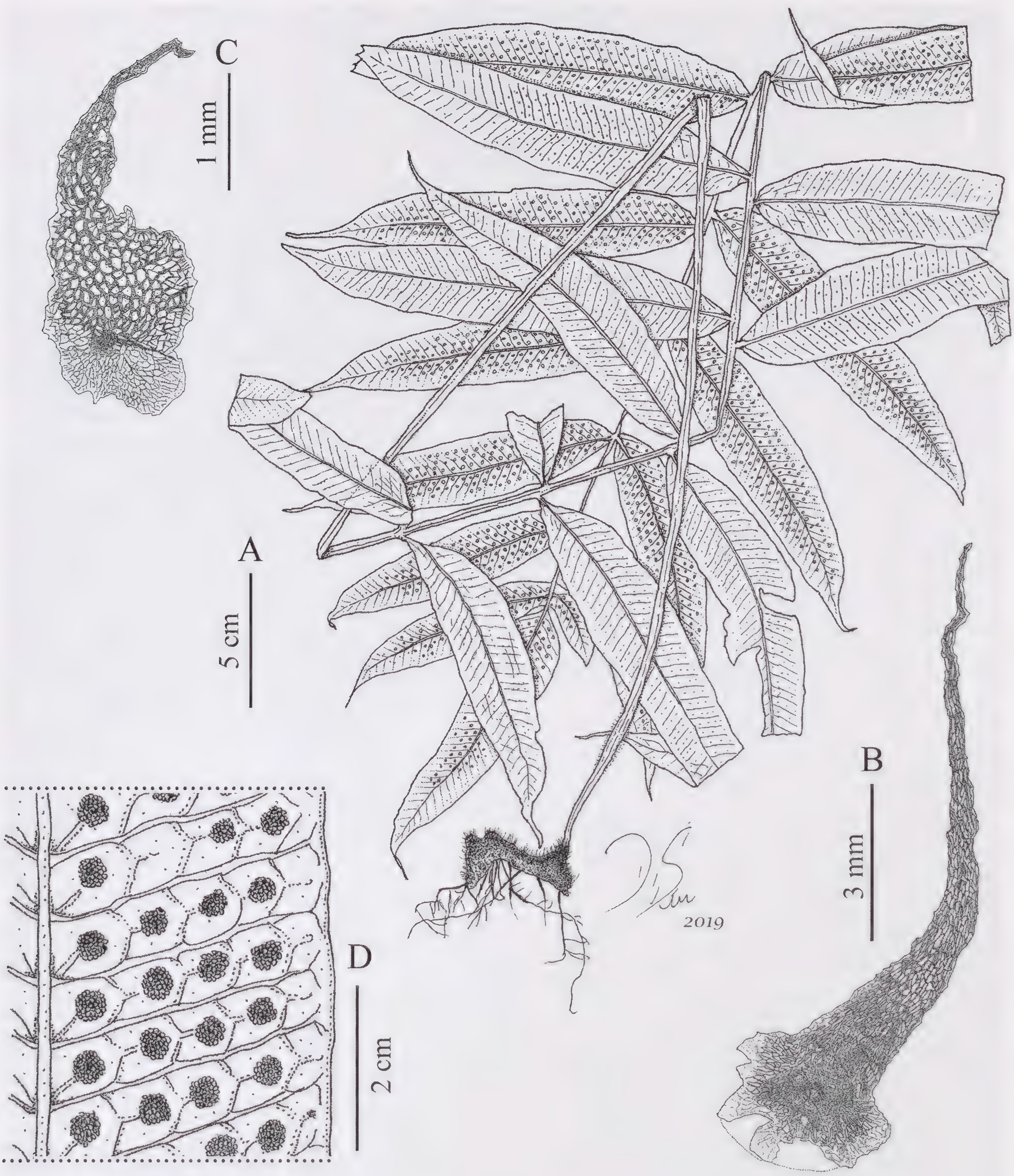

FIG. 1. *Serpocaulon psychotrium*: **A**. Habit. **B**. Rhizome scale. **C**. Laminar scale, near rachis. **D**. Venation, and soral array on laminar surface abaxially. From *L.J. Dorr et al. 7102* (NY).

S. richardii, S. psychotrium differs by its dark brown rhizome scales (Fig. 4), nearly glabrous laminae, and rounded to flattened spore verrucae (versus whitish to reddish rhizome scales, lamina densely pubescent, and gemmulate spores) (Fig. 5). Finally, from *S. fraxinifolium*, *S. psychotrium* can be distinguished by the spreading and subulate rhizome scales, and the adnate distal pinnae (versus appressed and rounded rhizomes scales and conform distal pinnae).

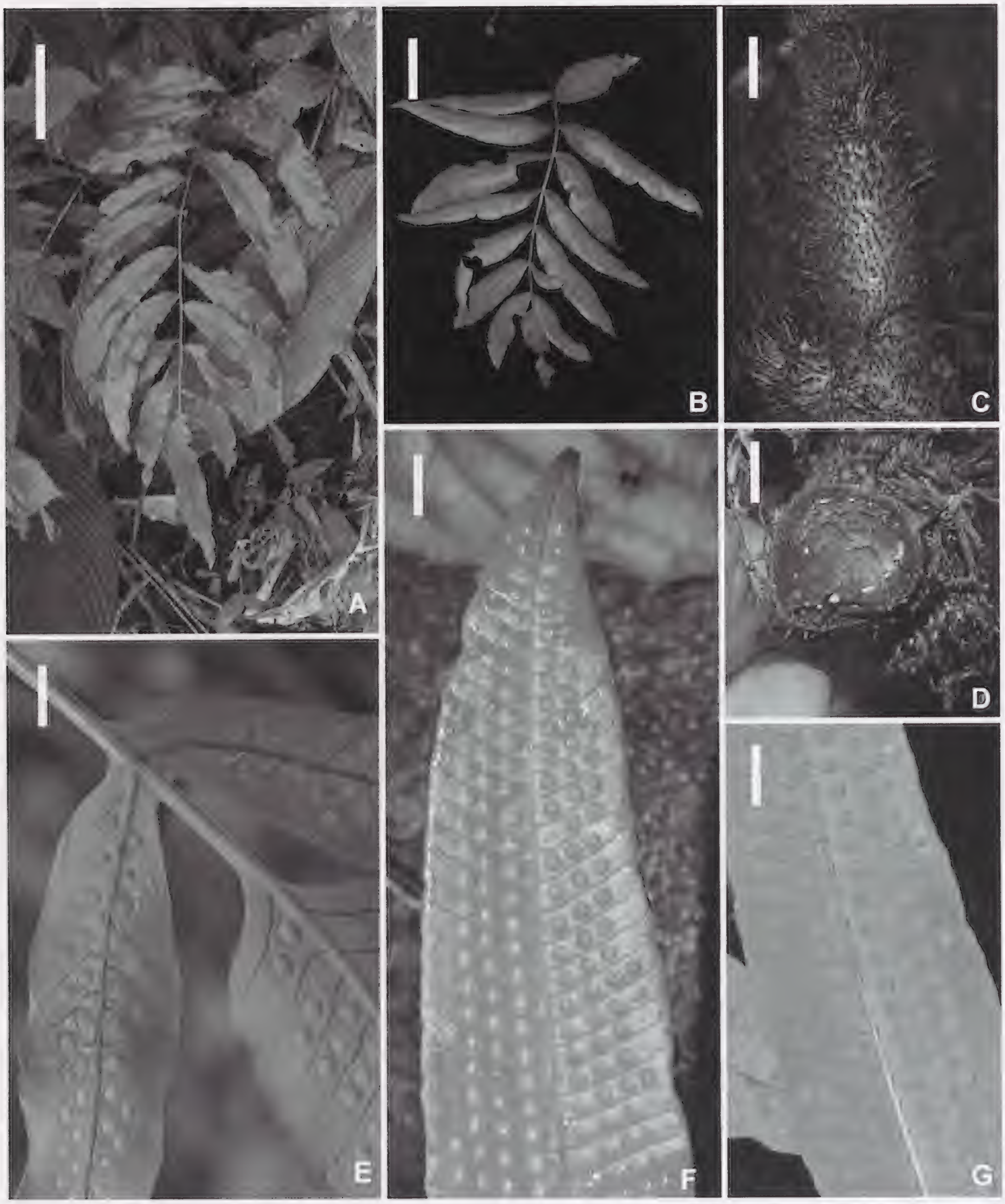

Fig. 2. *Serpocaulon psychotrium*: **A**. Habit, scale bar = 10 cm. **B**. Lamina, scale bar = 5 cm. **C**. Rhizome, scale bar = 5 mm. **D**. Cross-section of rhizome, scale bar = 5 mm. **E**. Laminar apex with adnate distal pinnae, scale bar = 1 cm. **F**. Adaxial view of the medial pinnae with prominent impressed sori, scale bar = 1 cm. **G**. Abaxial view of the medial pinnae showing the sori, scale bar = 1 cm. All from *D. Sanín et al. 6449* (HUA).

Specimens Examined (Paratypes).—COLOMBIA.—**Antioquia**: Amalfi, road between Amalfi and Medellín, 13.5 km SW of Amalfi, 06°54′N, 75°6′W, 1510 m, 17 Feb 1989, *J.M. MacDougal & J. Betancur 4088* (HUA three sheets, JAUM, MO, UC); Barbosa, vereda La Pradera, 06°30′N, 75°18′W, 1500 m, 5 Jul 1991,

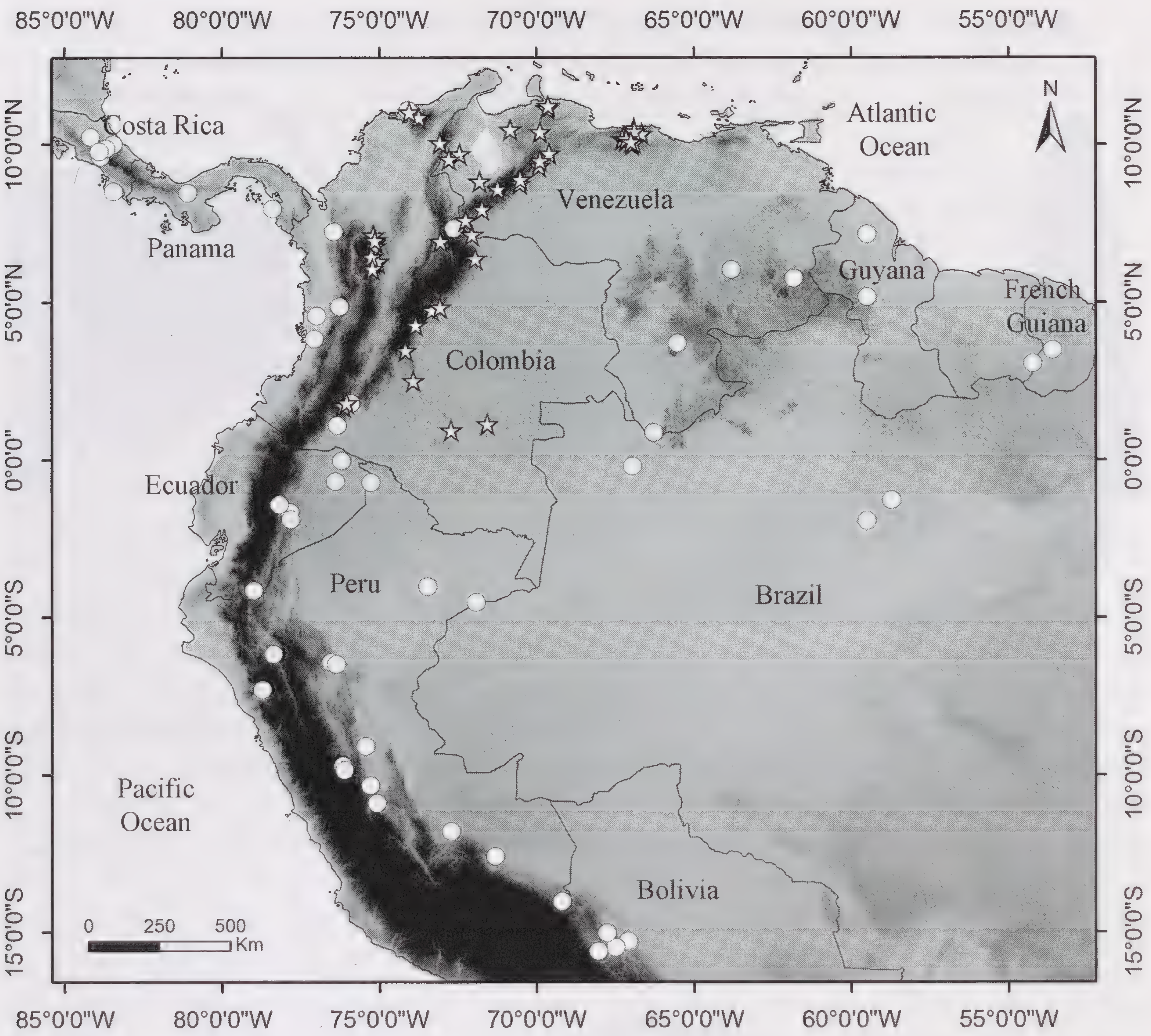

FIG. 3. Distribution of *Serpocaulon articulatum* (circles) and *S. psychotrium* (stars).

D.L. Echeverri B. 504 (HUA two sheets); Cocorná, vereda La Piñuela, carretera a San Francisco, 06°02′N, 75′08″W, 1000–1500 m, 13 Apr 1991, *D.A. Giraldo Cañas 71* (HUA two sheets); Guatapé, vereda Santa Rita, finca Montepinar, 06°15′N, 75°10′W, 1850 m, 22 May 1990, *N. Contreras & D.L. Echeverri 330* (HUA); Medellín, corregimiento de Santa Elena, sector Piedras Blancas, 2400 m, 06°15′N, 75°35′W, 1 Mar 1998, *F. Álzate 492* (HUA); San Carlos, vereda La Rápida, escampadero Cantarrana, 06°15′45″N, 75°01′55″W, 1100 m, 26 Mar 2005, *J. Colorado & J. Ramírez 2128* (JAUM three sheets); San Rafael, vereda La Luz, 06°18′N, 75°02′W, 1100 m, 10 Jun 1993, *D. Sánchez S. 1976* (MEDEL). **Arauca**: Tame, vereda La Casirba, 06°22′52″N, 71°55′04″W, 762 m, 19 Mar 2013, *D.M. Cabrera Amaya et al. 1666* (FMB). **Boyaca**: carretera entre Pauna y Borbur, 950 m, 14 Oct 1967, *R. Jaramillo M. et al. 3602* (COL); carretera Sogamoso Pajarito, Valle del río Cusiana, 1500 m, 20 Oct 1967, *R. Jaramillo M. et al. 3869* (COL), San Benito, valle del río Cuisana, entre Pajarito y Aguazul, 900–1000 m, 9 Dec 1970, *M.T. Murillo 1418* (COL); Santa María, carretera vía Mámbita, 04°45′27″N, 73°18′20″W, 907 m, 25 Mar 2001, *J.C. Murillo A. et al.*

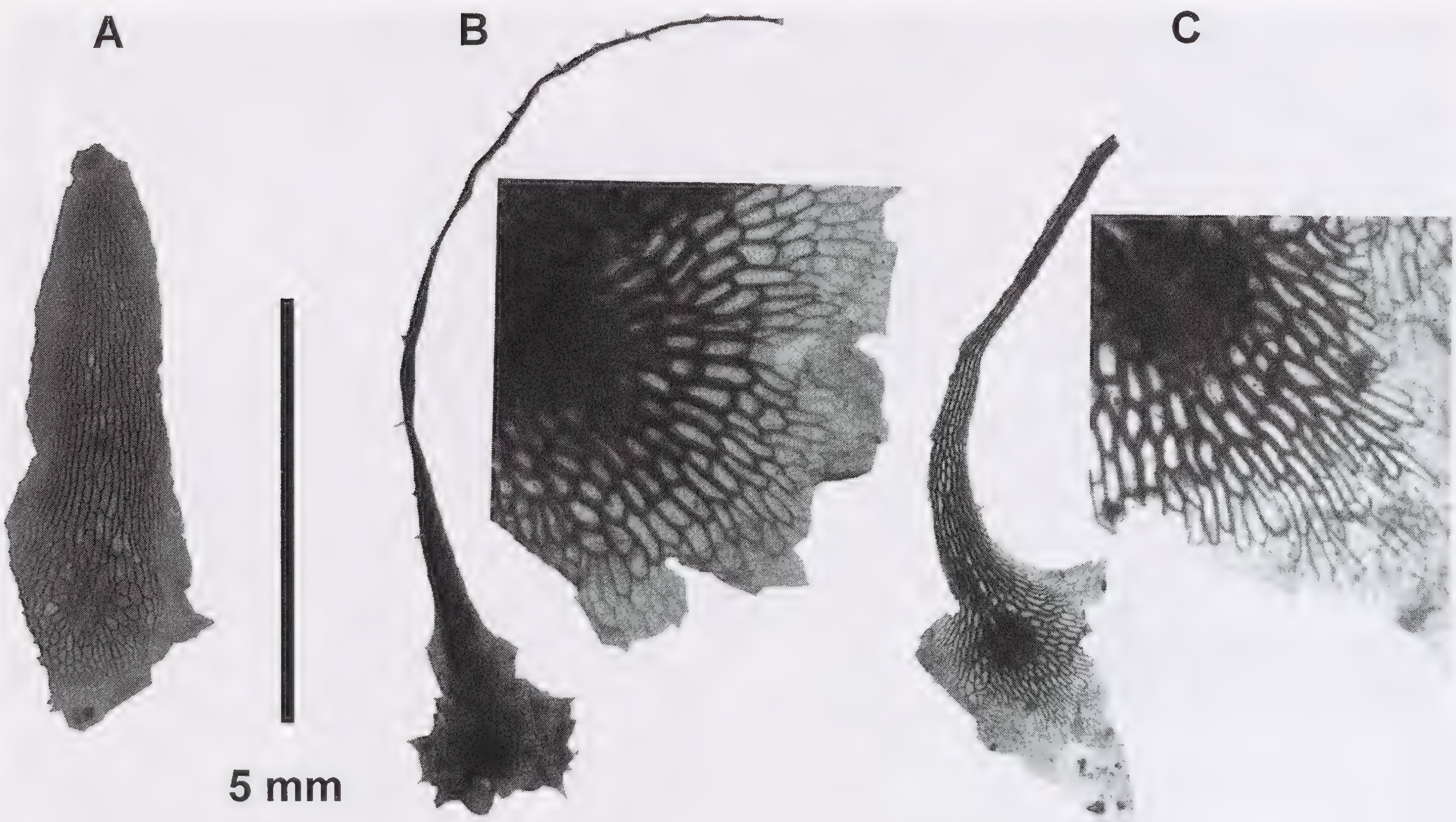

FIG. 4. Comparison between the rhizome scales of the related species of *Serpocaulon*: **A**. *S. articulatum* from *H. Pittier & T. Durand 3102* (BR). **B**. *S. psychotrium* from *J.M. MacDougal & J. Betancur 4088* (HUA). **C**. *S. richardii* from *R.E. Schultes & I. Cabrera 19049* (COL).

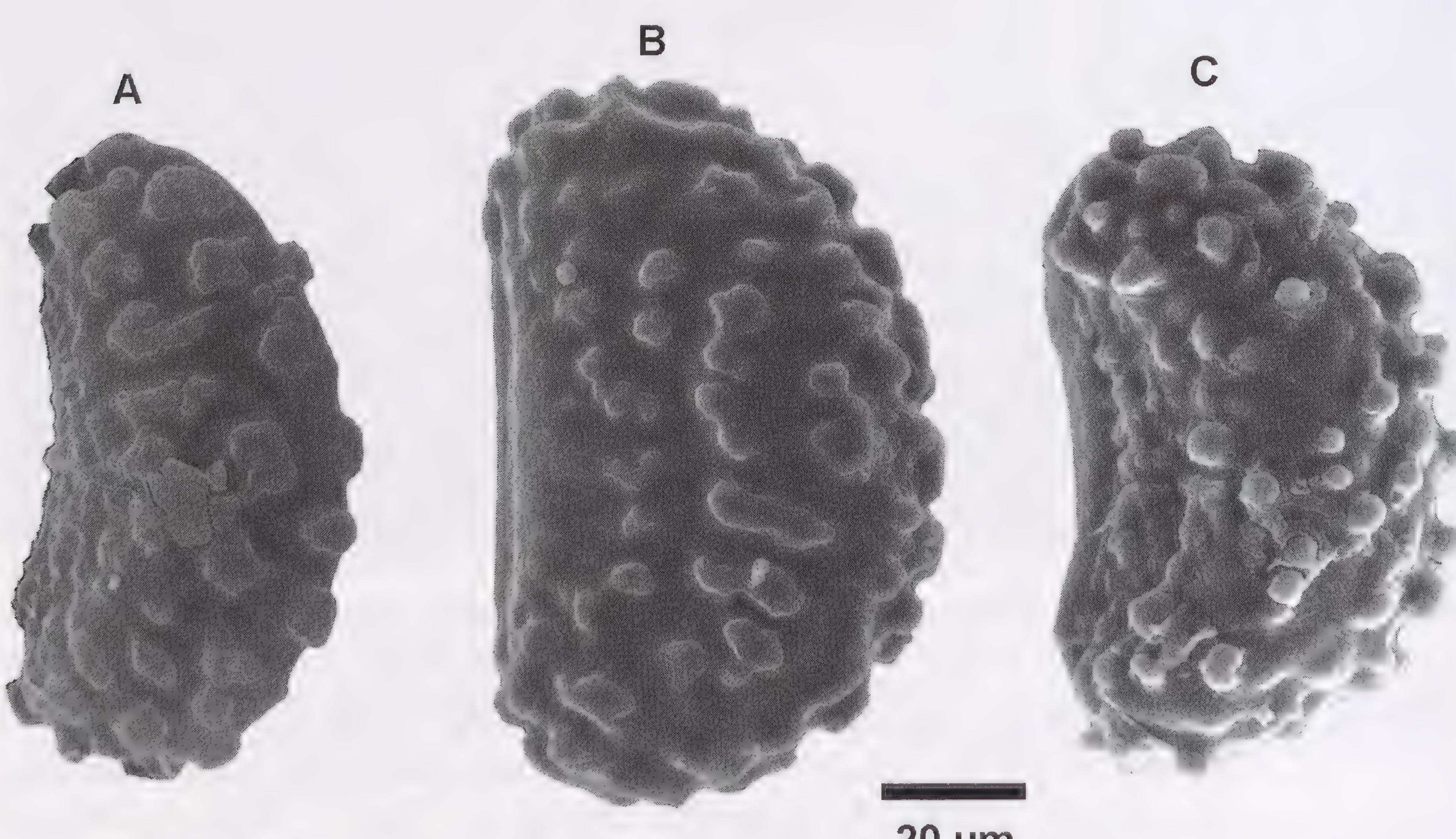

FIG. 5. Spores in related species of *Serpocaulon*. **A**. Lateral view of *S. articulatum* from *H. Pittier s.n.* (BR). **B**. Lateral view of *S. psychotrium* from *D.A. Giraldo-Cañas 71* (HUA). **C**. Lateral view of *S. richardii* from *R. Jaramillo-Mejia et al. 3650* (COL).

TABLE 1. Morphological comparison of three similar 1-pinnate species of *Serpocaulon*.

Character/Species	*S. articulatum*	*S. psychotrium*	*S. richardii*
Rhizome scale shape	Lanceolate	Subulate	Subulate
Rhizome scale color	Light brown	Dark brown	Whitish to redish
Vein impression	not impressed	prominent impressed	not prominent to less conspicuous
Laminar hairs	Scarce to glabrous	Scarce to glabrous	Dense
Apical pinna	Conform	Adnate	Adnate
prominent impressed sori	Absent	Present	Present
Spore ornamentation	Verrucae with flat apex	Verrucae with flat apex	Papillae with rounded apex

2760 (HUA); Sarare, Gibraltar, 700–900 m, 26–27 Mar 1959, *H. Bischler 2049* (COL); Páez, Vereda Vistahermosa, Jan 1994, *E. Barrera 3* (FMB); vía Mámbita, alrededores del río Guavio, 04°45′26″N, 73°18′20″W, 625 m, 9 Oct 2000, *J.C. Murillo A. et al. 2599* (HUA). **Caquetá**: base de los cerros cercanos al abrigo al norte del campamento base, bosque de *Cespedesia sp.*, 25 Nov 1992, *C. Barbosa et al. 8011* (COL three sheets); Sierra de Chiribiquete, cerca del campamento base, 00°56′15″N, 72°42′06″W, 600 m, 20 Nov 1992, *P. Palacios C. et al. 2737* (COL); Medio Caquetá, entre los Raudales El Tijereto y el Quinché, 01°07′83″N, 71°32′38″W, 21 Feb 2001, *A.M. Benavides et al. 118* (HUA). **Casanare**: Monterrey, Vereda El Porvenir, 1036235N, 1126653E, 1131 m, 8 Jun 2010, *P.A. Gil et al. 1074* (UPTC two sheets); Sabana Larga, cereda Caño Blanco, bosque en medio del Km 42 y 43 del oleoducto de Ecopetrol, 1039529 N, 1120225 E, 1512 m, 27 May 2010, *P.A. Gil et al. 842* (UPTC). **César**: Serranía del Perijá, Municipio Agustín Codazzi, Vereda El Milagro, Finca de Miguel San Juan, 10°03′N, 73°03′W, 1870 m, 28 May 1994, *O. Rangel et al. 12534* (COL). **Cundinamarca**: along road between Bogotá and Villavicencio, 8 km SE of Bogotá, 39 km SE of Caquesa, 04°17′N, 73°49′W, 1250 m, 23 Mar 1983, *T.B. Croat 55482* (COL); Buena Vista, Gazaguan Valley, 6 km W of Medina, Station 83, 800 m, 6 Oct 1944, *M.L. Grant 10417* (COL); Caparrapí, Hacienda "Saldaña", 1280 m, 10–13 Jun 1939, *H. García-Barriga 7680* (COL); carretera entre Albán y Sasaima, hacienda "Cataluña", 1820 m, 22 Dec 1967, *R. Jaramillo M. & T. van der Hammen 4772* (COL); Guaduas, vereda La Campeona, camino de La Cabaña-Cordillera Montefrío, bosque de *Quercus*, 19 Jul 1987, *E. Linares & M. Devia 1944* (COL lacking rhizome); Quetame, Kms 68–69, Quebrada La Marcelita (debajo de la quebrada Naranjal), 1300 m, 23 Mar 1974, *C.E. Acosta-Arteaga 195* (COL); Quipile, La Sierra, finca "El Nogal", 1310 m, 12 Mar 1967, *B. Jiménez A. 19* (COL); San Bernardo, vereda Portones, 1650 m, 28 Jul 1981, *S. Díaz P. et al. 3277* (COL lacking rhizome); Sasaima, Km 66, 1500 m, 31 Mar 1974, *C.E. Acosta-Arteaga 218* (COL); Pandi, vereda El Caracol, 1900 m, 29 Jul 1981, *S. Díaz P. et al. 3318* (COL); Ubala B, vereda Boca de Monte, 1000–1050 m, 29 Jun 1998, *J.L. Fernández et al. 16067* (COL two sheets); carretera Arbeláez-San Bernardo, Bar "La Gallega", 1000–1010 m, 2 Aug 1987, *J. Fuertes et al. 124* (COL); Yacopí, Insp. de Policía de Guadualito, vereda de La Laguna,

por el filo de la montaña, 1450 m, 31 Oct 1995, *G. Lozano et al. 7695* (1) (COL); Km 68 de la carretera Bogotá-Villavicencio, 1300 m, May 1974, *F. Sarmiento & M.T. Murillo 406* (COL); Viotá, Cerro La Vieja, Finca "La Turena", bosque de robles, 1200–1500 m, 21 Feb 1978, *J.H. Torres R. 753* (COL). **Huila**: Palestina, Vereda Santa Bárbara, finca La Esperanza, bajando 10 m por la ladera de la montaña hacia el río Guarapas, 01°43′42″N, 76°06′54″W, 1550 m, 25 Oct 2005, *G.A. Silva, V.M. Rico et al. 375* (FMB three sheets); Pitalito, vereda El Triunfo, finca El Pedregal, a 300 m arriba de la casa de doña Isabel Chaus, entrando 10 m desde el borde donde colinda con un cafetal, 01°48′32″N, 76°00′59″W, 1550 m, 1 Nov 2005, *G.A. Silva et al. 557* (FMB); Rivera, vereda Honda Alta, 1370–1550 m, 22 Aug 1992, *F. Llanos et al. 2375* (COL). **Magdalena**: San Pedro de La Sierra, 16 Dec 1966, *R. Romero-Castañeda 10728* (COL two sheets); Sierra Nevada de Santa Marta, transecto Buritaca, Alto Río Buritaca, Cuchilla, 1300 m, 3 Sep 1977, *R. Jaramillo M. et al. 5574* (COL). **Meta**: Acacías, Colonia Penal y Agrícola de Oriente, cerca del Campamento Las Blancas, 930 m, 14 Aug 1981, *R. Jaramillo M. 7737* (COL); La Macarena, vereda El Tapir, Parque Nacional Natural La Macarena, río Guayabero, bocas del río Duda, Caño Cabaña (parte alta), sector Cielo Roto, 02°31′N, 73°54′55′W, 29 Jun 1996, *D. Cárdenas et al. 7226* (COAH, COL); Mesetas, vereda Villa Lucía, hacia la Serranía de la Macarena, comunidad Páez, entre la Escuela del resguardo indígena de Villa Lucía y la casa de Hipólito Yandi, microcuenca de la quebrada La Cristalina, 03°28′05″N, 74°08′58″W, 1000–1200 m, 7 Oct 2002, *O. Rivera D. et al. 1133* (COAH, COL); Villavicencio, vereda El Carmen, caño Maizano, 9 Mar 1971, *C. Sastre & P. Pinto 1078* (COL). **Santander**: Piedecuesta, Mesa de los Santos, Guayabal, 2000 m, 5 May 1984, *G. Díaz et al. 123* (HUA).

VENEZUELA.—**Apure**: Distrito Páez, selva de Cutufi, between Cutufi on the río Cutufi and the río Sanare, 07°09–11′N, 71°56–58′W, 300 m, 8–12 Nov 1982, *G. Davidse & A.C. González 21843* (MO, NY, UC, VEN). **Aragua**: Cerro El Paují, Topo El Paují, al sur de El Consejo, alrededores de la torre, 10°11′N, 67°15′W, 1450 m, 14 Jul 1979, *J.A. Steyermark & A. Stoddart 118014* (MY, VEN); Parque Nacional Henri Pittier, bosque de Rancho Grande, without date [Oct-Nov 1965], *R.H. Tschudy 59* (VEN); Ricaurte, Fila de Tiara, 3 Oct 1976, *F. Ortega 207 A&B* (VEN two sheets each). **Barinas**: Bolívar, ladera Este al pie de la Peña del Gobernador, cerca de Altamira, sedimentos Eocenos de la Formación Pagüey, 1500 m, Dec 1985, *A. Fernández 1528* (PORT); Periférica del Municipio de Calderas en orilla del brazo del río Sto. Domingo, 8 Oct 1983, *B. Stergios et al. 6453* (MO). **Distrito Capital**: Los Flores, Sierra de El Ávila, 1600 m, 15 Dec 1938, *A.H.G. Alston 5526* (BM, NHN, NY lacking rhizome, U image, US, VEN); quebrada arriba de Maripérez, 1100 m, 11 Jun 1940, *L. Schnee 619* (MY). **Falcón**: Bolívar y Petit, Sierra de San Luis, 3 km NNE del Hotel Parador Turístico, 1500 m, 9 May 1979, *C. Burandt & R. Wingfield V0654* (UCOB); Sierra de San Luis, Fila Norte, Hoya de Curimagua, along road between Curimagua and La Chapa, 1.8 km NE of Uria, 11°09′N, 69°38′W, 1200 m, 6 Mar 1993, *T.B. Croat 74475* (UC, VEN); Carretera Coro-Curimagua, cerca de torre de relevo, 1700 m, 27 Aug 1962, *T. Lasser 4420* (VEN); Sierra de San

Luis, cerca del Hotel Parador, 1300 m, 3 Sep 1978, *H. van der Werff & R. Wingfield 3033* (MO, UC); Sierra de San Luis, cerca del Hotel Parador, 1400 m [1500 m, fide VEN], 25 Aug 1978, *R. Wingfield & H. van der Werff 6566* (MO lacking rhizome, UC, VEN). **Lara**: Jiménez, Parque Nacional Yacambú, 3 km E of Park headquarters, Quebrada El Blanco, 09°43′N, 69°34′W, 1300–1400 m, 24 Oct 1982, *G. Davidse & A.C. González 21090* (two sheets PORT, VEN); Iribarren, trocha Camino Real, margen derecho, zona Palo El Tigre, Parque Terepaima, 1200–1300 m, Aug 1983, *L. Iriarte & G. Morillo 167* (PORT, MER); Palavecino, Fila de Terepaima, entre el Alto de Chuparral y la Loma Redonda, 21–23 kms al sur de Cabudare, 1300–1460 m, 4 Aug 1970, *J.A. Steyermark et al. 103419* (VEN). **Lara/Falcón** (disputed area): Cerro Cerrón (western part), 1800–2000 m, 17 Jun 1979, *R. Liesner et al. 8242* (MO, VEN). **Mérida**: Páramo de Chacantá, 1800 m, 22 Jan 1922 [1921 at VEN], *A. Jahn 905* (US, VEN); Libertador, [ciudad de] Mérida, Campo de Oro, bosquete residual en la margen derecha del río Chama, entre el pie de la Cuesta de los Chucos y la quebrada Campo de Oro, 1370 m, 16 Jul 1977, *L. Ruíz-Terán & J.A. Dugarte 14003* (MERF two sheets, UC two sheets). **Miranda**: Guaicaipuro, al sureste de Las Tejerías, al sureste de la mina de Nickel (Loma de Hierro), Fila El Amparo, 10°08′N, 67°07′W, 750–1000 m, 7 Jul 2002, *W. Meier et al. 9023* (UC, VEN); Distrito Zamora, macizo del Ávila, vertiente sur, al noreste de Guatire, al noreste de El Bautismo, alrededores de El Oso, 1100–1300 m, 10°31′N, 66°28′W, 15 Jun 2003, *W. Meier & J.L. Hernández-Bretón 9266* (B, NY, UC, VEN); límite Municipio Baruta/Municipio El Hatillo, al sureste de Caracas, sureste de Baruta, El Volcán, vertiente sur, 10°25′N, 66°51′30″W, 1250–1350 m, 30 Mar 2006, *W. Meier & H.N. Cordido 13621* (MY, UC); Serranía del Interior, Municipio Urdaneta, vertiente N de la altiplanicie, Fila 1–3 km al S del Palacio de El Guayabal-pueblo de La Providencia, 10°02′29″N, 66°55′11″W, 1050–1100 m, 11 Oct 2005, *J. Mostacero & W. Meier 640* (UC two sheets, VEN); Baruta, fila montañosa al Oeste del sector El Naranjal y el tunel de Los Ocumitos, arriba de la Urb. Hacienda La Soledad, alrededores de torre repetidora de telefonía, 10°20′22″N, 66°53′03″W, ca. 1375 m, 10 Aug 2008, *J. Mostacero et al. 1529* (VEN); Baruta, carretera Hoyo de la Puerta, sector El Laurel, Estación Experimental de Agronomía "Dr. Jaime Henao Jaramillo" de la Universidad Central de Venezuela, 10°22′38″N, 66°53′51″W, ca. 1400 m, 16 Oct 2014, *J. Mostacero et al. 1897* (VEN); Parque Nacional Guatopo, along ridgetop, boundary between estado Miranda and estado Guárico, NE of highway, 18 km (by air) NNW of Altagracia de Orituco, 10°02′N, 66°26′W, 800–950 m, 28 Aug 1979, *M. Nee 17871* (F, VEN). **Miranda/Aragua** (border): bosque nublado de Loma de Hierro, 10°11′N, 67°7′W, 1350 m, 10 Jun 1984, *M. Colella & V. Morales 599* (PORT, VEN two sheets); límites distritos Urdaneta-San Casimiro, fila al sur del Topo Santo Domingo, 20 km distancia aérea al suroeste de Ocumare del Tuy, al oeste de Las Quebraditas, 10°04′30″N, 66°58′W, 1000–1150 m, 21 Jan 2002, *W. Meier & S. Nehlin 8876* (UC, VEN). **Portuguesa**: Guanare, Caserío "La Montaña", 4 km al NW de Córdoba, a lo largo de la quebrada "El Silencio", 10°24′N, 69°52′W, 1000 m, 11 Dec 1986, *G. Aymard 5167* (PORT, MO); Sucre, Villa Rosa, 15 km al SE de Biscucuy, bosques nublados a lo largo de la

Quebrada El Potrero, 09°19′N, 69°54′W, 1400–1600 m, 16 Jun 1985, *G. Aymard et al. 3712* (PORT lacking apex, UC); Ospino, 20 km W of La Estación, Laguna de San Bartolo and vicinity (turnoff from road to Palma Sola), 09°26′N, 69°38′W, 1400 m, 10 Nov 1982, *A.R. Smith et al. 1155* (MO, PORT, UC); laguna natural en la fila de la cumbre, 17.8 kms (por carretera) de La Estación, 30 kms (por carretera) al Norte de Ospino, 1170 m, 1 Nov 1982, *J.A. Steyermark et al. 127033* (PORT two sheets, UC, VEN). **Táchira**: Independencia, El Ron, 26 Dec 1968, *L. Cárdenas de Guevara 759* (MERF, MY); along highway between San Cristóbal and Páez, vía Rubio and Las Delicias, 13.8 km SW of plaza in Brammon, 07°39′N, 72°22′W, 1600 m, 12 Mar 1993, *T.B. Croat 74663* (MO, UC, VEN); Uribante, Quebrada between Cerro La Escalena and Cerro El Morro, 07°57′N, 71°42′W, 1150–1250 m, 23 Jun 1990, *L.J. Dorr & L.C. Barnett 7148* (MY, NY, PORT, VEN); Jáuregui, Seboruco, creciendo mas arriba del sector Torcoroma, 800 m, Nov 1982, *A. Fernández & J. Fernández 1059* (PORT, UC); vicinity of Las Minas, N of La Laguna, 16 km SE of Santa Ana, 07°36′N, 72°13′W, 1150–1250 m, 28 Jul 1979, *J.A. Steyermark & R. Liesner 118886* (UC, VEN); Uribante, Represa Las Cuevas near La Fundación, 08°50′N, 71°47′W, 900 m, 6 Jul 1983, *H. van der Werff 4937* (VEN); Uribante, along road from La Siberia to entrance to Las Cuevas Represa, 9 Jul 1983, *H. van der Werff & A. González 5208* (MO, VEN). **Trujillo**: Cerro vía Las Carmelitas (desde Las Pavas), 8 Feb 2007, *C. Berlingeri et al. 181* (MY). **Vargas**: on the old road from Caracas to La Guaira, 1100–1700 m, 28 Feb 1913, *H. Pittier 5911* (US). **Zulia**: [Machiques de Perijá], Kunana (Perijá), 1175 m, 26 Dec 1949, *F. Matos & S. Arias 1270* (CAR).

Despite its widespread distribution in northern South America, this species has been overlooked. One of the oldest collections from Venezuela was made in 1854 by the Prussian-born American botanist Augustus Fendler (1813–1883) around Colonia Tovar, Aragua State. Fendler noted that this fern was very different from plants now assigned to *Serpocaulon fraxinifolium* (see specimen 237 in Appendix I from Smith and Todzia, 1989), a species that can be readily distinguished by the ovate, appressed rhizome scales. This specimen was previously reported as *Polypodium* aff. *fraxinifolium* (Smith *et al.*, 1985).

2. ***Serpocaulon articulatum*** (C. Presl) Schwartsb. & A.R. Sm., J. Bot. Res. Inst. Texas 7(1): 85–93. 2013. – *Goniophlebium articulatum* C. Presl, Tent. Pterid. 186. 1836. *Polypodium articulatum* Desv., Mém. Soc. Linn. Paris 6: 236. 1827, nom. illeg. (non Juss. ex Poir. 1804, nec Vahl 1807).—TYPE: Brazil, *Anonymous*, ex Herb. Desvaux (lectotype, designated by Schwartsburd and Smith 2013: P [bc] 00624694 image!).

Serpocaulon caceresii (Sodiro) A.R. Sm., Taxon 55(4): 928, f. 3A. 2006. – *Polypodium caceresii* Sodiro, Crypt. Vasc. Quit. 360. 1893. —TYPE: ECUADOR. Crece en los bosques de Oriente en la orilla del río Napo, *R.P.R. Caceres s.n.* (**lectotype, here designated**: P [bc] 00624700 image!,

isolectotypes: BM, K, P [bc] 00624701 image!, P [bc] 00624703 image!, NHN-U [bc] 0007491!, US [bc] 00065813 image!). ***syn. nov.***

Polypodium fraxinifolium Jacq. subsp. *articulatum* (Desv.) Christ, Bull. Herb. Boissier, sér. 2, 6(1): 45–59. 1906. Costa Rica: Cartago, Turrialba, 550 m. *H. Pittier 9061* (lectotype designated by Lellinger 1985: 387: US [bc] 00065825; isolectotypes: CR, P).

Christ (1906) cited four collections from Costa Rica: *Pittier 1162* from Carrillo; *Pittier 9061* from Turrialba; *Tonduz 9451* from Tsaki, Talamanca; and *Wercklé* s.n. Lellinger (1985) typified *Polypodium fraxinifolium* subsp. *articulatum* Christ by selecting *Pittier 9061* (US). However, he wrongly cited the name as var. *articulatum*. Schwartsburd and Smith (2013) cited this name as a homotypic synonym of *Serpocaulon articulatum*, omitting the fact that Christ (1906) regarded this taxon as a subspecies.

Father Luis M. Sodiro arrived in Ecuador in 1870 from Italy (Acosta-Solís, 1937). Sodiro worked in Ecuador for more than 30 years and amassed around 60,000 specimens, many deposited in herbaria that he founded: QPLS and Q. Some of his duplicates are known to have gone to B, F, FI, K, NY, P, SI, UC, and other herbaria (Morton, 1972; Lellinger, 1980; Lehnert, 2008; Vivero Lovato, 2018).

Sodiro had a special preference for ferns, as indicated by his description of many new species (Sodiro, 1883; 1893; 1908) and his published works (Morton, 1972; Lellinger, 1980). However, most of the information from his specimens in Ecuadorian herbaria has not always been transcribed exactly on duplicates, and a perfect match of locality data on his labels with that in his publications is rare (Lehnert, 2008). Material from Paris (P) has often been chosen as type or authentic material for reference (Lehnert, 2008). In some cases, researchers (*e.g.*, Hensen, 1990) have not consulted Sodiro's collections in Ecuadorian herbaria (see Moran, 1990), but instead lectotypified names based on European collections.

This scenario perhaps applies to typification of *Polypodium caceresii* Sodiro. Hensen (1990) stated that type material of *Polypodium caceresii* was at Q (?), P, and K, without seeing material in Ecuadorian herbaria. This practice is contrary to Article 9, Recommendation 9A, of the International Code (Turland *et al.*, 2018). In addition, Hensen, and others, never compared *Polypodium caceresii* with the type of *Goniophlebium articulatum* C. Presl, which is also once-pinnate and has long-creeping rhizomes with patent scales (Schwartsburd and Smith, 2013; http://mediaphoto.mnhn.fr/media/1442925193543MokTaoVE9my27sa7).

The name *Polypodium caceresii* (= *S. caceresii*) has been frequently used in floras and other publications (*e.g.,* Hensen, 1990; Tryon and Stolze, 1993; Berry, Holst, and Yatskievych, 1995; Moran, 1995; Jørgensen and León-Yánez, 1999; Funk *et al.*, 2007; Hokche, Berry, and Huber, 2008; Kreier *et al.* 2008; Rodríguez, 2011; Jørgensen, Nee, and Beck, 2014; Murillo, Murillo, and León, 2016; Sanín, 2018; Smith *et al.*, 2018). Our investigations show that many of these previous usages apply, in part, to *S. articulatum*.

Like Hensen (1990), we were unable to find syntypes of *Serpocaulon caceresii* in any Ecuadorian herbaria. In other herbaria, we found syntypes of *S. caceresii* that were, in our opinion, representative of *S. articulatum*. This species was mentioned by Hensen (1990) as *P. articulatum* Desv. and recognized as a synonym of *P. caceresii* by him.

A description, illustration, and photos of the rhizome, rhizome scales, pinnae, and spores of *Serpocaulon articulatum* and *S. psychotrium* (treated as *S. caceresii*) are found in Sanín (2018). Schwartsburd and Smith (2013) also provided nomenclatural comments for *S. articulatum*, and Smith *et al.* (2006: Fig. 3a) illustrated the sori of *S. psychotrium* (treated by them as *S. caceresii*). Most likely, some of the specimens of *S. caceresii* cited in the literature pertain to *S. psychotrium*, and others apply to *S. articulatum*; thus, we provide a more detailed compilation of specimens for both taxa, and a key for identification of the pinnate species in the genus.

Specimens Examined.—BOLIVIA. **Beni**: Ballivian, lower slopes of Serrania Pilon Lajas, 14.3 km N of the bridge over the río Quiquibey, 700 m, 15°19′S, 67°3′W, 10 Jun 1985, *J.C. Solomon 13895* (LP, LPB). **La Paz**: Caranavi, serranía de Bella Vista, 47 km de Caranavi hacia Sospecho, 1150 m, 15°29′S, 67°28′W, 13 Aug 1997, *M. Kessler et al. 11656* (LPB); Larecaja, 7.1 km al SO de Tipuani por el camino a Unutuluni, 670 m, 15°36′S, 68°01′W, 24 Jan 1988, *J.C. Solomon 17724* (LPB, MO); Franz Tamayo, Parque Nacional Madidi, río Quendeque, campamento guardaparques, 300 m, 15°01′10″S, 67°44′31″W, 8 Feb 2002, *A. Fuentes et al. 3826* (LPB).

Brazil.—**Amazônia**: Camanaús, Basin of Rio Negro, [92 m], 31 Oct 1971, *G.T. Prance et al. 15866* (F); Presidente Figueiredo, Terra-Firme adjacente ao Lago da Usina Hidrelétrica de Balbina, 29 Nov 2006, *G. Zuquim & A.B. Junqueira 301* (SP). **Pará**: Oriximiná, Estação Ecológica Grão Pará, Serra do Acari, trilha 2 de 2800 m, 475 m, 01°16′17″N, 58°41′28″W, 30 Aug 2008, *M.R. Pietrobom & S. Maciel 7852* (SP).

Colombia.—**Caquetá**: Solano, 8 km SE, of Tres Esquinas on río Caquetá below mouth of río Orteguaza, 200 m, 6 Mar 1945, *E.L. Little 9622* (COL); Florencia, corregimiento El Caraño, vereda El Caraño, finca Las Brisas, relictos en la cima de la montaña, 1285 m, 01°44′50″N, 75°40′42″W, 16 Oct 2015, *D. Sanín 6151* (COL). **Cauca**: Piamonte, corregimiento de Nápoles, vereda La Florida, Serranía de los Churumbelos, 800 m, 9 May 2006, *Muñoz 2018* (CAUP). **Chocó**: hoya del río San Juan, quebrada La Serpiente, afluente del río San Juan, 5 m, 1 Apr 1979, *E. Forero 4451* (COL); San José del Palmar, vereda Damasco, escuela Santa Lucia, 641 m, 04°52′09″N, 76°15′02″W, 21 May 2009, *D. Sanín 2976* (FAUC); río Mutatá, ca. 3 km above its junction with río El Valle, NW of Alto del Buey, 800 m, *D.B. Lellinger 176* (COL). **Cundinamarca**: entre Albán y Sasaima, hacia Las Mercedes, 11 May 1961, *M.T. Murillo 84* (COL). **Guaviare**: San José del Guaviare, confluencia Caño Perdido-río Losada, 02°11′N, 74°03′W, 20 Jan 1990, *O. Marulanda & S. Marquez 1865* (HUA). **Huila**: Acevedo, carretera entre San Marcos y San Adolfo, 1300 m, 5 Apr 1983, *Osorio 161*

(COL). **Meta**: carretera Medina a San Pedro de Jagua, bosques sobre el río Gazuanta, 18 Jun 1986, *M.T. Murillo 2164* (COL). **Valle del Cauca**: Buenaventura, Corregimiento Los Tubos, vereda Péricos, vertiente occidental de la Cordillera Occidental, Km 43 Cali-Buenaventura, 521 m, 03°51′00″N, 76°47′19″W, 30 Aug 2011, *J. Home 224* (CUVC).

Costa Rica.—**Cartago**: Road to Moravia de Chirripó, near Finca los Quetzales, along Pacuare river, 1100–1300 m, 1 Oct 1982, *D.L. Hazlett 5077* (F); forêts de Turrialba, 550 m, 15 Sep 1894, *H. Pittier s.n.* (BR). **Heredia**: Braulio Carrillo National Park, 1865 m, 10°15′N, 84°10′W, 11 Nov 1986, *E. Hennipman et al. 6838* (F, CR, U). **Limón**: Cordillera de Talamanca, between headwaters of río Madre de Dios and Quebrada Barreal, 400–440 m, 10°02′N, 83°27′W, 5 Sep 1988, *M. Grayum et al. 8793* (F, CR). **Puntarenas**: Cantón de Golfito, P.N. Corcovado, Península de Osa, Estación Agujas, Quebrada Bonanza, Sendero Bonanza, 500 m, 08°31′40″N, 83°26′30″W, 12 Nov 1997, *A. Azofeifa 530* (INB).

Ecuador.—**Napo**: Cuyuja-Baeza, 1888, *A. Sodiro 2/905* (QPLS); Cantón Napo, trail from Zatzayacu to Las Palmas, 500 m, 17 Mar 1935, *Y. Mexia 7103a* (F, UC); Yasuni Scientific Research Station, ca. 1 km N of río Tiputini, Bridge II (road station Tivacuno oil well), 210 m, 00°40′S, 76°23′W, 22 Aug 1995, *H. Balslev 6364* (QCA, AAU). **Pastaza**: Finca Sta. Rosa, Km 60 carretera Puyo Macas, 5 km antes de la comunidad Shuar de Chuwitayo y 10 km antes del puente sobre el río Pastaza, 850 m, 01°53′05″S, 77°48′07″W, 7 Apr 1997, *H. Romero-Saltos & C. Kasent 498* (QCA). **Sucumbios**: Reserva Faunística Cuyabeno, N of Laguna Grande, 265 m, 00°01′N, 76°11′W, 26 Mar 1989, *H. Balslev et al. 84640* (QCA). **Tungurahua**: Cantón Baños, Parroquia de río Negro, 1500 m, 01°24′S, 78°10′W, 16–17 Jun 1987, *C.E. Cerón 1601* (QCA, MO). **Zamora-Chinchipe**: Parque Nacional Podocarpus, Bombuscaro, along trail "Higuerones", 1050 m, 04°07′S, 78°58′W, 23 Nov 2011, *M. Lehnert 2141* (QCA).

French Guiana.—**Cayenne**: Montagne de l' Inini, extrémité NW, sur la crête, 700–720 m, 03°30′N, 53°35′W, 17 Aug 1985, *G. Cremers et al. 8973* (BR). **Maripasoula**: Monts Kotika, plateau latéritique sommital, 730 m, 03°55′10″N, 54°11′10″W, 21 Feb 2005, *J.J. de Granville et al. 16870* (CAY image, NY, P, UC, US).

Guyana.—**Potaro-Siparuni**: Kaieteur Plateau, [05°10′30″N, 59°28′49″W], 15 May 1944, *B. Maguire & D.B. Fanshawe 23478* (F).

Panama.—**Darién**: Parque Nacional Darién, Serrania de Sapó, límite del Parque hasta la cima, 300–800 m, 75°58′N, 78°23′W, 26 Nov 1990, *H. Herrera & J. Polanco 812* (F, MO). **Veraguas**: NW of Santa Fé, 4.2 km from Escuela Agrícola Alto de Piedra, 25 Feb 1975, *S. Mori & J. Kallunki 4841* (RB).

Peru.—**Amazonas**: Bagua, Imaza, comunidad de Kampaensa, borde del río Shimutaz, 450 m, 04°55′S, 78°19′W, 21 Oct 1995, *E. Rodríguez 591* (UC, USM); Luya, Camporredondo, localidad Jaipe, 2050 m, 06°09′07″S, 78°21′05″W, 26 Mar 1997, *J. Campos et al. 3641* (MO, UC, USM). **Cajamarca**: San Ignacio, Dist.

Huarango, San Martín-Quebrada Colorada, 860 m, 15°17′S, 78°42′W, 15 May 1996, *J. Campos et al. 2739* (F, UC). **Cuzco**: La Convención, Distrito de Echarati, San Martín 3 site well, 400 m, 11°46″S, 72°42′W, 2 Nov 1998, *H. Beltrán et al. 3282* (USM). Junín: Jauja, Perené, 1500 m, 1918, *N. Esposto s.n.* (USM). **Loreto**: Amazonas, rivera de la Quebrada Sucusari, 140 m, 03°20′S, 72°55′W, 19 Apr 1991, *R. Vásquez & N. Jaramillo 16183* (COL); Maynas, from Iquitos, ca. 50 miles downriver on the Amazon at Peter Jensens's Explorama lodge, 26 Jun 1984, *R.C. Moran 3658* (USM). **Madre de Dios**: Manu, Cerro de Pantiacolla, río Palotoa, 10–15 km NW of Shintuya, transect to ridgetop, 700–1300 m, 12°35′S, 71°18′W, 14 Dec 1985, *R.B. Foster et al. 10820* (USM). **Pasco**: Oxapampa, Palcazu, río Alto, Iscozacin, Ozuz to río Pescado, 400–500 m, 10°19′S, 75°16′W, 12 May 1985, *R.B. Foster & B. d'Achille 10104* (F, USM). **Puno**: Sandia, Dist. Alto Inambari, sector Pacaysuizo, 1258 m, 14°01′S, 69°11′W, 21 Apr 2003, *C. Orocollo et al. 151* (USM). **San Martín**: Lamas, Alfonso de Alvarado, Quebrada de Poloponta, 4 km de San Juán de Pacayzapa, 800–900 m, 30 Apr 1973, *J. Schunke 6116* (LP); cataratas de Ahuashiyacu, Km 15 Tarapotó-Yurimaguas, 700 m, 06°29′S, 76°21′W, 19 Jun 1986, *S. Knapp & P. Alcorn 7783* (USM, MO). **Ucayali**: Padre Abad, Dist. Padre Abad, carretera San Miguel y Mapuya, 12 a 17 km de la Aguaytia, 350 m, 09°05′S, 75°26′W, 4 Oct 2004, *J. Schunke & J. Graham 16206* (F).

VENEZUELA.—**Amazonas**: Río Negro, swampy area between río Mawarinuma and headwaters of río Baria, 130 m, 00°53′N, 66°15′W, 29 Mar 1984, *R. Liesner 17018* (MO, UC, VEN). **Bolívar**: cerro Marahuaca, slopes, "Sima" área, 1200 m, 03°43′N, 65°30′W, 19 Oct 1988, *R. Liesner 25097* (MO, UC, VEN); selvas ribereñas del río Paragua, arriba de la boca del río Tonoro, 175 m, 06°03′N, 63°47′W, 13 May-13 June 1987, *B. Stergios 10313* (PORT, UC, VEN); Ptari-Tepuí, base of Cerro along río Karauai, 1220 m, [05°46′01″ N, 61°48′40″ W], 27 Nov 1944, *J.A. Steyermark 60656* (F); Auyán-tepui, Guayaraca, 1100 m, 1956, *V. Vareschi & E. Foldats 4599* (VEN).

KEY TO THE SPECIES OF *SERPOCAULON* WITH PINNATE LAMINAE

1. Rhizome scales appressed 2
    2. Laminae densely pubescent . . . . ***S. appressum***
    2. Laminae glabrous or sparingly pubescent 3
        3. Laminar apex adnate . . . . ***S. adnatum***
        3. Laminar apex free, pedicellate, or sessile 4
            4. Pinna bases cuneate, margin of the rhizome scales salmon color, areoles 36–57 rows along the middle pinna; Middle Magdalena Valley Basin of Colombia . . . . ***S. antioquianum***
            4. Pinna bases asymmetric, margin of the rhizome scales clear brown color, areoles 17–35 rows along the middle pinna; widespread in low-middle regions in the Andes and Central America . . . . ***S. fraxinifolium***
1. Rhizome scales spreading, at least their apices 5
    5. Rhizome scales lanceolate with straight apices 6
        6. Rhizomes long-creeping, space between phyllopodia twice (or more) the diameter of the rhizomes 7

7. Laminae coriaceous, venation inconspicuous .... ***S. articulatum***
7. Laminae chartaceous to papyraceus, venation conspicuous 8
8. Laminae 50–70 cm wide; 5–7 areoles between the costae and pinna margins; rhizome scales concolorous .... ***S. rex***
8. Laminae 13–30 cm wide; 3–4 areoles between the costae and pinna margins; rhizome scales bicolorous .... ***S. polystichum***
6. Rhizomes short-creeping, space between phyllopodia less than the diameter of the rhizomes 9
9. Rhizome scales iridescent, concolorous; spores with folded perine .... ***S. sessilifolium***
9. Rhizome scales opaque, bicolorous or concolorous; spores verrucate 10
10. Rhizome scales bicolorous; middle pinnae adnate .... ***S. meniscifolium***
10. Rhizome scales concolorous; middle pinnae free .... ***S. triseriale***
5. Rhizome scales subulate with reflexed apices 11
11. Laminae densely pubescent, rarely sparsely pubescent, papyraceous; rhizome scales reddish brown; sori not impressed on adaxial laminar surface . . . ***S. richardii***
11. Laminae sparsely pubescent or glabrous, chartaceous; rhizome scales dark brown; sori impressed on adaxial laminar surface .... ***S. psychotrium***

Acknowledgments

We thank the curators and staff of the herbaria cited in this paper for granting the authors access to their collections, mainly to Blanca León (USM), Consuelo Montalvo (Q), Sara Ruano (QLPS), Daniela Cevallos (QCA), Norma Deginani (SI), Christian Zanotti (SI), Juan C. Ospina (ICEGEM-UNJU), José Murillo (COL), Cristian Castro (COL), Nicolas F. Montoya Posada (QCA), and Álvaro Pérez (QCA). DS is in debt to Alexandre Salino (BHCB) for his kind support, the Coordenação de Aperfeiçoamento de Pessoal de Nível Superior, the Universidade Federal de Minas Gerais for a scholarship, and to Fundação de Amparo à Pesquisa do Estado de Minas Gerais (Fapemig) for financial support (APQ–03041–17). We are grateful to Robbin C. Moran, Christopher H. Haufler and the anonymous reviewers for their critical reading and suggestions.

Literature Cited

Acosta-Solís, M. 1937. La botánica hasta nuestros días. Anales de la Universidad Central del Ecuador LVII (298):568–609.

Berry, P. E., B. K. Holst, and K. Yatskievych. 1995. Pteridophytes, spermatophytes (Acanthaceae-Araceae). Pp. 1–327, *in* P. E. Berry, B. K. Holst, and K. Yatskievych (eds.). *Flora of the Venezuelan Guayana*. Vol. 2. Timber Press. Portland.

Christ, H. 1906. Primitiae Florae Costarricensis. Bulletin de L'Herbier Boissier, Seconde Série, Tome VI:45–58.

ESRI. 2016. ArcGIS release 10.5. Redlands. CA: Environmental Systems Research Institute.

Funk, V. A., T. H. Hollowell, P. E. Berry, C. L. Kelloff, and S. Alexander. 2007. Checklist of the plants of the Guiana Shield (Venezuela: Amazonas, Bolivar, Delta Amacuro; Guyana, Surinam, French Guiana). Contributions from the United States National Herbarium 55:1–584.

Hensen, R. V. 1990. Revision of the *Polypodium loriceum*-complex. Nova Hedwigia 50:279–236.

Hokche, O., P. E. Berry, and O. Huber (eds.). 2008. Nuevo Catálogo de la Flora Vascular de Venezuela. Pp. 1–859. Caracas: Fundación Instituto Botánico de Venezuela.

Jørgensen, P. M., and S. León-Yánez (eds.). 1999. Catalogue of the Vascular Plants of Ecuador. Monographs in Systematic Botany from the Missouri Botanical Garden 75: i–viii. Pp. 1–1181. Missouri Botanical Garden Press. St. Louis.

Jørgensen, P. M., M. H. Nee, and S. G. Beck (eds.). 2014. Catálogo de las Plantas Vasculares de Bolivia, Monographs in Systematic Botany from the Missouri Botanical Garden 127(1–2): i–viii. Pp. 1–1744. Missouri Botanical Garden Press. St. Louis.

Kreier, H. P., M. Rex, K. Weising, M. Kessler, A. R. Smith, and H. Schneider. 2008. Inferring the diversification of the epiphytic fern genus *Serpocaulon* (Polypodiaceae) in South America

using chloroplast sequences and amplified fragment length polymorphisms. Plant Systematics and Evolution 274:1–16.

Lehnert, M. 2008. On the identification of *Cyathea pallescens* (Sodiro) Domin (Cyatheaceae): typifications, reinstatements and new descriptions of common neotropical tree ferns. Botanical Journal of the Linnean Society 158:621–649.

Lellinger, D. B. 1980. Date of publication of Sodiro's "Sertula Florae Ecuadorensis". American Fern Journal 70:96–98.

Lellinger, D. B. 1985. Nomenclatural and taxonomic notes on the pteridophytes of Costa Rica, Panama, and Colombia. II. Proceedings of the Biological Society of Washington 98: 366–390.

Lellinger, D. B. 2002. A modern multilingual glossary for taxonomic pteridology. Pteridologia 3. American Fern Society.

Moran, R. C. 1990. Review of R. V. Hensen's Revision of the *Polypodium loriceum* complex. American Fern Journal 80:118–119.

Moran, R. C. 1995. Polypodiaceae. Pp: 333–366 *in* G. Davidse, M. S. Sousa, and S. Knapp (eds.). *Flora Mesoamericana, Psilotaceae a Salviniaceae.* Universidad Nacional Autónoma de México. Ciudad de México.

Morton, C. V. 1972. Date of publication of Sodiro's "Cryptogamae Vascaulares Quitensis. American Fern Journal 62:57–64.

Murillo, M. T., J. C. Murillo, and A. León. 2016. *Helechos de Colombia.* Pp. 1–370. Universidad Nacional de Colombia (Sede Bogotá), Instituto de Ciencias Naturales, Ed. ARFO Ltda. Bogotá.

Pinkley, H. V. 1969. Etymology of *Psychotria* in view of a new use of the genus. Rhodora 71:535–540.

Ramírez-Valencia, V., D. Sanín, and A. Pardo. 2013. Análisis morfológico de las esporas de *Serpocaulon* (Polypodiaceae) de la Cordillera Central de Colombia. Caldasia 35:177–197.

Ramírez-Valencia, V., and D. Sanín, 2016. Spores of *Serpocaulon* (Polypodiaceae): morphometric and phylogenetic analysis. Grana 56:1–18.

Rödl-Linder, G. 1990. Monograph of the genus *Goniophlebium.* Blumea 34:277–423.

Rodríguez, W. D. 2011. *Pteridophyta*, Pp. 9–939 *in* A. Idárraga-Piedrahita, R. D. C. Ortíz, R. Callejas Posada, and M. Merello (eds.). *Flora de Antioquia: Catálogo 2*: Universidad de Antioquia. Medellín.

Sanín, D. 2018. *Serpocaulon* (Polypodiaceae), Flora de Colombia. No. 32. Pp. 1–137. Instituto de Ciencias Naturales, Universidad Nacional de Colombia, Bogotá.

Schwartsburd, P., and A. R. Smith. 2013. Novelties in *Serpocaulon* (Polypodiaceae). Journal of the Botanical Research Institute of Texas 7:85–93.

Smith, A. R., and C. A. Todzia. 1989. Augustus Fendler's Venezuelan collections of ferns and fern allies. Annals of the Missouri Botanical Garden 76:330–349.

Smith, A. R., J. T. Mickel, B. Øllgaard, R. C. Moran, R. J. Hickey, and D. M. Johnson. 1985. *Pteridophytes of Venezuela, an annotated list.* Pp. 254. University of California, Berkeley.

Smith, A. R., H. P. Kreier, C. H. Haufler, T. A. Ranker, and H. Schneider. 2006. *Serpocaulon,* a new genus segregated from *Polypodium.* Taxon 55:919–930.

Smith, A. R., M. Kessler, B. León, T. E. Almeida, I. Jiménez-Perez, and M. Lehnert. 2018. Prodromus of a fern flora for Bolivia. XL. Polypodiaceae. Phytotaxa 354:1–67.

Sodiro, L. 1883. *Recensio cryptogamae vasculares quitenses.* Typis Universitatis, Pp. 1– 656. Quito.

Sodiro, L. 1893. *Cryptogamae vasculares quitensis adiectis speciebus in aliis provinciis ditionis ecuadoriensis.* Typis Universitatis, Pp. 1–660. Quito.

Sodiro, L. 1908. *Sertula Florae Ecuadoriensis.* Pteridophyta, series 2. Typis Universitatis, Quito.

Thiers, B. 2020. Index Herbariorum: A Global Directory of Public Herbaria and Associated Staff. New York Botanical Gardens Virtual Herbarium. Available from: http://sweetgum.nybg.org/ih/ (accessed 28 January 2020).

Tryon, R. M., and R. G. Stolze. 1993. 18. Aspleniaceae–21 Polypodiaceae. 32: Pp 1–190, *in* R. M. Tryon and R. G. Stolze (eds.) Pteridophyta of Peru Part V. 18. Fieldiana, Bot. n.s. Field Museum of Natural History, Chicago.

Turland, N. J., J. H. Wiersema, F. R. Barrie, W. Greuter, D. L. Hawksworth, P. S. Herendeen, S. Knapp, W.-H. Kusber, D.-Z. Li, K. Marhold, T. W. May, J. McNeill, A. M. Monro, J. Prado, M. J. Price, and G. F. Smith (eds.). 2018. International Code of Nomenclature for algae, fungi, and plants

(Shenzhen Code) adopted by the Nineteenth International Botanical Congress Shenzhen, China, July 2017. Regnum Vegetabile 159. Glashütten: Koeltz Botanical Books. DOI https://doi.org/10.12705/Code.2018

Vivero Lovato, D. A. 2018. *Padre Luis Sodiro S. J.: Importancia de su aporte al conocimiento de la botánica en el Ecuador y sus antecesores.* Pp. 55. Facultad de Ciencias Exactas y Naturales, Pontificia Universidad Católica de Ecuador. Quito.

Appendix 1. Index to collector's numbers. Specimens are in alphabetic order and labeled as (1) for *S. psychotrium* and (2) for *S. articulatum*.

Barkley 1885 (1); *Beltrán 5687* (2); *Bunting 2417* (1); *Castillo 2943* (1); *Croat 55020* (1); *Hno. Daniel 1902* (1); *Davidse 21091* (1); *Delgado 23* (1); *Díaz 1003* (1); *Escalona 11* (1); *Farreras 20* (1); *Fay 1409* (1); *Fay & Fay 2732* (2); *A. Fernández 139* (1), *146* (1), *148* (1); *J.L. Fernández 16159* (1); *Ferrer-Pereira 246* (1); *García 414* (1); *Gaydos 4* (1); *Gil 695* (1); *Giraldo 3019* (1); *de Granville 16743* (2); *Haught 3826* (1); *Iriarte 69* (1); *Iskandar 828* (1); *Jaramillo M. 4795* (1); *Killip 34844* (2); *Liesner 8355* (1); *López 6727* (1), *6728* (1); *Maciel 836* (2); *Meier 8555* (1), *12543* (1), *14025* (1); *Mejía P. 55* (1); *Montoya 990* (1), *1005* (1); *Mostacero 1884* (1); *Palacios C. 2738* (1); *Pinilla 8* (1), *73* (1); *Pittier 3102* (2); *Orozco 369* (1); *Ortega 1452* (1); *Rangel 12551* (1); *Rivas 56* (1); *Rodríguez 4138* (1); *Roldán* (1); *Salinas 523* (2); *Sodiro 1/905* (2); *Schwarz 38* (1); *Stergios 1106* (1), *6485* (1); *Steyermark 98926* (1), *99042* (1), *120017* (1), *126734* (1); *Trujillo-Q. 7016* (1); *Tuomisto 6463* (2); *van der Werff 5030* (1); *Velasco 575* (1); *Velásquez 1705* (1).

American Fern Journal 111(2):86–109 (2021)
Published on 7 June 2021

Microscopic and Metagenomic Evidence for Eukaryotic Microorganisms Associated with Atacama Desert Populations of Giant *Equisetum*

Anchittha Satjarak
Plants of Thailand Research Unit, Department of Botany, Faculty of Science, Chulalongkorn University, Bangkok, Thailand 10330, email: anchittha.s@chula.ac.th

Michael J. Piotrowski
Department of Botany, University of Wisconsin, Madison, WI 53706, USA, email: mpiotrowski5575@gmail.com

Linda E. Graham*
Department of Botany, University of Wisconsin, Madison, WI 53706, USA, email: lkgraham@wisc.edu

Marie T. Trest
Department of Botany, University of Wisconsin, Madison, WI 53706, USA, email: mttrest@wisc.edu

Lee W. Wilcox
Department of Botany, University of Wisconsin, Madison, WI 53706, USA, email: lwwilcox@wisc.edu

Jennifer J. Knack
Department of Biology, University of Minnesota, Duluth, MN 55812, USA, email: jennack3315@gmail.com

Martha E. Cook
School of Biological Sciences, Illinois State University, Normal IL 61790, USA, email: mecook1@lstu.edu

Patricia Arancibia-Avila
Department of Basic Sciences, University of Bío-Bío, Chillan, Chile, email: parancib@ubiobio.cl

Abstract.—Understanding features that fostered the persistence of *Equisetum*–Earth's oldest extant vascular plant genus–since Mesozoic times and through episodes of significant global environmental change, is of current interest in view of modern challenges to plant survival. In addition to known structural and physiological adaptations, we hypothesized that microscopy and shotgun metagenomic sequencing might reveal eukaryotic microorganisms such as fungi that may aid *Equisetum* survival. Here, we report evidence for several lineages of eukaryotic microbes associated with giant *Equisetum xylochaetum*, which dominates vegetation in saline streambeds of remote valleys in the hyper-arid Atacama Desert, Chile. Plant material was collected and field-preserved at two comparatively low-disturbance sites; DNA extracted in Chile using low-shear methods was later sequenced, 18S and 28S rDNA taxonomic marker sequences were selected for SILVAngs classification, allowing comparisons to eukaryotic microorganisms previously inferred for earlier-diverging plant lineages. SEM, fluorescence microscopy, and/or LM of toluidine blue-stained sections of roots indicated protists, epiphytic and endophytic fungi, and cortical nematodes. Eukaryotic genera inferred from 18S rDNA at >100X mean sequencing depth included the ciliate *Engelmanniella*, hyphal chytrid *Monoblepharella*, predatory ascomycete

* corresponding author

Cephaliophora, a salpingoecid choanoflagellate, and an annelid worm. 23S rDNA sequences indicated ascomycete Capnodiales fungi at one site and four types of Pezizomycotina fungi at the other. No evidence for vesicular-arbuscular mycorrhizal fungi was found, but we hypothesized that *Equisetum* may benefit from other types of fungal associations, some possibly inherited from ancestral plant lineages.

KEY WORDS.—horsetails, metagenomic sequencing, scouring rushes, seedless plant microbiomes

The globally widespread genus *Equisetum,* commonly known as "horsetail" or "scouring rush," has been described as the world's oldest and most successful vascular plant genus (Rothwell, 1996). *Equisteum* is the only modern representative of a once-diverse clade of equisetophytes (Class Equisetopsida or Sphenopsida) that originated in the Upper Devonian; the history of genus *Equisetum* extends back to the Mesozoic, indicated by definitive fossil remains of Late Jurassic age (Channing *et al.*, 2011), and possibly the Lower/Middle Triassic (~230 Ma) (Gould, 1968) or even earlier (White, 1894). These dates are consistent with molecular diversification ("timetree" or "molecular clock") analyses indicating a stem age for *Equisetum* of 304.2 Ma (later Carboniferous) (Laenen *et al.*, 2014), and a crown age of 203 Ma (earliest Jurassic) (Clark, Puttick, and Donoghue, 2019). *Equisetum* crown age was estimated at mid-Mesozoic in an analysis that included molecular and fossil data (Elgorriaga *et al.*, 2018).

Structural features shared with the tree-sized (30 m tall) Carboniferous hydrophyte genus *Calamites* (Gifford and Foster, 1989) have been proposed to explain the persistence of genus *Equisetum* over such long geological time periods, and in diverse modern locales (Rothwell, 1996): determinate aerial shoots; production of aerenchyma that fosters growth even in anoxic waterlogged soils; and a persistent, branched, fire- and drought-resistant subterranean rhizome, which produces elongate roots able to access deep water and minerals even when the soil surface is dry. Modern *Equisetum*, which differs from other modern ferns and lycophytes in having a distinctive type of vascular system (Nopun *et al.* 2016), is said to differ structurally from *Calamites* mainly in the absence of secondary xylem (Rothwell and Ash, 2015). Among the modern *Equisetum* species, *E. xylochaetum* Mett., related to, but recently segregated from *E. giganteum* L. (Christenhusz *et al.*, 2019), which forms lush glades in streambeds in Atacama Desert valleys of southern Peru and northern Chile, most closely approaches ancient *Calamites* in size, having stems up to 4.0 cm diameter that reach more than 4 meters in height (Husby, 2013). Experimental field studies have demonstrated that *Equisetum xylochaetum* possesses several physiological adaptations to high salinity conditions associated with arid environment: sodium exclusion and a high degree of homeostasis in stomatal conductance, photosynthesis, and root function over a broad range of groundwater salinities (Husby *et al.*, 2011; 2014). An ancient whole genome duplication (WGD) event was proposed to have helped *Equisetum* to survive the dramatic K-Pg extinction event (Vanneste *et al.*,

2015). Later studies have indicated the occurrence of Carboniferous and Triassic WGD events in the stem lineage, prior to the divergence of modern *Equisetum* beginning in the early Jurassic, raising questions about the role of WGD in long-term lineage survival of Equisetaceae (Clark, Puttick, and Donoghue, 2019).

We hypothesized that in addition to structural, physiological, and possible genomic features, microorganisms might also contribute to *Equisetum* survival under modern stressful conditions such as the hyperarid Atacama Desert, and may also have aided equisetophyte persistence in the remote past. Microorganisms can be transmitted between plant generations and plant microbiomes display evidence of inheritance/evolutionary impacts (*e.g.*, Gehring *et al.*, 2017; Fitzpatrick *et al.* 2018; Walters *et al.* 2018; Yeoh *et al.* 2017). Genetically-determined plant secretions are known to play important roles in establishing and mediating microbiome composition (*e.g.*, Stringlis *et al.*, 2018), indicating a mechanistic explanation for inheritance effects. These findings suggest the possibility that modern *Equisetum* might have inherited the capacity to acquire beneficial microorganisms from ancestral plant populations.

A deep-time perspective of Atacama Desert *Equisetum* microbial associations can be justified by spore evidence for presence of terrestrial plants in northern Chile (Zorritas Formation, Antofagasta Region) since the early Carboniferous (Rubinstein, Petus, and Niemeyer, 2017) and >150 million years of regional geographic stability. Northern Chile has remained at approximately the same latitude since the Late Jurassic (Hartley *et al.*, 2005; Clarke, 2006; Placzek *et al.*, 2014), with relatively moist climate indicated for much of this time and present extreme aridity ensuing in the Holocene (Arroyo *et al.*, 1988). Analysis of organic carbon along aridity gradients in this region has indicated that plant life was likely present in the past in regions that today lack conspicuous vegetation (Knief *et al.*, 2020).

Excepting El Niño-associated rain events (Chávez *et al.*, 2019; Ortega *et al.*, 2019), annual rainfall in the northern Chilean coastal cities of Arica and Iquique is typically 0.5-0.6 mm, the result of subtropical high pressure, cold offshore current, and wind. Very low rates of erosion over long time periods have led to accumulation of usual salts (perchlorates, iodates, and nitrates) in addition to halite and gypsum (Knief *et al.*, 2020; Voight *et al.*, 2020), conditions that also challenge plant growth. Given these extreme environmental conditions, modern Atacama Desert vegetation is sparse; the region has been used as an analog of Mars conditions (*e.g.*, Azua-Bustos *et al.*, 2019). We hypothesized that comparing eukaryotic microorganisms associated with Atacama Desert *Equisetum* with microorganisms previously inferred by similar methods for modern representatives of earlier-diverging plant lineages (Knack *et al.*, 2015; Graham *et al.*, 2017) might indicate microbiome features associated with long-term lineage survival (Graham *et al.*, 2018).

However, at present, the suite of eukaryotic microorganisms associated with *Equisetum* in general, and *E. xylochaetum* in particular, is not well understood. For example, some authorities note that *Equisetum* generally lacks mycorrhizae that would foster nutrient acquisition (Read *et al.*, 2000), but

other studies have provided evidence from microscopy that some species of *Equisetum* harbor vesicular-arbuscular mycorrhizae (VAM) and other fungal associates (Dhilion, 1993; Hodson *et al.*, 2009; Koske *et al.*, 1985). Imaging and metagenomic sequence data have revealed that liverworts and mosses can associate with diverse eukaryotic microbes, including fungi (Knack *et al.*, 2015; Graham *et al.*, 2017). To look for evidence of fungal associations, compare eukaryotic microorganisms among seedless plant lineages, and generally improve knowledge of plant-associated microorganisms, particularly in stressful environments, we employed several microscopy approaches and taxonomic marker genes derived from shotgun metagenomics to survey eukaryotic microorganisms associated with *E. xylochaetum* populations sampled from relatively undisturbed locales in the Atacama Desert, Chile.

Materials and Methods

Source of plant material.—In January 2016, replicate samples of *Equisetum* plants having distinctive stem height and diameter consistent with those described for giant *E. xylochaetum* (Christenhusz *et al.*. 2019) were taken from upper and lower aerial shoots, and rhizomes and/or roots. Plant collections were made from public lands at two sites in the Chilean Atacama Desert by four of the authors (LG, JK, MT, PA-A) for microscopic and metagenomic study. These plant materials were sampled from saline streambeds in deep quebradas (canyons) that occur in the northern part of the Central Depression (Valle Central). The hyper-arid Central Depression lies east of a coastal range of Mesozoic igneous and sedimentary rocks known as the Cordillera de la Costa (Oligocene-Pliocene sediments) and west of the Precordillera (Mesozoic to Eocene) pre-Andean basins of Miocene to Holocene sediments west of the Andes. The collection sites had been employed previously for physiological studies of the same species of *Equisetum* by Husby *et al.* (2011; 2014), who reported some environmental metadata. Soil features, including soil bacterial abundance and diversity, have been reported in some detail for a nearby area of the Atacama (Knief *et al.*, 2020). Geo-reference and other site information related to the current report are provided in Appendix 1.

Plant collectors visited five of the same Atacama locales described by Husby *et al.*, (2011), judging that the two sites for which data are reported here–Huasquiña (also spelled Guasquiña) (HUA) and Chiza (CHI) (names referencing nearby villages)–were the least-disturbed by human activities. These locales are mapped in Husby *et al.*, (2011). In 2016, the particularly remote HUA locale seemed the least-disturbed; although ancient remains of agricultural terraces were present, modern human agriculture was not practiced near the sampled area. The CHI collection site was located approximately 100 meters from Chile Highway 5, but agricultural fields were not observed in the near vicinity. High water tables (0.5 m or less) were previously described for these two locales (Husby *et al.*, 2011), but during our 2016 excavations up to a 1-meter depth, we did not encounter groundwater at

these sites, only moist soil, possibly reflecting annual or seasonal climate variability.

Collectors used new nitrile gloves and implements to reduce the potential for sample contamination. Three technical replicates each from upper and lower stems, rhizomes, and roots, plus one sample of internal tissue at a joint, were represented in collections from HUA from which DNA was subsequently sequenced. By contrast, CHI collections sampled for DNA sequencing included three technical replicates each of upper and lower stems and roots, because rhizomes were not encountered during excavation to a 1-meter depth. We note that underground rhizomes and roots of *Equisetum* are structurally-distinctive (Gifford and Foster, 1989) and therefore easily distinguished from those of co-occurring angiosperms. Although *E. xylochaetum* collections were made from both sites as voucher specimens, the brittle materials were fragmented by compression during transport, so were not appropriate for formal herbarium archiving; these fragmented specimens were stored in author P. A.-A.'s lab at the University of Bio-Bio, Chillan, Chile.

Imaging.—Preliminary microscopic examinations of fresh materials were conducted in the field using a Zeiss Primo Star compound microscope equipped with sub-stage illumination and adaptors for international current (B&H Photo Video, NY, NY). This microscopic examination helped to ensure that plant samples were as free as possible from soil or other loosely-adherent materials. To enable further microscopic imaging after transport to the US, representative plant samples were fixed immediately after collection in 2% glutaraldehyde that was freshly prepared in the field from 70% EM-grade glutaraldehyde (Ted Pella, Inc. Redding, CA, USA). To prepare fresh glutaraldehyde solution just prior to use, 6.8 ml of 0.1M pH 7 phosphate buffer was used to dilute 0.2 ml of 70% glutaraldehyde that had been stored free of air in a 5ml syringe, which was wrapped with Parafilm and double-bagged in plastic to retard leakage or air entry during transport. Fixed plant materials were washed three times in phosphate buffer prior to transport in phosphate buffer; USDA APHIS determined that such materials were not under jurisdiction. No living materials were transported from Chile.

Glutaraldehyde-fixed/buffer-washed roots sampled from CHI were first hand-sectioned for light microscopic examination. Because structures large enough to be eukaryotes were observed within roots, other root samples were further processed for light microscopy and for SEM. Some hand-sections were viewed with use of a Zeiss Axioplan epifluorescence microscope equipped with UV filter G365 FT395 LP420 for assessment of Calcofluor White staining specific for chitin (or cellulose). For microtome-sectioning, a glutaraldehyde-fixed root was dehydrated in an ethanol series, then embedded in LR White resin, hard grade (Ted Pella, Inc., Redding, CA). Following polymerization at 50°C, sections of ~250 nm-thickness were cut using an MT2B Sorvall ultramicrotome and a DuPont diamond knife with water-filled boat, and sections were transferred from the water surface to glass slides using a hand-made wire loop, which was cleaned in 95% EtOH after each use. After low-level heating on a hot plate to evaporate water and adhere microtome-cut

sections to slides, an aqueous solution of 1% toluidine blue + 1% sodium borate was used to stain sections for a short time at low heat. Toluidine blue has been recommended for observation of the hyphae of arbuscular mycorrhizal fungi in embedded plant root tissues (Hulse, 2018), has also been employed to study ectomycorrhizae (Ragonezi and Zavattieri, 2018), and is a recognized method for visualizing root-infecting nematodes (Zhang *et al.*, 2017). Stained slides were rinsed with distilled water to remove excess stain, then returned to low heat to dry, after which Permount (Thermo Fisher Scientific, Waltham, MA) was employed to make permanent preparations. Light microscopic images were recorded using a Nikon D300s digital camera and Camera Control Pro software (Nikon, Melville, NY, USA) or an Olympus BX50 compound microscope equipped with Nikon D810 camera.

For SEM, roots that had been glutaraldehyde-fixed and buffer-washed in the field were hand-sectioned with a razor blade before dehydration in an ethanol series, then critical point dried and coated with iridium prior to examination with a Hitachi S-4800 ultra-high-resolution cold cathode field emission SEM operated at 5 kV.

DNA processing.—Plant samples taken aseptically for metagenomic analyses were stored immediately after field collection in 90% ethanol (EtOH) in sterile conical tubes. Sealing screw caps with a strip of Parafilm (Bemis, Inc. Neenah, WI, USA) proved essential to preventing ethanol evaporation during transport. After 4-8 days of transport in the field, samples for DNA extraction were further processed. Samples were carefully washed to remove EtOH, soil, and any other loosely-associated materials by swirling in three changes of sterile water in sterile petri dishes, before transfer to bead beater tubes. No conspicuous parts of other plants were observed. To improve the proportion of microbial DNA to host plant DNA and to reduce DNA shearing, we did not employ grinding. The goal of reducing shearing was to obtain longer segments of native DNA to reduce the likelihood of artifact sequence formation during downstream contig assembly. These processing methods mirrored those we had earlier used to prepare field-sampled species representing earlier-diverging seedless plant lineages in our previous metagenomic studies (Knack *et al.*, 2015; Graham *et al.*, 2017). For the current study of *E. xylochaetum*, we deliberately employed similar cleaning, sequencing, and analytic methods to facilitate between-lineage comparisons.

To reduce the potential for introduction of exogenous microbes, transfers of plant materials were accomplished using forceps that were dipped into 95% EtOH and then flamed, by operators using new nitrile gloves. DNA extraction was done using the MoBio PowerSoil kit (Qiagen, Hilden, Germany) employing a modified lysis procedure designed to reduce DNA shearing, as suggested by Qiagen technical personnel: samples were vortexed for only a few seconds prior to heating at 70°C for 5 min, a process that was then repeated. Extracted DNA was transported to the US in freezer tubes at ambient temperature, a procedure determined by USDA APHIS not to be under jurisdiction, then kept frozen at -80° F for a few days prior to delivery to the University of Wisconsin-Madison Biotechnology Center for quantification and

sequencing. DNA quantification data indicated that 13 samples obtained from site HUA should be pooled, as were 9 samples from locale CHI. DNA quantities for individual technical replicates were insufficient for finer scale partitioning among plant parts. More than 52 Gb of shotgun metagenomic sequence was obtained using the Illumina HiSeq 2500 platform.

Bioinformatic processing.—Raw reads were trimmed using Trimmomatic version 0.39 (Bolger, Lohse, and Usadel, 2014). MEGAHIT version 1.2.6, designed for handling large, complex metagenomics data sets (Li *et al.* 2015), was employed for assembling contigs from raw sequences. The assembler used paired reads to detect and resolve chimeric contigs produced from misassembly (Ayling, Clark, and Leggett, 2020). Assembly statistics and chimera detection information are provided in Appendix 2. The SILVAngs 1.3 portal was employed to classify contigs containing 18S rDNA and 28S rDNA sequences because eukaryotic microbes are particularly well-represented in the reference databases (Quast *et al.*, 2013), and because this classifier had been employed in our earlier metagenomic analyses of eukaryotic microbes associated with seedless plants (Knack *et al.*, 2015; Graham *et al.*, 2017). UCHIME (ver. 4.2.40; Edgar *et al.* 2011), implemented in Geneious version 9.1.3 (https://www.geneious.com) was used to filter out chimeric contigs (see Appendix 2). Contigs containing annotated 18S rDNA and 28S rDNA sequences were compared against the SSU and LSU SILVA database (Quast *et al.*, 2013) using default parameters: minimum score to report chimera = 0.3, minimum divergence ratio = 0.5, weight of a no vote = 8, pseudo-count prior on number of no votes = 1.4, weight of an abstain vote = 1, number of chunks to extract from the query sequence when searching for parents = 4, minimum length of a chunk = 64 bp, maximum number of candidate parents to consider = 2, minimum unaligned sequence length = 10, maximum unaligned sequence length = 10,000, the length of id smoothing window = 32, global alignment.

Contigs were taxonomically processed using the SILVA incremental aligner (SINA SINA version 1.2.10 for ARB SVN, revision 21008; Pruesse, Peplies, and Glöckner, 2012) applied against the SILVA small subunit (SSU) and large subunit (LSU) rRNA SEED and quality controlled (Quast *et al.*, 2013). Reads shorter than 50 aligned bases and those with 12% ambiguities or homopolymers were excluded before further processing, as were likely contaminants and artifacts and those having low alignment quality scores. Identical reads were identified and unique reads clustered using cd-hit-est software (ver. 3.1.2; Li and Godzik, 2006) running in accurate mode, ignoring overhangs, and applying identity criteria of 1.00 and 0.98 as operational taxonomic units (OTUs) for classification performed by local nucleotide BLAST search against the non-redundant version of the SILVA SSU and LSU reference data sets (release 132), using blastn, version 2.2.30+, with standard settings (Camacho *et al.*, 2009). Classification of each OTU reference read was mapped onto all reads assigned to the respective OTU. Reads for which there were no or weak (% sequence identity + % alignment coverage)/2 = <93) BLAST hits remained unclassified and were labeled “no relative” in SILVAngs fingerprint and Krona charts (Ondov, Bergman, and Phillippy, 2011). These

methods were initially used by Klindworth *et al.*, (2013) and Ionescu *et al.*, (2012). The above paragraph has been paraphrased from SILVAngs project reports, as recommended in those reports. Quality and settings information can be found in Appendix 3.

Genomic coverage was estimated for most of the classified eukaryotic taxa as a means of gaining some insight into relative abundance. Because the sequence data were obtained by shotgun metagenomic methods, amplification bias was not an issue, as can be the case when input sequences are amplicons. However, we note that for eukaryotes, sequencing depth levels may be influenced by multicellularity or genomic duplication history, and do not represent accurate quantitative assessment of microbial population levels.

For calculation of genomic coverage, trimmed raw reads were aligned to SILVA references using BWA version 0.7.4 non-model species alignment (Li and Durbin, 2009). Mapped reads were filtered and converted to fastq format using SAMtools version 1.7 and BEDtools version 2.26.0 (Quinlan and Hall, 2010). Reads were then mapped to their corresponding SILVA reference sequence using Geneious version 9.1.3 (https://www.geneious.com). Mean and maximum coverage were calculated using the Geneious function "statistics." We employed coverage for the gene region of greatest abundance, indicated by use of the CyVerse Discovery Environment (https://de.cyverse.org/de/). Taxa inferred from 18S or 28S rDNA sequences at a mean coverage level ≥10X were considered to have been detected, and were employed for evolutionary comparisons. Taxa inferred at a mean coverage level ≥50X were considered relatively abundant. Because assembler pipelines change with time and investigators may have reasons for choosing particular assemblers, to facilitate use by others, we have archived raw, rather than assembled, metagenomic sequence in the NCBI Short Read Archive (http://www.ncbi.nlm.nih.gov/sra) as BioProject PRJNA555713. Sequence data for the HUA site are in accession SAMN12326833, and sequence data for the CHI site are in accession SAMN15794710.

Because this report focuses on eukaryotic microbial associates, *E. xylochaetum*-associated prokaryotic microorganisms and their genes and most sequences related to the host plant genome, which are present in the metagenome, are not described here. However, plastid marker sequences *rbcL*, *rps4*, and *trnL-F*, previously employed to explore species relationships within extant *Equisetum* species (Christenhusz *et al.*, 2019) were extracted from metagenomic data for use in corroborating our identification of the host plant as *E. xylochaetum* based on distinctive structural traits.

Phylogenetic analysis.—Reference *Equisetum* plastid sequences were obtained from GenBank, accessed in July, 2020. *Equisetum bogotense* isolates 40800, 40801, 40802, and 40827 were used as an outgroup cluster, as this species was previously known to represent the earliest-diverging of the modern species (Christenhusz *et al.*, 2019). Nucleotide sequences were aligned using MAFFT v7.402 (Katoh et al. 2013) and the substitution model computed using ModelTest-NG v0.1.5 (Darriba et al. 2020). Maximum likelihood (ML) analysis was performed using RAxML v8.2.12 (Stamatakis 2014) on the XCEDE

Portal for CIPRES (Miller, Pfeiffer, and Schwartz, 2010) using GTR+I+G substitution model. Bayesian analysis were performed with MrBayes v3.2.6 (Ronquist and Huelsenbeck 2003). Four independent chains were run for 100,000 cycles and consensus topologies calculated after 25,000 burn-in cycles.

Results

Microscopy.—LM observations of glutaraldehyde-fixed roots sampled from the Chiza (CHI) site revealed evidence for eukaryote-sized structures on the surfaces of roots and root hairs, and within root cortex cells. Hyaline branched-filaments having diameters <10 μm, which were observed by LM on and within cross-sectioned root cells in which amyloplasts were also visible (Fig. 1a), and which fluoresced blue-white in UV excitation after Calcofluor White staining (and did not display red autofluorescence typical of chlorophyll) (data not shown) were interpreted as fungal hyphae. Thin filaments having similar features present on or within root hairs were also interpreted as fungal hyphae. Septa were sometimes visible in putative hyphae of Calcofluor White-stained material. Darkly-pigmented septate hyphae (commonly known as "dark septate hyphae") were not observed by microscopic examination in the field or lab. Cortical cells of some portions of microtome-sectioned, toluidine blue-stained roots contained larger diameter structures consistent with putative identification as nematodes; such profiles sometimes traversed root cell walls (Fig. 1b). The surfaces of putative nematodes exhibited fine cuticular annulations when viewed at high magnification (Fig. 1c). *Equisetum* root cortical cells that contained nematode-like structures and nearby cells were devoid of cytoplasmic contents such as amyloplasts (Fig. 1b,c).

SEM examination of hand-cut cross sections revealed evidence that microbes of dimensions consistent with classification as prokaryotes and/or eukaryotes were present on outer surfaces of root epidermal cells and contorted root hairs (Fig. 2 a-d). Some of the epimicroorganisms displayed sizes and shapes consistent with unicellular protists (Fig. 2c) and fungi having branched hyphae and specialized cells (Fig. 2d). Higher magnification SEM views revealed the presence of structures consistent with identification as fungal hyphae within root cortical cells, including cells containing rounded structures interpreted as amyloplasts (Fig. 3a). Some of the root cortical cells containing fungal hyphae-like structures lacked structures interpreted as amyloplasts (Fig. 3b). No microscopic evidence for vesicular-arbuscular mycorrhizal fungi was observed for either of the sampled locales.

Sequence-based eukaryotic classifications.—Metagenomic evidence included relatively high coverage of host *Equisetum* 18S rDNA at the lowest-disturbance site, Huasquiña (HUA). Host plant 18S rDNA was likewise confirmed for Chiza (CHI). Phylogenetic analysis employing multiple plastid marker genes indicated that the host plant was *E. xylochaetum* (Fig. 4). At both sites, 18S rDNA sequences were classified as Poales angiosperms: *Juncus* at HUA; *Echinochloa* and *Setaria* at CHI. Eukaryotic taxa whose 18S rDNA

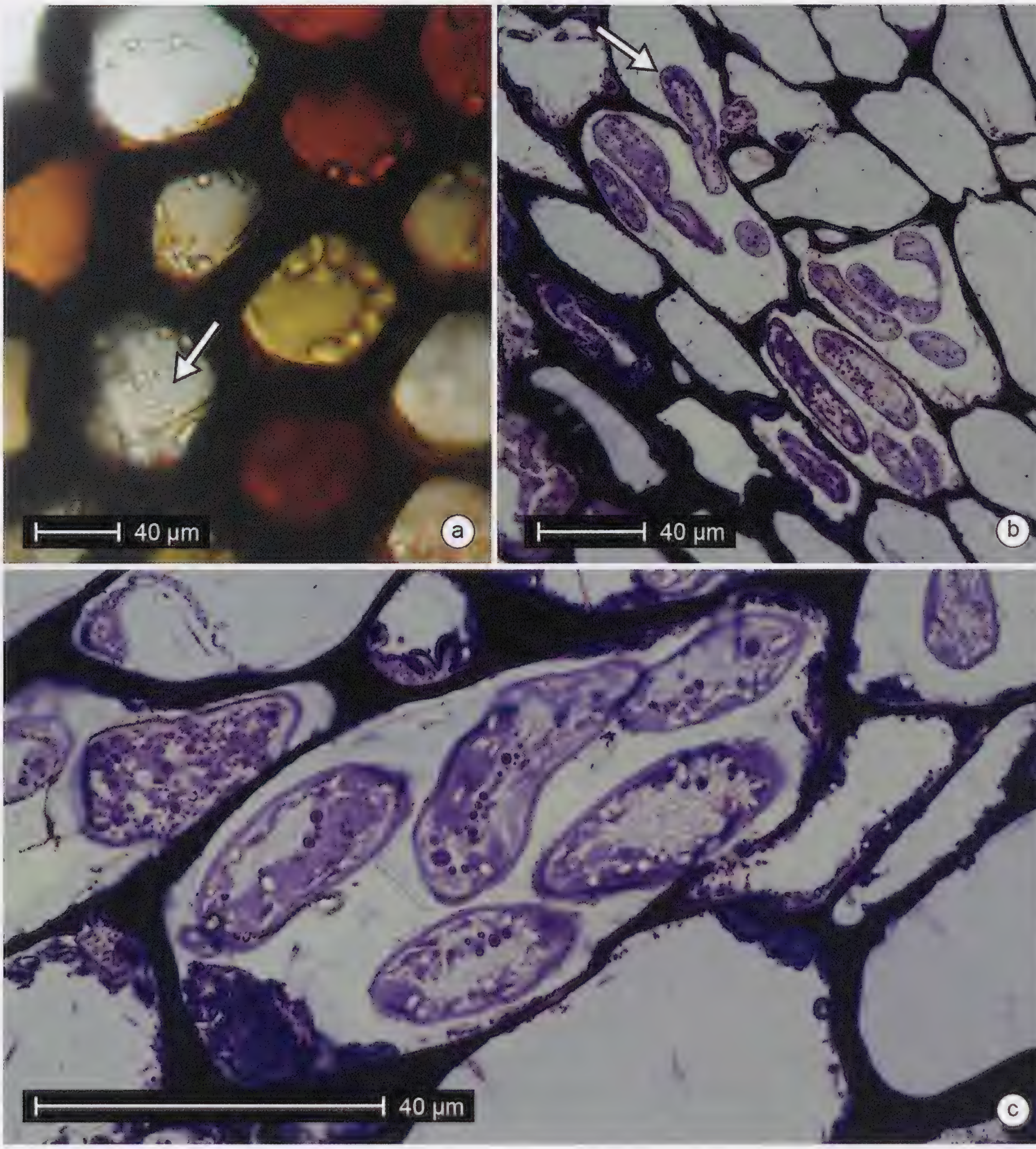

FIG. 1. LIGHT MICROSCOPY. Sections showing eukaryotic microbial associates of *E. xylochaetum* root sampled from the Chiza (CHI) site. **(a)** Hand-cut section showing hyaline branched filaments interpreted as fungal hyphae within root cortical cells (arrow), whose walls are thick and darkly-pigmented. **(b)** Toluidine blue-stained thick section made with microtome and diamond knife. Structures interpreted as profiles of nematodes are located within cortical cells and in apparent transit between cortical cells (arrow). **(c)** Enlarged view of a root cortical cell containing structures interpreted as profiles of nematodes whose surfaces bear fine annulations. Such cortical cells in root regions infected by putative nematodes lack cytoplasmic features such as amyloplasts that occur in un-infected root regions.

sequences were present in mean coverage levels ≥100X at HUA and CHI are summarized with mean and maximum coverage levels in Table 1. At site CHI no eukaryotic taxa were inferred from 18S or 28S rDNA at mean sequencing depths ≥100X, except the host plant *Equisetum* (mean sequencing depth =

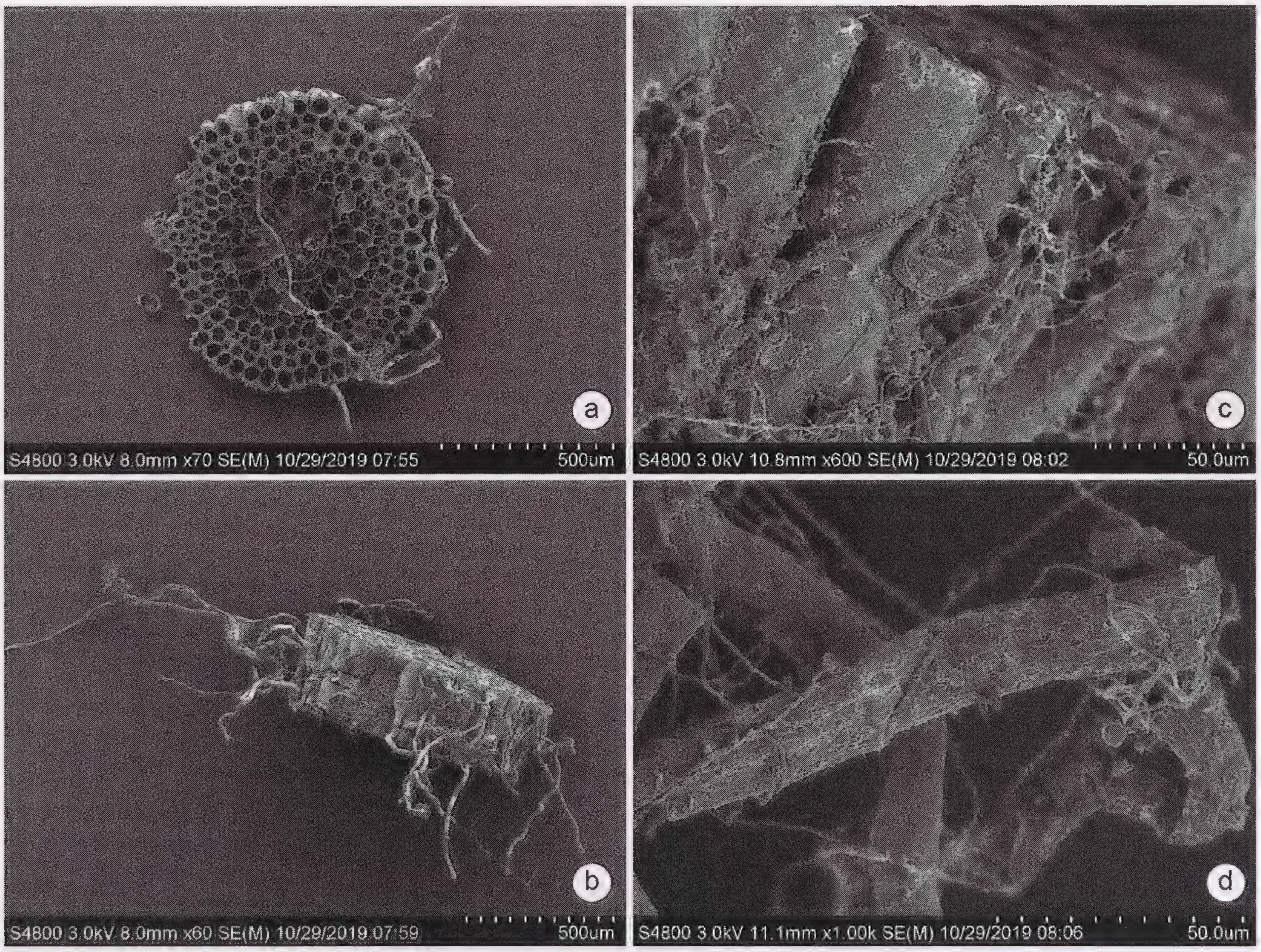

FIG. 2. SCANNING ELECTRON MICROSCOPY. **(a)** Top-view of a hand-cut section of an *E. xylochaetum* root, showing central stele of relatively thin-walled cells, cortex cells having thicker cells, scalloped outer root surface, and emergence of contorted root hairs from root epidermal cells. **(b)** Side-view of the same hand-cut section of an *E. xylochaetum* root showing scalloped root surface and emergence of contorted root hairs from epidermal cells. **(c)** Magnified side-view of root showing an attached biofilm of structures interpreted as eukaryotic and prokaryotic epibionts. The flattened spherical object at center was interpreted as a possible unicellular protist. Narrow threads are of sizes consistent with fungal hyphae and filamentous bacteria. (d) Magnified view of contorted root hairs, showing associated structures interpreted as eukaryotic and prokaryotic microorganisms. A branched filament at the right side was interpreted as fungal hyphae.

1184X, maximum depth = 2420X). 28S rDNA sequences classified as (Pezizomycotina) Capnodiales ascomycete fungi were noted from CHI, but not detected by 18S rDNA.

At site HUA, four types of Pezizomycotina fungi were indicated by 28S rDNA; one of these, classified as Pezizales, had a mean sequence coverage of 146X (maximum 2181X). An HUA Pezizales ascomycete classified as *Cephaliophora* was detected by 18S rDNA signal (212X mean coverage, 1304 maximum coverage). At HUA, 18S rDNA also indicated presence of the chytrid *Monoblepharella* (mean 270X, max 2235X coverage). No sequence evidence for the presence of arbuscular mycorrhizal fungi was found at either site.

At HUA, additional types of microbial eukaryotes were indicated by 18S rDNA sequence data. A salpingoecid choanoflagellate protist was inferred by mean of 291X and maximum 2297X sequence coverage. A haplotaxid annelid

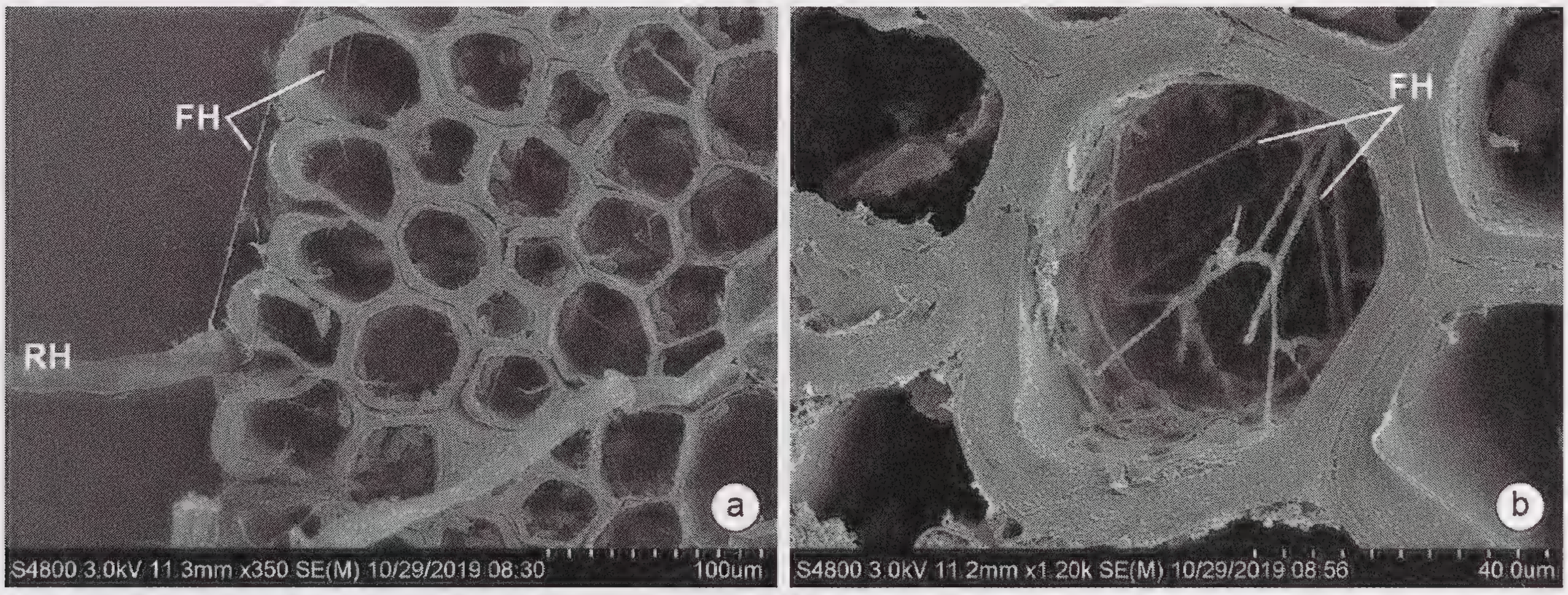

FIG. 3. SCANNING ELECTRON MICROSCOPY. **(a)** A higher magnification view of part of the root section shown in Fig. 2a, showing root hairs (RH) and thin filaments interpreted as epiphytic and endophytic fungal hyphae (FH). Inner cortical cells contain rounded structures interpreted as amyloplasts. No evidence for nematode infection was observed in this root section. **(b)** A root cortical cell containing thin, branching filaments interpreted as fungal hyphae (FH). At this magnification, root cortical cell wall layering is apparent.

microanimal was inferred at mean 121X, maximum 1031X. The unicellular hypotrich ciliate *Engelmanniella* was inferred at a mean 191X, maximum 1397X sequence coverage. A thaumatomonad rhizarian protist was also inferred to occur at HUA in high sequence coverage (mean 136X, maximum 2145X).

Krona analysis of SSU (16S rDNA + 18S rDNA) sequences filtered from the metagenomic data for site HUA indicated that 51% of SSU sequences were not classifiable based on the current content of taxonomic databases, and that bacterial sequences represented a higher proportion of classifiable sequences than did eukaryotic sequences (Fig. 5). Similar Krona analysis for site CHI likewise indicated dominance by bacterial taxa, with 26% of sequences not classifiable on the basis of current taxonomic databases; among eukaryotes, only vascular plants were indicated (analysis not visualized).

DISCUSSION

Overview.—Phylogenetic analysis of multiple plastid marker genes previously employed to study *Equisetum* species diversification (Christenhusz *et al.*, 2019) was consistent with structural information indicating that the host plant was *E. xylochaetum*. Microscopy and molecular data were consistent in indicating the close association of eukaryotic microorganisms, including fungi, with *E. xylochaetum* sampled from two relatively undisturbed Atacama Desert sites. The 28S rDNA marker revealed aspects of eukaryotic diversity not apparent from the 18S rDNA data alone, indicating the value of employing more than one taxonomic marker. Although replicate DNA samples were taken from multiple plant parts, to achieve DNA levels needed for shotgun sequencing, DNA from replicates and

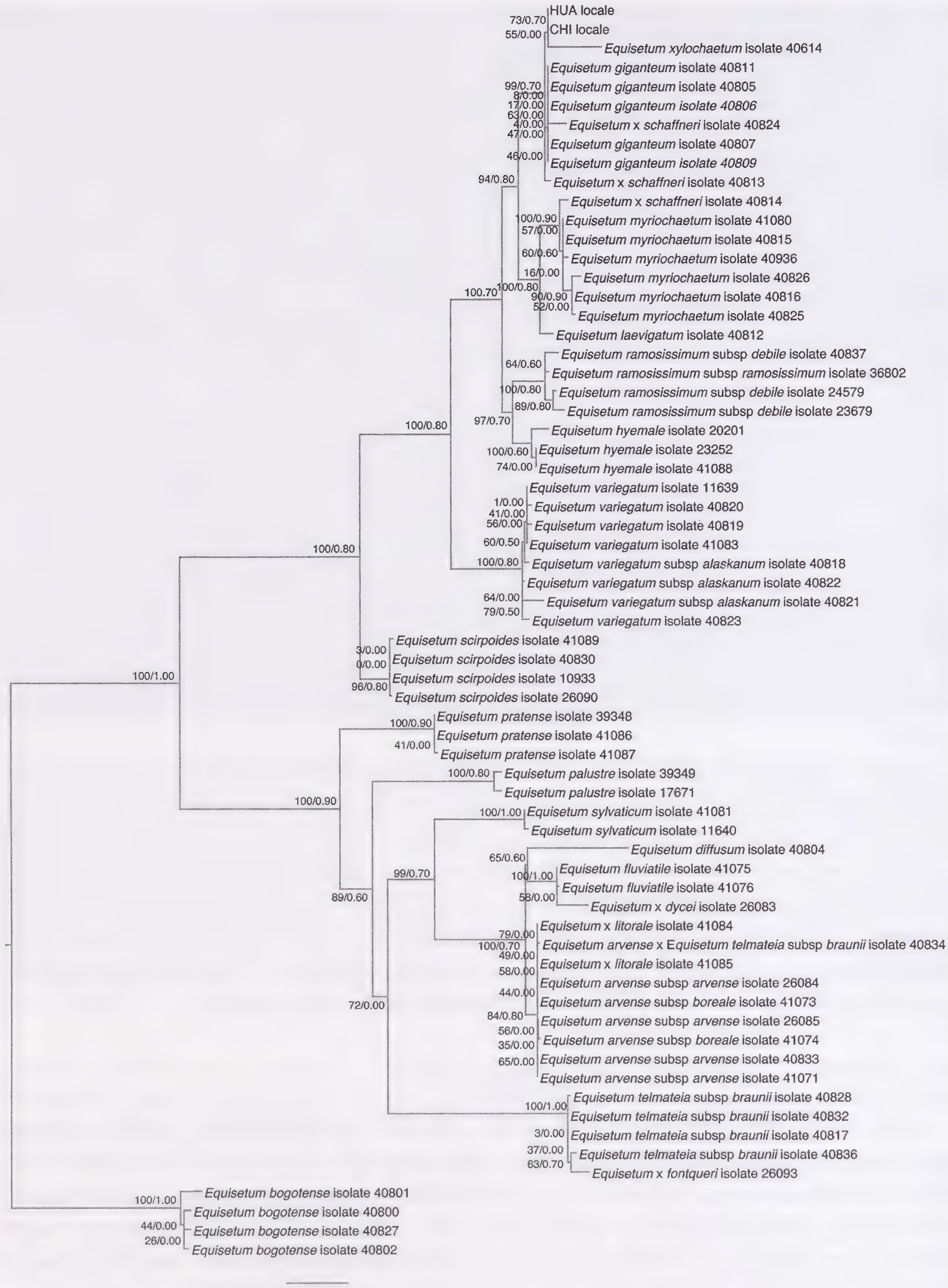

FIG. 4. HOST PHYLOGENETIC RELATIONSHIPS. Phylogenetic relationships of *Equisetum* sampled from the HUA and CHI locales, based on multiple plastid marker genes. Maximum likelihood/Bayesian values indicate that the sampled plants are more closely related to reference *E. xylochaetum* isolate 40614 than to other databased *Equisetum* sequences, a result consistent with distinctive structural features.

TABLE 1. Eukaryotic taxa inferred from 18S rDNA sequence at >100X mean sequencing depth from *Equisetum xylochaetum* sampled at the HUA and CHI sites.

Taxa at HUA	**Informal name; phylum**	**Mean sequencing depth**	**Maximum sequencing depth**
Equisetum	giant horsetail plant; Monilophyta	1021X	2402X
Juncus	rush plant; Anthophyta	1651X	2498X
Engelmanniella	hypotrich ciliate protist; Ciliophora	191X	1397X
Monoblepharella	hyphal chytrid; Chytridiomycota (Spatafora *et al.*, 2016) or Monoblepharomycota (Tedersoo *et al.*, 2018)	270X	2235X
Cephaliophora	Ascomycota	212X	1304X
Salpingoecidae	choanoflagellate protist; Choanoflagellata	391X	2297X
Haplotaxida	haplotaxid worm; Annelida	121X	1031X
Taxa at CHI			
Equisetum	Giant horsetail plant; Monilophyta	1184X	2429X

plant parts had to be pooled, thereby precluding statistical comparisons or efforts to localize microbes on plants. The proportions of sequence contigs that could not be classified based on the information content of current taxonomic databases indicate high potential for future discovery of microorganisms new to science. Comparisons of eukaryotic microbial components of *E. xylochaetum* microbiomes to those inferred in our previous, similarly-conducted metagenomic studies of modern representatives of earlier-diverging, non-vascular plant lineages revealed some commonalities of evolutionary interest.

Locale comparison.—Relatively-abundant 18S rDNA sequence classified as *Equisetum* was obtained for both sampling sites. Sequences indicating co-occurring Juncaceae were likewise consistent with observations of such plants at the sampled locales, though *E. xylochaetum* was judged to dominate the vegetation. Although the sequencing depth of 18S rDNA we report for the host was similar to that of 18S rDNA signal for co-occurring flowering plants (Juncaceae), this is not evidence that the microbiome information obtained in this study might apply to plants other than *E. xylochaetum*. No visible parts of plants other than *E. xylochaetum* were included in microscopically-examined and well-washed samples subjected to DNA sequencing, but it is possible that small amounts of pollen or small seeds from co-occurring angiosperm species might have been attached to surfaces of sequenced *Equisetum*. We had purposefully not employed grinding during DNA extraction, to avoid flooding metagenomic DNA with that from the large host plant, and to reduce DNA shearing, to obtain longer pieces of native DNA to reduce potential impacts of artifact formation during contig assembly. This lack of grinding constrained the sequencing depth of 18S rDNA for the host plant, explaining why the mean sequencing depth inferred for the *E. xylochaetum* host was not noticeably larger than those of sequences indicating co-occurring flowering plants likely represented by microscopic pieces. Despite the advantages of not grinding, it is

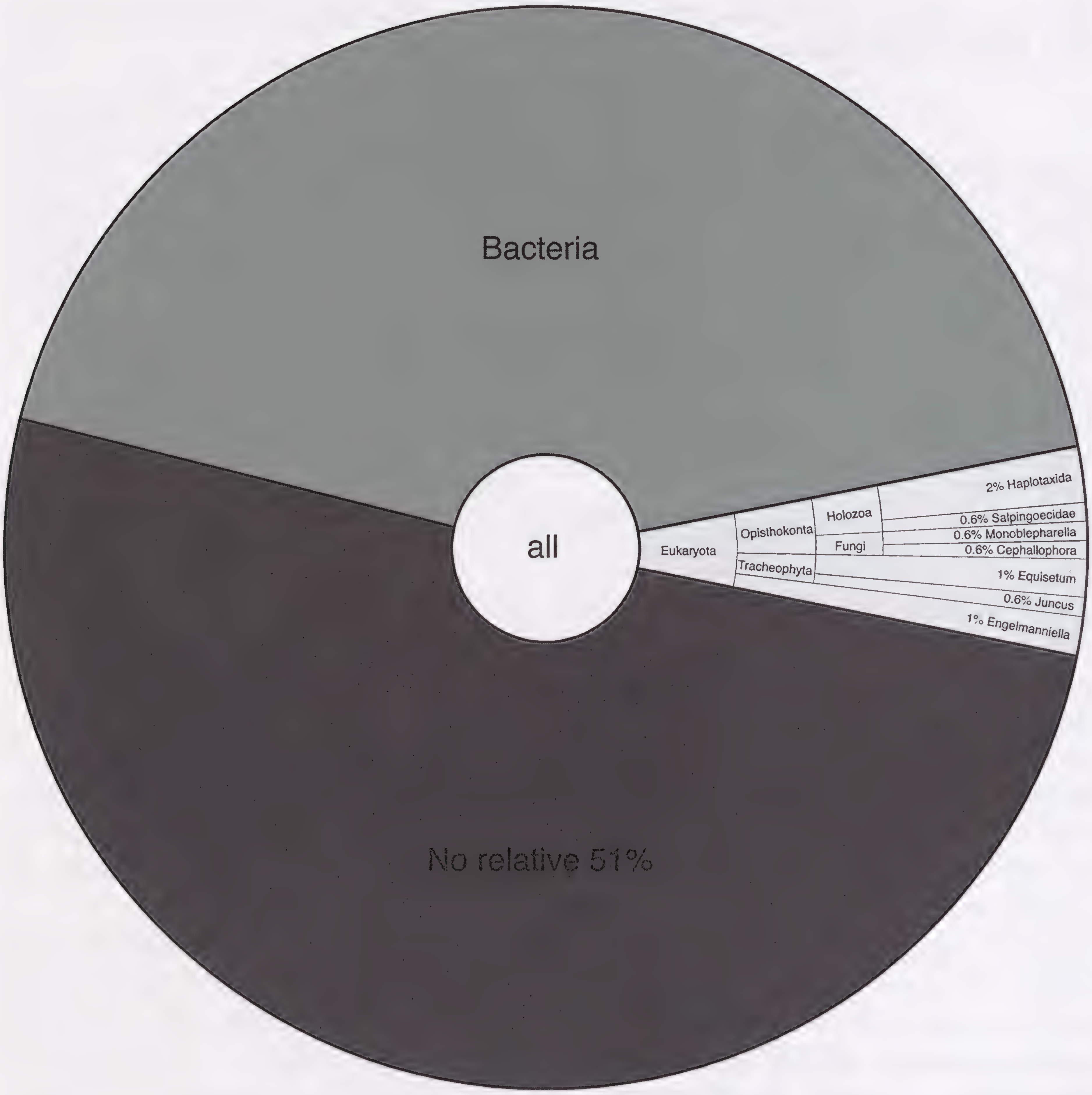

FIG. 5. SILVANGS KRONA ANALYSIS. Pie chart showing relative proportions of metagenomic contigs classified as Eukaryota, Bacteria, and No Relative. About 6% of sequences classified as the host plant *Equisetum*, a co-occurring angiosperm (*Juncus*), the protist *Engelmanniella*, fungi, or microanimals. The large percentage of sequences not classifiable based on the current content of taxonomic databases suggests high potential for discovery of microorganisms new to science.

possible that grinding might have increased the chances of obtaining DNA sequence for endophytic taxa.

Relatively abundant 18S rDNA evidence at the HUA site for the hypotrich ciliate *Engelmannia* was consistent with relatively abundant HUA 28S rDNA indicating a hypotrich ciliate, but neither marker detected ciliates at CHI. Relatively abundant 28S rDNA also indicated the presence at HUA of a thaumatomonad rhizarian not detected at CHI, and relatively-abundant 18S rDNA indicated presence at HUA but not at CHI of a salpingoecid choanoflagellate–member of a bacterivorous opisthokont lineage closely

related to animal ancestry. Although these observations might suggest that the microorganisms associated with *E. xylochaetum* at the HUA site were richer in protist diversity than at CHI, the difference might have resulted from lack of rhizome samples for CHI.

Sequence evidence from both sites for fungal associates of *E. xylochaetum* was consistent with evidence from microscopy studies of samples from CHI by indicating the likely importance of fungi. Immediate field-processing of samples for later shotgun metagenomic DNA sequencing and microscopy, followed by longer-term freezer storage of extracted DNA and refrigerator storage of glutaraldehyde-fixed/buffer washed samples for microscopy, reduced the potential for later contamination with exogenous fungi. Sequence and microscopy data were consistent in indicating the presence of narrow fungal filaments, but not arbuscular mycorrhizal fungi (AMF), whose hyphae are often relatively wide and may bear distinctive large spores. Because our sampling was necessarily limited in scope, it is theoretically possible that AMF were present, but our collections missed them. If AMF were absent, a number of possible causal factors might be invoked.

Such factors include the typical presence in *Equisetum* tissues of high silica content, which has been hypothesized to retard fungal invasion (Guerriero *et al.*, 2018). *Equisetum* species are also known to produce alkaloids such as nicotine that might influence microbial associations; *E. giganteum* (closely related to *E. xylochaetum*) produces some alkaloids, such as palustridiene, that are not present in all *Equisetum* species (Tipke *et al.*, 2019). Extreme environmental conditions peculiar to the Atacama Desert might also be involved.

Another possible factor is the moist stream-bed environments from which we sampled Atacama *Equisetum*. A meta-analysis of 34 studies of the occurrence of arbuscular mycorrhizal fungi (AMF) in the roots of wetland plants worldwide concluded that though AMF colonization was widespread, the level of colonization was relatively low, particularly in lakes and streams, possibly reflecting locale-specific features (Fusconi and Mucciarelli, 2018). High salinity is an ecological feature that could in theory influence AMF colonization, because high salinity conditions were documented for the particular streambed populations of *E. xylochaetum* (Husby *et al.*, 2011) that we sampled some years later. However, a recent molecular sequence analysis of the effects of salinity on soil microbial communities (in China) indicated that glomalean fungi were present up to the highest level surveyed (>4 grams per kilogram), though species shifts were noted (Zhang *et al.*, 2019). While some evidence for presence of AMF fungi was observed in association with subsurface parts of *Equisetum* sampled from Canadian locales, other types of fungi were considered to be more abundant (Hodson *et al.*, 2009), raising the possibility that *Equisetum* may employ beneficial fungal associates in addition to AMF.

Experimental studies have indicated that ascomycete (*Pezoloma ericae*, Helotiales, Pezizomycotina) associations similar to those of ericoid flowering plants occur in leafy liverworts; radiolabeled phosphorus was used to

demonstrate provision of P by fungi to the plants, and radiolabeled carbon to demonstrate movement of plant photosynthate to fungi (Kowal *et al.*, 2018). Helotiales were among diverse ascomycetes we had earlier inferred from 18S and 28S rDNA sequences (derived from metagenomic data) to associate with the thalloid liverwort *Conocephalum conicum* (Knack *et al.*, 2015). Although Helotiales fungi were not identified using similar methods in our samples of Atacama *E. xylochaetum*, several other Pezizomycotina orders (Pezizales, Glomerellales, Sordiariales, Capnodiales) were inferred. Pezizales includes ectomycorrhizal representatives (Tedersoo *et al.*, 2006; Nouhra *et al.*, 2013). These observations raise the possibility that some of the Pezizomycotina inferred in the current analysis to occur in the eukaryotic microorganisms associated with *E. xylochaetum* might provide similar nutrient provisioning functions that might be explored in future studies.

Atacama Desert populations of *E. xylochaetum* might also benefit by partnering with predatory ascomycete fungi to reduce root nematode infestation. We found abundant sequence evidence (18S rDNA mean sequence depth = 212X, maximum 1304X) for the ascomycete *Cephaliophora*, whose narrow hyphae can produce adhesive pegs that attract rotifers and tardigrades within which hyphae ramify (Barron, Morikawa, and Saikawa, 1990), or wind around nematodes (Tubaki, 1956). Our microscopic evidence for the presence in *Equisetum* roots of nematode-like structures (at the CHI locale) demonstrates that root nematode infestation can be an issue for Atacama Desert *Equisetum* populations. The fossil record suggests that plant parasitic nematodes were present prior to the origin of roots; today several clades of nematodes parasitize parts of diverse vascular plants (Smant, Helder, and Goverse, 2018). Leaf-infecting nematodes are known for ferns and lycophytes (*e.g.*, Wu *et al.*, 2016), though we did not locate any previous reports of nematode attack of *Equisetum* roots. Nematode feeding involves the secretion of plant cell wall-degrading enzymes, possibly explaining cell wall breaches and evidence for cell-to-cell nematode movement we detected in Atacama *E. xylochaetum* roots, using microscopy. Our microscopy-based evidence that nematode-infected *Equisetum* roots are devoid of cellular contents (*e.g.*, amyloplasts) generally present in non-infected roots suggests that nematodes were ingesting root cell contents; we did not observe evidence in *E. xylochaetum* for the formation of root cell syncytia, such as were described from toluidine blue-stained microtome sections of nematode-infected angiosperm roots by Zhang *et al.*, (2017). Given the possibility that *Equisetum*-like plants have occupied northern Chile over geological time periods, including the transition from mesic to xeric environmental conditions, nematode attack might have selected for partnerships involving nematode-feeding ascomycete fungi such as *Cephaliophora*.

Although we detected substantial 18S rDNA sequence evidence for the presence of a haplotaxid annelid at the HUA site, sequences classified as nematodes were not found in our Atacama data. Microscopic examination of multiple sections of roots sampled from CHI suggested that nematodes were

localized, because evidence of these microanimals or their feeding (*e.g.*, cortical cell wall damage, absence of amyloplasts) was not always present. It is likely that by chance, none of the technical replicate samples we employed for sequencing included nematode-infected tissues. Alternatively, our purposeful lack of grinding to reduce host DNA input and increase read length to reduce potential assembly artifact, might also have reduced the chances of finding sequence evidence for nematodes and other types of intracellular eukaryotic microorganisms.

Comparisons to eukaryotic microorganisms associated with representatives of other seedless plant lineages.—Our previous metagenomic and microscopy studies of *Conocephalum conicum* (sampled from rock surfaces to reduce input from soil) and the peat moss *Sphagnum fimbriatum* (sampled from Chilean Patagonia) revealed the presence of diverse types of fungal associates (Knack *et al.,* 2015; Graham *et al.*, 2017), including potentially mutualistic glomaleans (in the case of *C. conicum*) and Mortierellales. Physiological evidence for carbon-for-nitrogen exchange was obtained for a representative lycophyte associated with Mucoromycotina root fungi (Hoysted *et al.*, 2019). Amplicon analyses have indicated the presence of both Mucoromycotina and Glomeromycotina observed to be associated with gametophytes of the ferns *Angiopteris lygodiifolia* and *Osmunda japonica* (Ogura-Tsujita *et al.*, 2019). By contrast, neither of these fungal groups was inferred to be represented among microbial associates of *E. xylochaetum*.

Ascomycete associations seem to be more prevalent in our samples of Atacama *E. xylochaetum*. Molecular evidence for Capnodiales ascomycetes at CHI was a feature shared with both *C. conicum* and *S. fimbriatum*, as were sequences classified as Sordariomycetes at HUA. These commonalities might reflect ancient association traits that could be further explored by characterizing additional seedless plant microbiomes for comparative study. Additional approaches to classification of molecular sequences (*e.g.*, other rDNA sequence regions) could be employed using our archived metagenomic sequence data for these seedless plant species, to potentially gain more definitive fungal classifications, particularly as sequence databases enlarge. Future physiological studies of ascomycete associations with seedless plants may provide clues regarding the functional nature of the *Equisetum*-fungal associations we detected in the Atacama Desert.

Metagenomic evidence for hyphal chytrid (*Monoblepharella*) association with *E. xylochaetum* at HUA, consistent with a report of this genus from South America (Brazil) (Rocha *et al.*, 2015), is of interest because chytrids were also inferred to associate with *C. conicum* (Knack *et al.*, 2015). *Monoblepharella* represents a lineage thought to have evolved hyphae independently of other hyphal fungi, and is thus of evolutionary interest (Powell, 2017), although potential functional aspects of interactions with seedless plants remain to be determined. The metagenomic sequence evidence we found for *E. xylochaetum* association with a ciliate (*Engelmanniella*) at the HUA site recalls sequence evidence for several other ciliate types associated with *S. fimbriatum*; rhizarian protists and a choanoflagellate were also inferred to

associate with both *E. xylochaetum* and the peat moss *S. fimbriatum* (Graham *et al.*, 2017). These protist commonalities may reflect moist habitat conditions and possibly reflect earlier, more mesic conditions likely present in the Atacama region prior to the Holocene onset of aridity (Arroyo *et al.*, 1988; Knief *et al.*, 2020). An emerging deep-time view of the Atacama region is of an ancient mesic, vegetated terrain that might have supported extensive plant populations–including species of *Equisetum*–for long time periods, with such populations gradually becoming restricted to the streambeds of deep valleys as landscape aridity increased. Modern global climate change effects on water supplies might ultimately impact the hardy, persistent *Equisetum xylochaetum* groves of the Atacama Desert.

Acknowledgements

Professor José Delatorre-Herrera (Universidad Arturo Prat, Iquique, Chile) provided key logistical assistance and chemical supplies that were much appreciated. Professor Luis Sobrevia (Pontificia Universidad Católica de Chile, Santiago) kindly provided access to a well-equipped molecular biology laboratory essential for DNA extractions. Computing resources employed for metagenomic sequence analyses were funded by NSF grant DEB-1119944 to L. E. Graham. We thank Sarah Friedrich for generating illustrations.

Literature Cited

Arroyo, M. T. K., F. A. Squeo, J. J. Armesto, and C. Villagran. 1988. Effects of aridity on plant diversity in the northern Chilean Andes: Results of a natural experiment. Annals of the Missouri Botanical Garden 75:55-78.

Ayling, M., M. D. Clark, and R. M. Leggett. 2020. New approaches for metagenome assembly with short reads. Briefings in Bioinformatics 21:584-594.

Azua-Bustos, A., C. Gonzalez-Silva, M. A. Fernandez-Martinez, and C. Arenas-Fajardo. 2019. Aeolian transport of viable microbial life across the Atacama Desert, Chile: Implications for Mars. Scientific Reports 9:11024.

Barron, G. L., C. Morikawa, and M. Saikawa. 1990. New *Cephaliophora* species capturing rotifers and tardigrades. Canadian Journal of Botany 68:685-690.

Bolger, A. M., M. Lohse, and B. Usadel. 2014. Trimmomatic: A flexible trimmer for Illumina sequence data. Bioinformatics 30:2114-2120.

Camacho, C., G. Coulouris, V. Avagyan, N. Ma, J. Papadopoulos, K. Bealer, and T. Madden. 2009. BLAST+: architecture and applications. BMC Bioinformatics 10:421.

Channing, A., A. Zamuner, D. Edwards, and D. Guido. 2011. *Equisetum thermale sp. nov.* (Equisetales) from the Jurassic San Agustín hot spring deposit, Patagonia: Anatomy, paleoecology and inferred paleoecophysiology. American Journal of Botany 98:680-697.

Chávez, R. O., A. Moreira-Muñoz, M. Galleguillos, M. Olea, J. Aguayo, A. Latin, I. Aguilera-Betti, A. A. Muñoz, and H. Manríquez. 2019. GIMMS NDVI time series reveal the extent, duration, and intensity of "blooming desert" events in the hyper-arid Atacama Desert, Northern Chile. International Journal of Applied Earth Observation and Geoinformation 76:193-203.

Christenhusz, M. J. M., L. Bangiolo, M. W. Chase, M. F. Fay, C. Husby, M. Witkus, and J. Viruel. 2019. Phylogenetics, classification and typification of extant horsetails (*Equisetum*, Equisetaceae). Botanical Journal of the Linnaean Society 189:311-352.

Clark, J. W., M. N. Puttick, and P. C. J. Donoghue. 2019. Origin of horsetails and the role of whole-genome duplication in plant macroevolution. Proceedings of the Royal Society B 286:2019.1662.

Clarke, J. D. A. 2006. Antiquity of aridity in the Chilean Atacama Desert. Geomorphology 73:101-114.

Darriba, D., D. Posada, A. M. Kozlov, A. Stamatakis, B. Morel, and T. Flouri. 2020. ModelTest-NG: a new and scalable tool for the selection of DNA and protein evolutionary models. Molecular Biology and Evolution 37:291-294.

Dhilion, S. S. 1993. Vesicular-arbuscular mycorrhizas of *Equisetum* species in Norway and the U.S.A.: occurrence and mycotrophy. Mycological Research 97:656-660.

Edgar, R. C., B. J. Haas, J. C. Clemente, C. Quince, and R. Knight. 2011. UCHIME improves sensitivity and speed of chimera detection. Bioinformatics 27:2194-2200.

Elgorriaga, E., I. H. Escapa, G. W. Rothwell, A. M. F. Tomescu, and N. R. Cuneo. 2018. Origin of *Equisetum*: Evolution of horsetails (Equisetales) within the major euphyllophyte clade Sphenopsida. American Journal of Botany 105:1286-1303.

Fitzpatrick, C. R., J. Copeland, P. W. Wang, D. S. Guttman, P. M. Kotanen, and M. T. J. Johnson. 2018. Assembly and ecological function of the root microbiome across angiosperm plant species. Proceedings of the National Academy of Sciences, U. S. A. 115:E1157-E1165.

Fusconi, A. and M. Mucciarelli. 2018. How important is arbuscular mycorrhizal colonization in wetland and aquatic habitats? Environmental and Experimental Botany 155:128-141.

Gehring, C. A., C. M. Sthultz, L. Flores-Rentería, A. V. Whipple, and T. G. Whitham. 2017. Tree genetics defines fungal partner communities that may confer drought tolerance. Proceedings of the National Academy of Sciences, U. S. A. 114:11169-11174.

Gifford, E. M. and A. S. Foster. 1989. *Morphology and Evolution of Vascular Plants*, Freeman, NY, NY.

Gould, R. E. 1968. Morphology of *Equisetum laterale* Phillips, 1829, and *E. bryanii sp. nov.* from the Mesozoic of South-Eastern Queensland. Australian Journal of Botany 16:153-176.

Graham, L. E., J. M. Graham, J. J. Knack, M. T. Trest, M. J. Piotrowski, and P. Arancibia-Avila. 2017. A sub-Antarctic peat moss metagenome indicates microbiome resilience to stress and biogeochemical functions of early Paleozoic terrestrial ecosystems. International Journal of Plant Sciences 178:618-628.

Graham, L. E., J. M. Graham, L. W. Wilcox, M. E. Cook, P. Arancibia-Avila, and J. J. Knack. 2018. Evolutionary roots of plant microbiomes and biogeochemical impacts of nonvascular autotroph-microbiome systems over deep time. International Journal of Plant Sciences 179:505-522.

Guerriero, G., C. Law, I. Stokes, K. L. Moore, and C. Exley. 2018. Rough and tough. How does silicic acid protect horsetail from fungal infection? Journal of Trace Elements in Medicine and Biology 47:45-52.

Hartley, A. J., G. Chong, J. Houston, and A. E. Mather. 2005. 150 million years of climatic stability: Evidence from the Atacama Desert, northern Chile. Journal of the Geological Society of London 162:421-424.

Hodson, E., F. Shahid, J. Basinger, and S. Kaminskyi. 2009. Fungal endorhizal associates of *Equisetum* species from Western and Arctic Canada. Mycological Progress 8:19-27.

Hoysted, G. A., A. S. Jacob, J. Kowal, P. Giesemann, M. I Bidartondo, J. G. Duckett, G. Gebauer, W. R. Rimington, S. Schornack, S. Pressel, and K. J. Field. 2019. Mucoromycotina fine root endophyte fungi form nutritional mutualisms with vascular plants. Plant Physiology doi:https//doi.org/10.1104/pp.00729.

Hulse, J. D. 2018. Review of comprehensive staining techniques used to differentiate arbuscular mycorrhizal fungi from plant root tissues. Acta Scientific Agriculture 2.7:39-44.

Husby, C. 2013. Biology and functional ecology of *Equisetum* with emphasis on the giant horsetails. Botanical Review 79:147-177.

Husby, C., J. Delatorre, V. Oreste, S. F. Oberbauer, D. T. Palow, L. Novara, and A. Grau. 2011. Salinity tolerance ecophysiology of *Equisetum giganteum* in South America: a study of 11 sites providing a natural gradient of salinity stress. AoB Plants plr022 doi:10.1093/aobpla/plr022.

Husby, C. E., J. Delatorre-Herrera, S. F. Oberbauer, A. Grau, and L. Novara. 2014. Stomatal conductance patterns of *Equisetum giganteum* stems in response to environmental factors in South America. Botany 92:701-712.

Ionescu, D., C. Siebert, L. Polerecky, Y. Y. Munwes, C. Lott, S. Häusler, M. Bozoc-Ionescu, C. Quast, J. Peplies, F. O. Glöckner, A. Ramette, T. Rödiger, T. Dittmar, A. Oren, S. Geyer, H.-J. Stärk, M. Sauter, T. Licha, J. B. Laronne, and D. de Beer. 2012. Microbial and chemical characterization of underwater fresh water springs in the Dead Sea. Public Library of Science One 7:e38319.

Katoh, K. and D. M. Standley. 2013. MAFFT multiple sequence alignment software version 7: improvements in performance and usability. Molecular Biology and Evolution 30:772-780.

Klindworth, A., E. Pruesse, T. Schweer, J. Peplies, C. Quast, M. Horn, and F. O. Glöckner. 2013. Evaluation of general 16S ribosomal RNA gene PCR primers for classical and next-generation sequencing-based diversity studies. Nucleic Acids Research 41:e1.

Knack, J. J., L. W. Wilcox, P.-M. Delaux, J.-M. Ané, M. J. Piotrowski, M. E. Cook, J. M. Graham, and L. E. Graham. 2015. Microbiomes of streptophyte algae and bryophytes suggest that a functional suite of microbiota fostered plant colonization of land. International Journal of Plant Sciences 176:405-420.

Knief, C., R. Bol, W. Amelung, S. Kusch, K. Frindte, E. Eckmeier, A. Jaeschke, T. Dunai, B. Fuentes, R. Mörchen, T. Schütte, A. Lücke, E. Klumpp, K. Kaiser, and J. Rethemeyer. 2020. Tracing elevational changes in microbial life and organic carbon sources in soils of the Atacama Desert. Global and Planetary Change 184:103078.

Koske, R. E., C. F. Friese, P. D. Olexia, and R. L. Hauke. 1985. Vesicular-arbuscular mycorrhizas in *Equisetum*. Transactions of the British Mycological Society 85:350-353.

Kowal, J., S. Pressel, J. G. Duckett, M. I. Bidartondo, and K. J. Field. 2018. From rhizoids to roots. Experimental evidence of mutualism between liverworts and ascomycete fungi. Annals of Botany 121:221-227.

Laenen, B., B. Shaw, H. Schneider, B. Goffinet, E. Paradis, A. Désamoré, J. Heinrichs, J. C. Villarreal, S. R. Gradstein, S. F. McDaniel, D. G. Long, L. L. Forrest, M. L. Hollingsworth, B. Crandall-Stotler, E. C. Davis, J. Engel, M. Von Konrat, E. D. Cooper, J. Patiño, C. J. Cox, A. Vanderpoorten, and A. J. Shaw. 2014. Extant diversity of bryophytes emerged from post-Mesozoic diversification bursts. Nature Communications 5:5134.

Li, D., C. M. Liu, K. Sadakane, and T. W. Lam. 2015. MEGAHIT: an ultra-fast single-node solution for large and complex metagenomics assembly via succinct de Bruijn graph. Bioinformatics 15:1674-1676.

Li, H. and R. Durbin. 2009. Fast and accurate short read alignment with Burrows-Wheeler transform. Bioinformatics 25:1754-1760.

Li, H., B. Handsaker, A. Wysoker, T. Fennell, J. Ruan, N. Homer, G. Marth, G. Abecasis, and R. Durbin. 2009. 1000 genome project data processing subgroup, the sequence alignment/map format and SAMtools. Bioinformatics 25:2078-2079.

Li, W. and A. Godzik. 2006. Cd-hit: a fast program for clustering and comparing large sets of protein or nucleotide sequences. Bioinformatics 22:1658-1659.

Miller, M. A., W. Pfeiffer and T. Schwartz. 2010. Creating the CIPRES Science Gateway for inference of large phylogenetic trees. In 2010 gateway computing environments workshop (GCE), Ieee pp.1-8.

Nopun, P., P. Traiperm, T. Boonkerd, and T. Jenjettikul. 2016. Systematic importance of rhizome stellar anatomy in selected Monilophytes from Thailand. Taiwania 61:175-184.

Nouhra, E., C. Urcelay, S. Longo, and L. Tedersoo. 2013. Ectomycorrhizal fungal communities associated to *Nothofagus* species in northern Patagonia. Mycorrhiza 23:487-496.

Ogura-Tsujita, Y., K. Yamamoto, Y. Hirayama, A. Ebihara, N. Morita, and R. Imaichi. 2019. Fern gametophytes of *Angiopteris lygodiifolia* and *Osmunda japonica* harbor diverse Mucoromycotina fungi. Journal of Plant Research 132:581-588.

Ondov, B., N. Bergman, and A. Phillippy. 2011. Interactive metagenomic visualization in a web browser. BMC Bioinformatics 12:385.

Ortega, C., G. Vargas, M. Rojas, J. A. Rutlant, P. Muñoz, C. B. Lange, S. Pantoja, L. Dezileu, and L. Ortlieb. 2019. Extreme ENSO-driven torrential rainfalls at the southern edge of the Atacama Desert during the Late Holocene and their projection into the 21st century. Global Planetary Change https://doi.org/10, 1016/j.gloplacha. 2019.02.011.

PLACZEK, C., D. E. GRANGER, A. MATMON, J. QUADE, and U. RYB. 2014. Geomorphic process rates in the Central Atacama Desert, Chile: Insights from cosmogenic nuclides and implications for the onset of hyperaridity. American Journal of Science 314:1462-1512.

POWELL, M. J. 2017. Chytridiomycota. Pp. 1523-1558, *in:* J. M. Archibald, A. G. B. Simpson, C. H. Slamovits, L. Margulis, M. Melkonian, D. J. Chapman, and J. O. Corliss (eds), *Handbook of the Protists.* Springer, New York.

PRUESSE, E., J. PEPLIES, and F. O. GLÖCKNER. 2012. SINA: accurate high throughput multiple sequence alignment of ribosomal rna genes. Bioinformatics doi:10.1093/bioinformatics/bts252.

QUAST, C., E. PRUESSE, P. YILMAZ, J. GERKEN, T. SCHWEER, P. YARZA, J. PEPLIES, and F. O. GLÖCKNER. 2013. The SILVA ribosomal RNA gene database project: improved data processing and web-based tools. Nucleic Acids Research 41:D590-D596.

QUINLAN, A. R. and I. M. HALL. 2010. BEDTools: a flexible suite of utilities for comparing genomic features. Bioinformatics 26: 841-842.

RAGONEZI, C. and M. A. ZAVATTIERI. 2018. Histological studies of mycorrhized roots and mycorrhizal-like-structures in pine roots. Methods and Protocols 1:34.

READ, D. J., J. G. DUCKETT, R. FRANCIS, R. LIGRONE, and A. RUSSELL. 2000. Symbiotic fungal associations in 'lower' land plants. Philosophical Transactions of the Royal Society of London B 355:815-831.

ROCHA, J. R. S., N. D. C. SOUSA, M. A. M. MACEDO, L. W. SARAIVA, L. A. SANTOS, A. L. M. SOUSA, P. C. L. SALES, A. A. CRONEMBERGER, A. S. GOMES, E. P. RODRIGUES, L. M. A. SOUSA, and D. F. M. SILVA. 2015. First records of *Monoblepharella taylori* Sparrow (Monoblepharidales) in Brazil. Current Research in Environmental and Applied Mycology 5:74-77.

RONQUIST, F. and J. P. HUELSENBECK. 2003. MrBayes 3: Bayesian phylogenetic inference under mixed models. Bioinformatics 19:1572-1574.

ROTHWELL, G. W. 1996. Pteridophytic evolution: An often underappreciated phytological success story. Review of Palaeobotany and Palynology 90:209-222.

ROTHWELL, G. W. and S. R. Ash. 2015 Internal anatomy of the Late Triassic *Equisetocaulis gen. nov.*, and evolution of modern horsetails. Journal of the Torrey Botanical Society 142:27-37.

RUBINSTEIN, C. V., E. PETUS, and H. NIEMEYER. 2017. Palynostratigraphy of the Zorritas Formation, Antofagasta region, Chile: Insights on the Devonian/Carboniferous boundary in western Gondwana. Geoscience Frontiers 8:493-506.

SMANT, G., J. HELDER, and A. GOVERSE. 2018. Parallel adaptations and common host cell responses enabling feeding of obligate and facultative plant parasitic nematodes. Plant Journal 93:686-702.

SPATAFORA, J. W., Y. CHANG, G. L. BENNY, K. LAZARUS, M. E. SMITH, M. L. BERBEE, G. BONITO, N. CORRADI, I. GRIGORIEV, A. GRYGANSKYI, T. Y. JAMES, K. O'DONNELL, R. W. ROBERSON, T. N. TAYLOR, J. UEHLING, R. VILGALYS, M. M. WHITE, and J. E. STAJICH. 2016. A phylum-level phylogenetic classification of zygomycete fungi based on genome-scale data. Mycologia 108:1028-1046.

STAMATAKIS, A. 2014. RAxML version 8: a tool for phylogenetic analysis and post-analysis of large phylogenies. Bioinformatics 30:1312-1313.

STRINGLIS, I. A., K. YU, K. FEUSSNER, R. DE JONGE, S. VAN BENTUM, M. C. VAN VERK, R. L. BERENDSEN, P. A. H. M. BAKKER, I. FEUSSNER, and C. M. J. PIETERSE. 2018. MYB72-dependent coumarin exudation shapes root microbiome assembly to promote plant health. Proceedings of the National Academy of Sciences, U. S. A. 115:E5213-E5222.

TEDERSOO, L., K. HANSEN, B. A. PERRY, and R. KJOLLER. 2006. Molecular and morphological diversity of pezizalean ectomycorrhizal. New Phytologist 170:581-596.

TEDERSOO, L., S. SANCHEZ-RAMIREZ, U. KOLJALG, M. BAHRAM, M. DORING, D. SCHIGEL, T. MAY, M. RYBERG, and K. ABARENKOV. 2018. Hi-level classification of the Fungi and a tool for evolutionary ecological analyses. Fungal Diversity 90:135-159.

TIPKE, I., L. BUCKER, J. MIDDELSTAEDT, P. WINTERHALTER, M. LUBIENSKI, and T. BEUERLE. 2019. HILIC HPLC-ESI-MS/MS identification and quantification of the alkaloids from the genus *Equisetum.* Phytochemical Analysis 2019:1-10.

TUBAKI, K. 1956. *Cephaliophora irregularis* newly found in Japan. Journal of Japanese Botany 31:161-164.

Vanneste, K., L. Sterck, A. A. Myburg, Y. Van de Peer, and E. Mizrachi. 2015. Horsetails are ancient polyploids: Evidence from *Equisetum giganteum*. Plant Cell 27:1567-1578.

Voight, C., S, Klipsch, D, Herwartz, G. Chong, and M. Staubwasser. 2020. The spatial distribution of soluble salts in the surface soil of the Atacama Desert and their relationship to hyperaridity. Global and Planetary Change 184:103077.

Walters, W. A., Z. Jin, N. Youngblut, J. G. Wallace, J. Sutter, W. Zhang, A. González-Peña, J. Peiffer, O. Koren, Q. Shi, R. Knight, S. G. Tringe, E. S. Buckler, J. L. Dangl, and R. E. Ley. 2018. Large-scale replicated field study of maize rhizosphere identifies heritable microbes. Proceedings of the National Academy of Sciences, U. S. A. 115:7368-7373.

White, D. 1894. Equiseta in the Carboniferous. Botanical Gazette 19:71.

Wu, G.-L., T.-H. Kuo, T.-T. Tsay, I. J. Tsai, and P. J. Chen. 2016. Glycoside hydrolase (GH) 45 and 5 candidate cellulases in *Aphelenchoides besseyi* isolated from bird's-nest fern. Public Library of Science One 11:e0158663.

Yeoh, Y. K., P. G. Dennis, C. Paungfoo-Lonhienne, L. Weber, R. Brackin, M. A. Ragan, S. Schmidt, and P. Hugenholtz. 2017. Evolutionary conservation of a core root microbiome across plant phyla along a tropical soil chronosequence. Nature Communications 8:215.

Zhang, L., C. J. Lilley, M. Imren, J. P. Knox, and P. E. Urwin. 2017. The complex cell wall composition of syncytia induced by plant parasitic cyst nematodes reflects both function and host plant. Frontiers in Plant Science 8:1087.

Zhang, W.-W., C. Wang, R. Xue, and L.-J. Wang. 2019. Effects of salinity on the soil microbial community and soil fertility. Journal of Integrative Agriculture 18:1360-1368.

Appendix 1. Ecological and geographical metadata for two sampled Atacama Desert locations.

	Huasqueña (HUA)	**Chiza (CHI)**
Sampling date	1/9/2016	1/10/2016
GPS coordinates	-19.752535 -69.404068	-19.198696 -70.043582
Temperature	31°C	30°C
Altitude	1983 m	350 m
Additional locale information	Remote roadside stream bed; ~0.3 m of dry sedge debris over soil; dry to 20 cm depth, then moist	Chiza valley ~100 m from Chilean highway 5; sandy upper banks of stream bed
Rhizome depth in soil	~0.3 m	>1 m; not collected
Root depth in soil	~0.3 m	~0.3 m

Appendix 2. Shotgun Metagenomic Assembly Statistics and Chimera Detection

Site	**HUA**	**CHI**
Number final contigs	432,156	256,891
Minimum contig length, bp	200	362
Maximum contig length, bp	811,711	294,792
Average contig length, bp	362	637
N50, bp	622	664
Number of non-chimeric sequences	SSU 156 LSU 14,231	SSU 113 LSU 11,308
Number of chimeric sequences	SSU 14 LSU 0	SSU 24 LSU 0

APPENDIX 3. SILVAngs Classification Project information: SSU (18S + 16S rDNA) and LSU (23S + 28S rDNA) for sites HUA and CHI, SINA v1.2.10 for ARB SVN (revision 21008)

	SSU HUA	**LSU HUA**	**SSU CHI**	**LSU CHI**
Number samples	1	1	1	1
Number of assembled contigs	432,156	432,156	256,891	256,891
Number of rejected contigs	431,979 (99.96%)	417,906 (96.7%)	256,747 (99.94%)	245,524 (95.58%)
Raw sequence information				
Minimum length	200	200	200	200
Average length	632	632	637	637
Maximum length	811,711	811,711	294,792	294,792
Aligned sequence information				
Minimum length	1	1	1	1
Average length	598	623	589	625
Maximum length	811,711	811,711	294,792	294,792
Quality information: rejected by				
Alignment BP score	39	2951	23	1587
Alignment identity	351018	317010	240132	213804
Alignment score	1528	20884	1244	16601
Ambiguous bases	-	-	-	-
Homopolymers	72978	72693	10652	10481
Quality	-	-	-	-
Length	6416	4368	4696	3051
Clustering information				
Number OTUs	170	14,231	137	11,308
Number clustered sequences	4	18	4	57
Number replicates	3	1	3	2
Classification information				
Number classified sequences	87	185	106	135
Number No-relative	79	14,046	7	11,173
Project settings				
Minimum alignment identity	50	40	50	40
Minimum alignment score	40	30	40	30
Minimum basepair score	30	30	30	30
Quality control				
Minimum sequence quality	30	30	30	30
Minimum length aligned nucleotides	50	50	50	50
Maximum ambiguities (%)	2	2	2	2
Maximum homopolymers (%)	2	2	2	2
Clustering				
CD-Hit Version	3.1.2	3.1.2	3.1.2	3.1.2
Minimum OTU identity	98	98	98	98
Classification				
BLAST version	2.2.30+	2.2.30+	2.2.30+	2.2.30+
Reference	SILVA	SILVA	SILVA	SILVA
Reference version	132	132	132	132
Similarity %	93	93	93	93

American Fern Journal 111(2):110–116 (2021)
Published on 7 June 2021

New Leaves of *Dryopteris intermedia* Develop More Slowly When the Petioles of Overwintering Leaves are Broken

Jack T. Tessier
SUNY Delhi – 454 Delhi Dr., Delhi, NY 13753 USA

Abstract.—Wintergreen ferns keep their leaves for an entire year before replacing them with new leaves in the spring. The overwintering leaves of *Dryopteris intermedia* provide carbon to the new leaves, and if these old leaves cannot become prostrate before winter via the hinge that develops at the base of the petiole, they are frost damaged and broken, which may affect the development of the new leaves in the subsequent year. I compared the vernal development of new leaves in *D. intermedia* between plants whose old leaves were intact and those whose petioles had been experimentally broken in the fall to determine the importance of the softening of the petiole-base in old leaves to the development of new leaves. Compared to the control, plants whose old leaves had broken petioles had a one-week delay in the development of their new leaves. This delay demonstrates that the evolutionary development of the petiole hinge may have been critical to the functional benefit associated with new leaf development in the wintergreen leaf habit in ferns.

Key Words.—deciduous forest, fern, leaf phenology, northeast United States, wintergreen

Ferns encompass a range of patterns in leaf longevity (Karst and Lechowicz, 2007). Deciduous species, which keep their leaves for one growing season, include *Dennstaedtia punctilobula* (Michx.) T. Moore and *Onoclea sensibilis* L. (Hill and Silander, 2001; Reudink *et al.*, 2005). Evergreen species, which maintain individual leaves for multiple growing seasons, include *Polypodium virginianum* L. (Reudink *et al.*, 2005; Tessier, 2008). Wintergreen species, which keep their leaves for one year before replacing them each spring, include *Dryopteris marginalis* (L.) A. Gray and *Polystichum acrostichoides* (Michx.) Schott (Reudink *et al.*, 2005; Tessier, 2008). Generally, keeping leaves beyond the growing season can provide a storage organ for resources and permit non-growing season photosynthesis (Goldblum and Kwit, 2012, 2013; Minoletti and Boerner, 1993; Tani and Kudo, 2003). What is less well understood is how some of the adaptations seen in these different leaf habits (timing of senescence, timing of bud break, percent retranslocation, leaf positioning, etc.) contribute to the evolutionary success of the habits.

Dryopteris intermedia (Muhl. ex Willd.) A. Gray is a wintergreen fern that is common in the northeast United States (Siccama and Bormann, 1970; Tessier, 2008; Yorks, Leopold, and Raynal, 2000). It grows in deciduous forests (Brach, MacNaughton, and Raynal, 1993; Siccama and Bormann, 1970; Tessier and Raynal, 2003), where it can make use of the higher light intensity for photosynthesis at times when canopy trees do not have leaves (Goldblum and

tessiejt@delhi.edu

Kwit, 2012, 2013; Tessier, 2001). A hinge (softening of the tissues) develops at the base of the petiole in old leaves in fall (Noodén and Wagner, 1997). While this new orientation reduces insolation, it allows those old leaves to lie prostrate and be protected from frost by snow cover (Tessier, 2014). When the old leaves are experimentally removed at the start of spring, the new leaves develop later and more slowly than for intact plants (Van Buskirk and Edwards, 1995). This delay is a result of the lost carbon provided by the old leaves to the new leaves (Tessier and Bornn, 2007). If the old leaves are experimentally kept upright in winter, they experience significantly more frost damage and breakage than if they are prostrate (Tessier, 2018), calling into question the utility of the wintergreen leaf habit in *D. intermedia* without the ability to become prostrate for winter.

This study addressed the question: can leaves with broken petioles facilitate the development of new leaves? I hypothesized that the break in the petiole (which would happen without the softening of the base of the petiole) would damage the vascular tissues and hinder photosynthesis and the movement of resources. This hypothesis led to the prediction that plants with broken petioles on old leaves would break bud later and develop new leaves more slowly in the spring than plants with intact old leaves (*sensu* Van Buskirk and Edwards, 1995).

MATERIALS AND METHODS

This study was conducted in the same second growth northern hardwood forest near Delhi, NY USA used by Tessier (2018). In October 2017, three parallel transects of 100 m each set 10 m apart were established. Every ten meters along these transects, the two closest plants of *D. intermedia* were chosen for use in the study. One plant was the control plant and was left intact. The other plant was the experimental plant, and its petiole was snapped (but left intact) near the ground where the hinge would have formed in a few weeks. This breakage simulated damage from contact with ground debris, such as sticks and rocks, or from the weight of snow, which would happen if the base did not soften to allow a prostrate position (Noodén and Wagner, 1997; Tessier, 2018). This breaking was done in October rather than in the spring to mimic the damage that would be suffered between the normal autumnal development of the petiole hinge (Noodén and Wagner, 1997) and the vernal development of new leaves (Tessier, 2008). Effectively, the broken leaves mimic what would happen if a hinge did not develop via a softening at the base of the petiole. The closest plant and the second closest plant to the 10 m mark alternated along the transect, determining which plant became the control plant and which became the experimental plant. Collectively, a paired, systematic design was used for this study (Hurlbert, 1984). Thirty pairs of plants were included in the study.

Beginning at the end of snowmelt in 2018, I monitored the plants on a weekly basis to assess bud opening and leaf development. Monitoring began on April 13 and ended on June 14 for 10 weeks of observations. At each observation, I counted the total number of leaves on each of the 60 plants and

documented the percentage of leaves in the following condition for each plant: buds closed, buds opening, leaves less than half unrolled, leaves more than half unrolled, leaves unrolled but not fully expanded, and leaves fully expanded.

All statistical tests were conducted using Minitab version 18 (Minitab, Inc., State College, PA). To compare the developmental status of plants in the control and broken treatment, I used paired t-tests to compare the Julian date when the first leaf, 50% of leaves, and 100% of leaves of the plant reached each developmental stage.

Results

All 60 plants survived the winter. Buds and leaves from the control plants were developmentally ahead of the experimental plants in a statistically significant way at every stage (Table 1). However, a paired t-test was not possible for the first leaf reaching full expansion and all leaves reaching full expansion because there was no variability in both control and the broken treatment for those stages, making statistical analysis moot. All of the buds in the control plants were open by May 10, and this did not happen for the experimental plants until May 17 (Table 1). The control plants stayed significantly ahead of the plants in the broken treatment throughout the study (Table 1). Leaves in control plants were all fully expanded by May 31 but not until June 6 in experimental plants (Table 1).

Discussion

The breakage of petioles of old leaves results in a delay in the development of new leaves in *D. intermedia* (Table 1). This result supports the hypothesis that petiole breakage prevents typical functioning in the old leaves, which could relate to photosynthesis in the old leaves or the flow of resources to the new leaves from the old leaves (Minoletti and Boerner, 1993; Tessier and Bornn, 2007). There was roughly a one week delay in the full development of new leaves as a result of the breakage (Table 1), which reduces the capacity for vernal photosynthesis (Goldblum and Kwit, 2012, 2013) while light intensities are high on the forest floor of the deciduous forests (Anderson, 1964; Canham *et al.*, 1994; Federer and Tanner, 1966; Hutchison and Matt, 1977) where this and other wintergreen fern species live (Brach, MacNaughton, and Raynal, 1993; Siccama and Bormann, 1970; Tessier and Raynal, 2003). With nearly half of annual photosynthesis happening before canopy leaf out in *D. intermedia* (Goldblum and Kwit, 2012) and the photosynthetic rate dropping in old leaves as spring progresses (Tessier, 2001), a delay in the development of new leaves represents a significant reduction in the ability of the plants to capture energy that is necessary for growth and reproduction (Britton and Watkins, 2016; Hammen 1993; Watkins, Churchill, and Holbrook 2016). To compensate for this loss of photosynthetic time, leaves would have to photosynthesize faster, but they are already near their maximum photosynthetic rate during high light

TABLE 1. Comparison of development of new leaves in *Dryopteris intermedia* during the spring of 2018 between control plants and plants whose petioles were broken on old leaves before winter in a second-growth mixed hardwood forest in Delhi, NY USA. Data are Julian date ± standard error. Statistical results are for a paired t-test between control and broken treatment within a developmental stage (N = 30). * No statistical analysis due to lack of variability in both treatments.

Phenological Stage	Control	Broken Leaves	Statistical Result
First Bud Opening	123.93±0.442	129.07±0.442	T = 8.93 P < 0.0001
Half of Buds Opening	127.43±0.626	130.00±0.336	T = 3.61 P = 0.001
All Buds Opening	129.53±0.324	132.57±0.626	T = 4.18 P < 0.0001
First Leaf Less than Half Unrolled	130.70±0.390	132.33±0.613	T = 2.54 P = 0.017
Half of Leaves Less than Half Unrolled	131.17±0.484	133.27±0.648	T = 2.76 P = 0.010
All Leaves Less than Half Unrolled	132.57±0.626	137.47±0.575	T = 5.89 P < 0.0001
First Leaf More than Half Unrolled	137.4±0.324	139.33±0.699	T = 2.50 P = 0.018
Half of Leaves More than Half Unrolled	137.47±0.324	139.33±0.699	T = 4.96 P < 0.0001
All Leaves More than Half Unrolled	139.80±0.637	144.23±0.626	T = 5.19 P < 0.0001
First Leaf Fully Unrolled	144.47±0.324	146.80±0.637	T = 3.34 P = 0.0002
Half of Leaves Fully Unrolled	144.47±0.324	150.53±0.324	T = 13.73 P < 0.0001
All Leaves Fully Unrolled	147.97±0.644	151.00±0.000	T = 4.71 P < 0.0001
First Leaf Fully Expanded	151.00±0.000	151.00±0.000	T = * P = *
Half of Leaves Fully Expanded	151.00±0.000	153.57±0.626	T = 4.10 P < 0.0001
All Leaves Fully Expanded	151.00±0.000	158.00±0.000	T = * P = *

periods in the spring (Hutchison and Matt, 1977; Brach, MacNaugton, and Raynal, 1993).

When leaves reach the end of their photosynthetic lifespan, they become time-limited sources of resources for the rest of the plant. Deciduous species translocate nutrients from senescing leaves (del Arco, Escudero, and Garrido, 1991; DeMars and Boerner, 1997; Killingbeck *et al.*, 2002; Ryan and Bormann, 1982), which limits the loss of nutrients from the plant when the leaves drop. Similarly, old leaves in wintergreen ferns are sources of energy and nutrients as they reach the end of their lifespans (Minoletti and Boerner, 1993; Tessier and Bornn, 2007). These results show that unless the base of the petiole softens prior to winter to prevent breakage (Tessier, 2018), the old leaf has a reduced ability to provide resources for the new leaves and promote leaf development

(Table 1), which diminishes the plant's access to the high light opportunity in the spring. Therefore, the ecological and evolutionary success of the wintergreen leaf habit may have been dependent on the concomitant evolutionary development of the petiole hinge (Noodén and Wagner, 1997). A multi-generational study would be required to quantify the impact of broken leaves on plant mass and reproductive fitness.

Plants have evolved a wide variety of mechanisms to prevent damage. Herbivore damage can be deterred by chemical and physical defenses (Forrester, Leopold, and Underwood, 2006; Johnson, Erb, and Hartley, 2016; Li *et al.*, 2016). Damage from wind is prevented via flexibility in the stem anatomy and short stature (Asner and Goldstein, 1997; Grime, 1977; Holbrook and Putz, 1989). Frost damage is prevented via physiological mechanisms that prevent breakage of cell walls and membranes (Gusta and Wisniewski, 2013; Mazzucotello *et al.*, 2006; Moellering, Muthan, and Benning, 2010). Fire tolerance is associated with thickness and moisture content of bark (Pinard and Huffman, 1997; Spalt and Reifsnyder, 1962). Likewise, these results combined with other work (Noodén and Wagner, 1997; Tessier, 2014, 2018) show that the petiole hinge is a critical mechanism in wintergreen ferns to prevent damage to old leaves and to stimulate the development of new leaves (Minoletti and Boerner, 1993; Tessier and Bornn, 2007).

In conclusion, breakage to the petiole of old leaves slows the development of new leaves in the wintergreen fern *D. intermedia*. These results indicate that the petiole hinge allowing old leaves to become prostrate before winter (Noodén and Wagner, 1997) prevents damage to the old leaves (Tessier, 2014, 2018), allowing them to furnish resources to the new leaves (Tessier and Bornn, 2007) and hasten their development to establish the new set of photosynthetically active components of the plant (Table 1). The petiole hinge is, therefore, likely to be an evolutionarily critical component of the wintergreen leaf habit in ferns.

Acknowledgments

The author thanks Dana Reiff and three anonymous reviewers for providing constructive suggestions about iterations of the manuscript.

Literature Cited

Anderson, M. C. 1964. Studies of the woodland light climate. II. Seasonal variation in the light climate. Journal of Ecology 52:643–663.

Asner, G. P. and G. Goldstein. 1997. Correlating stem biomechanical properties of Hawaiian canopy trees with hurricane wind damage. Biotropica 29:145–150.

Brach, A. R., S. J. MacNaughton, and D. J. Raynal. 1993. Photosynthetic adaptability of two fern species of a northern hardwood forest. American Fern Journal 83:47–53.

Britton, M. R. and J. E. Watkins Jr. 2016. The economy of reproduction in dimorphic ferns. Annals of Botany 118:1139–1149.

Canham, C. D., A. C. Finzi, S. W. Pacala, and D. H. Burbank. 1994. Causes and consequences of resource heterogeneity in forests: interspecific variation in light transmission by canopy trees. Canadian Journal of Forest Research 24:337–349.

del Arco, J. M., A. Escudero, and M. V. Garrido. 1991. Effects of site characteristics on nitrogen retranslocation from senescing leaves. Ecology 72:701–708.

DeMars, B. G. and R. E. J. Boerner. 1997. Foliar phosphorus and nitrogen resorption in three woodland herbs of contrasting phenology. Castanea 62:43–54.

Federer, C. A. and C. B. Tanner. 1966. Spatial distribution of light in the forest. Ecology 47:555–560.

Forrester, J. A., D. J. Leopold, and H. B. Underwood. 2006. Isolating the effects of white-tailed deer on the vegetation dynamics of a rare maritime American holly forest. American Midland Naturalist 156:135–150.

Goldblum, D. and M. C. Kwitt. 2012. The relative photosynthetic contribution of old and new fronds of the wintergreen fern *Dryopteris carthusiana*, Ontario, Canada. Journal of the Torrey Botanical Society 139:270–282.

Goldblum, D. and M. C. Kwitt. 2013. Erratum. Journal of the Torrey Botanical Society 140:245.

Grime, J. P. 1977. Evidence for the existence of three primary strategies in plants and its relevance to ecological and evolutionary theory. American Naturalist 111:1169–1194.

Gusta, L. V. and M. Wisniewski. 2013. Understanding plant cold hardiness: an opinion. Physiologia Plantarum 147:4–14.

Hammen, S. C. L. 1993. Density-dependent phenotypic variation in the hay-scented fern, *Dennstaedtia punctilobula*. Bulletin of the Torrey Botanical Club 120:392–396.

Hill, J. D. and J. A. Silander Jr. 2001. Distribution and dynamics of two ferns: *Dennstaedtia punctilobula* (Dennstaedtiaceae) and *Thelypteris noveboracensis* (Thelypteridaeae) in a northeast mixed hardwoods-hemlock forest. American Journal of Botany 88:894–902.

Holbrook, N. M. and F. E. Putz. 1989. Influence of neighbors on tree form: effects of lateral shade and prevention of sway on the allometry of *Liquidambar styraciflua* (sweet gum). American Journal of Botany 76:1740–1749.

Hurlbert, S. H. 1984. Pseudoreplication and the design of ecological field experiments. Ecological Monographs 54:187–211.

Hutchison, B. A. and D. R. Matt. 1977. The distribution of solar radiation within a deciduous forest. Ecological Monographs 47:185–207.

Karst, A. L. and M. J. Lechowicz. 2007. Are correlations among foliar traits in ferns consistent with those in seed plants? New Phytologist 173:306–312.

Killingbeck, K. T., S. L. Hammen-Winn, P. G. Vecchio, and M. E. Goguen. 2002. Nutrient resorption efficiency and proficiency in fronds and trophopods of a winter-deciduous fern, *Dennstaedtia punctilobula*. International Journal of Plant Sciences 163:99–105.

Johnson, S. N., M. Erb, and S. E. Hartley. 2016. Roots under attack: contrasting plant responses to below- and aboveground insect herbivory. New Phytologist 210:413–418.

Li, X., W. Guo, E. Siemann, Y. Wen, W. Huang, and J. Ding. 2016. Plant genotypes affect aboveground and belowground herbivore interactions by changing chemical defense. Oecologia 182:1107–1115.

Mazzucotelli, E., A. Tartari, L. Cattivelli, and G. Forlani. 2006. Metabolism of γ-aminobutyric acid during cold acclimation and freezing and its relationship to frost tolerance in barley and wheat. Journal of Experimental Botany 57:3755–3766.

Minoletti, M. L. and R. E. J. Boerner. 1993. Seasonal photosynthesis, nitrogen and phosphorus dynamics, and resorption in the wintergreen fern *Polystichum acrostichoides* (Michx.) Schott. Bulletin of the Torrey Botanical Club 120:397–404.

Moellering, E. R., B. Muthan, and C. Benning. 2010. Freezing tolerance in plants requires lipid remodeling at the outer chloroplast membrane. Science 330:226–228.

Noodén, L. D. and W. H. Wagner Jr. 1997. Photosynthetic capacity and leaf reorientation in two wintergreen ferns, *Polystichum acrostichoides* and *Dryopteris intermedia*. American Fern Journal 87:143–149.

Reudink, M. W., J. P. Snyder, B. Xu, A. Cunkelman, and R. A. Balsamo. 2005. A comparison of physiological and morphological properties of deciduous and wintergreen ferns in southeastern Pennsylvania. American Fern Journal 95:45–56.

Pinard, M. A. and J. Huffman. 1997. Fire resistance and bark properties of trees in a seasonally dry forest in eastern Bolivia. Journal of Tropical Ecology 13:727–740.

Ryan, D. F. and F. H. Bormann. 1982. Nutrient resorption in northern hardwood forests. BioScience 32:29–31.

Siccama, T. G. and F. H. Bormann. 1970. The Hubbard Brook ecosystem study: productivity, nutrients, and phytosociology of the herbaceous layer. Ecological Monographs 40:289–402.

Spalt, K. W. and W. E. Reifsnyder. 1962. *Bark characteristics and fire resistance: a literature survey.* Southern Forest Experiment Station. US Forest Service. Asheville, NC.

Tani, T. and G. Kudo. 2003. Storage ability of overwintering leaves and rhizomes in a semi-evergreen fern, *Dryopteris crassirhizoma* (Dryopteridaceae). Ecological Research 18:15–24.

Tessier, J. T. 2001. Vernal photosynthesis and nutrient retranslocation in Dryopteris intermedia. American Fern Journal 91:187–196.

Tessier, J. T., and D. J. Raynal. 2003. Use of nitrogen to phosphorus ratios in plant tissues as an indicator of nutrient limitation and nitrogen saturation. Journal of Applied Ecology 40:523–534.

Tessier, J. T. and M. P. Bornn. 2007. Old fronds serve as a vernal carbon source in the wintergreen fern *Dryopteris intermedia* (Aspleniaceae). American Journal of Botany 94:25–28.

Tessier, J. T. 2008. Leaf habit, phenology, and longevity of eleven forest understory plant species in Algonquin State Forest, northwest Connecticut, USA. Botany 86:457–465.

Tessier, J. T. 2014. Reduced winter snowfall damages the structure and function of wintergreen ferns. American Journal of Botany 101:965–969.

Tessier, J. T. 2018. Upright fronds of *Dryopteris intermedia* suffer frost damage and breakage during winter. American Fern Journal 108:19–26.

Van Buskirk, J. V. and J. Edwards. 1995. Contribution of wintergreen leaves to early spring growth in the wood fern *Dryopteris intermedia.* American Fern Journal 85:54–57.

Watkins Jr., J. E., A. C. Churchill, and N. M. Holbrook. 2016. A site for sori: ecophysiology of fertile-sterile leaf dimorphy in ferns. American Journal of Botany 103:845–855.

Yorks, T. E., D. J. Leopold, and D. J. Raynal. 2000. Vascular plant propagule banks of six eastern hemlock stands in the Catskill Mountains of New York. Journal of the Torrey Botanical Society 127:87–93.

American Fern Journal 111(2):117–128 (2021)
Published on 7 June 2021

Fatty Acids Composition of the Epiphytic Ferns, *Platycerium bifurcatum* and *Asplenium nidus,* and the Terrestrial Fern, *Asplenium trichomanes*

Alexander S. Voronkov* and Tatiana V. Ivanova
K.A. Timiryazev Institute of Plant Physiology RAS, IPP RAS, 35 Botanicheskaya St., Moscow, 127276 Russia

Abstract.—Ferns are the second most diverse group of higher plants on the planet. However, the metabolic processes of these plants, as well as their reaction to the influence of various environmental factors, benefit from new investigation. In seed plants, an important role of the lipid fatty acid (FA) composition in plant response to a variety of environmental conditions has been repeatedly demonstrated. In this paper, the composition of FAs in the epiphytic ferns, *Platycerium bifurcatum* and *Asplenium nidus*, and the terrestrial fern, *Asplenium trichomanes* was analyzed by gas-liquid chromatography with mass spectrometry. The data obtained clearly indicate that epiphytic ferns have several distinctive features in the composition of their FAs. They are characterized by a high level of saturated FAs (about 50%) and a great variety of very-long-chain FAs (VLCFA). This strongly contrasts with the FAs composition in the terrestrial fern in which unsaturated FAs prevail. High levels of saturated fatty acids, in particular palmitic acid (16:0), together with a high VLCFA content, can be a necessary component in complex interactions with microorganisms. Thus, the specific FA composition of *P. bifurcatum* and *A. nidus* may act both as a protective mechanism against the penetration of bacteria and pathogenic fungi, and as a mechanism for the interaction of the epiphytes with saprophytic fungi. It is likely that the composition of FAs in the epiphytic ferns is determined by their habitat and plays an active role in the interaction of plants with their environment.

Key Words.—*Asplenium nidus, Asplenium trichomanes, Platycerium bifurcatum,* unsaturated fatty acids, very-long-chain fatty acids

Ferns are an ancient group of vascular plants. They were once the dominant group of plants in forests but are now outcompeted by gymnosperms and angiosperms. There are currently around 12,000 fern species, and they are found around the globe in a variety of habitats. Ferns have amazing ecological plasticity and are widespread in many natural areas on all continents except Antarctica. They grow in forests in the lower and upper tiers. If epiphytic, they grow on the branches and trunks of large trees. Ferns can also be found, in rock crevices, swamps, rivers, and lakes, on the walls of urban houses, on agricultural lands where they can grow as weeds, and along roadsides (Christenhusz, Fay, and Byng, 2018). Ferns are omnipresent, but do not always attract attention.

Despite such a variety of life forms and broad distribution, ferns receive undeservedly little attention in research, especially compared to angiosperms. In terms of human utility, ferns may have healing properties (Nath *et al.*, 2013),

* voronkov_as@mail.ru

they may be a source of biofuels (Brouwer *et al.*, 2016), or they could serve as bio-indicators for assessing the ecological status of forests (Andama, Michira, and Luilo, 2003). Therefore, the economic potential of fern use is enormous, but, unfortunately, still hidden.

The physiology of ferns has been poorly studied and their metabolism, including the metabolism of lipids, is poorly understood (DeLong *et al.*, 2011, 2013). In seed plants, lipid fatty acids (FAs) composition has been shown to play an important role in plant adaptation under combined stress (Voronkov *et al.*, 2020), and significant variation in FA composition was detected for the plants from different ecological groups (Ivanova *et al.*, 2009). Thus, the goal of this work is to study the total lipid FAs composition of two epiphytic ferns *Platycerium bifurcatum* and *Asplenium nidus* as compared to the terrestrial fern *Asplenium trichomanes*. Our study will help to elucidate the effect of habitat on the lipid fatty acid composition in ferns.

Materials and Methods

Plant material.—Three fern species were grown under greenhouse conditions at the Institute of Plant Physiology RAS. The first, *Platycerium bifurcatum* (Cav.) C.Chr., is a typical epiphyte and has two types of leaves: sporiferous leaves, resembling deer antlers in shape, wedge-shaped at the base and expanding upward and branching twice or thrice dichotomously into obtuse lobes at the top; and sterile leaves, rounded, solid or lobed along the edge, pressed to the substrate, forming a "pocket", where organic residues and water are collected and additional roots are located. The latter become brown and dry with age (Hoshizaki and Price, 1990; Pemberton, 2003). To analyze total lipid FA composition, generative leaves without sori were collected.

The second, *Asplenium nidus* L., is an epiphytic species from the family Aspleniaceae, native to tropical regions. *Asplenium nidus* often lives in palm trees, where it collects water and humus in its leaf-rosette (Martin, 2009). To analyze the composition of FAs from total lipids, leaves that had not yet formed sori were selected.

The third, *Asplenium trichomanes* L., is a terrestrial plant, 10-35 cm high. The rhizome is short and covered with blackish scales and the leaves are feathery with short petioles and numerous segments (Cody, 1968; Metzgar, 2016). To analyze the total lipid FAs composition, whole young leaves that had not yet formed sori were used.

Lipid extraction.—Freshly collected fern leaves were weighed and fixed in boiling isopropyl alcohol for 1 h to preserve native lipid composition. The samples were stored at +4°C until extraction. To extract lipids, isopropanol was separated by filtration through a Schott glass filter into a 250 ml volumetric flask and plant material was homogenized with a porcelain mortar and extracted as previously described with slight modifications (Voronkov *et al.*, 2019). Lipids were extracted three times sequentially in 50 ml of $CHCl_3$/CH_3OH/H_2O (30:20:1.7, by vol) and 90 ml of $CHCl_3$/CH_3OH/HNO_3 (20:10:0.1, by vol). All extracts were combined in a volumetric flask and the total volume

was adjusted to 250 ml with isopropanol containing 0.001% butylated hydroxytoluene (Sigma-Aldrich, 34750) as an antioxidant. The extracts were stored at +4°C.

Preparation of fatty acid methyl esters.—FA methyl esters (FAMEs) were prepared according to the previously described method with slight modifications (Ivanova *et al.*, 2019, 2020). 50 μg of margaric acid (Sigma Aldrich, H3500) was added to 50 ml of extract as an internal standard. The sample was evaporated to dryness using a rotary evaporator under standard conditions and saponification was carried out in a 5 ml of boiling solution of 4% NaOH in CH_3OH/H_2O (1:1, by vol). The sample was then rotovapped, H_2O (1–2 ml) was added to the dry sample and the unsaponifiable FAs were washed out several times with hexane until the latter became clear. Subsequently, a few drops of methyl orange (Aronis, 9594) were added to the remaining water-soluble fraction and it was acidified with 20% H_2SO_4 until the solution changed to a pink color. The FAs were then extracted six times with 5 ml of hexane. The collected hexane was evaporated, and 3 ml of methanol and a few drops of acetyl chloride were added to the sample, and it was boiled for 1 h. Then the sample was evaporated again, 1–2 ml of H_2O and a few drops of methyl orange were added, and methyl esters of fatty acids were extracted six times with hexane. After that, hexane was evaporated and 500 μl of benzene were added.

The benzene extract was pipetted onto a chromatographic plate, and a mixture of $C_6H_{14}/C_2H_5\text{-}O\text{-}C_2H_5/CH_3COOH$ (8:2:0.1, by vol.) was used as the mobile phase. When the front passed to the top of the plate, the plate was removed and airdried for 1–2 min. Then the plate was treated with a 0.001% solution of 2′,7′-dichlorofluorescein (Acros, 19153) in ethanol and air-dried for 5–7 min. The FAME-containing zones were visualized with UV light ($\lambda = 365$ nm). The sorbent from the FAME-containing chromatographic plate area was then removed with a scalpel and transferred to a Schott glass filter, and the FAMEs were eluted from the sorbent by washing with hexane six times (Voronkov, Ivanova, and Kumachova, 2020).

The identification and quantification of FAMEs was performed using GLC-MS with an Agilent 7890A GC (Agilent Technologies, Santa Clara, CA, USA) fitted with a capillary column (DB-23, 60 m×0.25 mm) containing a grafted (50%-cyanopropyl)-methylpolysiloxane polar liquid phase as a 0.25 μm thick film. The FAMEs were separated under the conditions as indicated in Voronkov *et al.* (2020). To identify individual FAME species and calculate their relative concentrations in the mixture (mol-%), a NIST search library and the MSD Chem Station software were used.

To characterize the unsaturation level of lipid fatty acids, the unsaturation index, $UI = \sum P_i n_i/100$, and saturation coefficient, $SC = \Sigma P_i^{sat.}/\Sigma P_i^{unsat.}$, were calculated; where: P_i is % of FA, n_i is the number of double bonds in each of the FA.

The activity efficiencies of the ω-9, ω-6 and ω-3 desaturases were calculated, as percentages, as the stearic desaturation ratio, SDR = (18:1)/(18:0 + 18:1), as the oleic desaturation ratio, ODR = (18:2 + 18:3)/(18:1 + 18:2 + 18:3), and as the

linoleic desaturation ratio, LDR = (18:3)/(18:2 + 18:3). Simple ratios 18:2/18:0 (2/0), 18:2/18:1 (2:1), and 18:2/18:3 (2:3) were also calculated.

Statistical analyses.—All the experiments were performed in triplicate with at least three independent runs. The data are presented in tables and a graph as means ± SEM. Statistical analysis was performed using one-way ANOVA followed by post-hoc analysis using Tukey's honest significant difference (HSD) for unequal N test. Different letters show significantly different values. Mean values were considered significantly different at $p < 0.05$. To check if there is a correlation between the FAs content or between the FAs groups in *A. nidus* and *A. trichomanes* or in *P. bifurcatum* and *A. nidus,* correlation coefficient (r) was calculated using Microsoft Excel software.

Results

The lipids of *P. bifurcatum, A. nidus,* and *A. trichomanes* were comprised of 14, 27, and 23 (respectively) species of individual 12–28 FAs (Table 1). In all three studied ferns, the major FAs were palmitic (16:0), oleic (18:1n-9), linoleic (18:2n-6), and α-linolenic (18:3n-3). In addition, *P. bifurcatum* had stearic (18:0) and arachidic (20:0) acids, whereas *A. nidus* had lignoceric (24:0) and cerotic (26:0) acids for major components. It should be noted that the content of 16:0 was significantly higher in the epiphytic ferns, whereas the content of unsaturated 18:1n-9 and 18:2n-6 was significantly higher in *A. trichomanes.* Moreover, the content of 18:3n-3 was much higher in *P. bifurcatum* than in the representatives of the *Asplenium* genus under study. Such significant differences in the content of mono-, di-, and triene acids in the ferns led to the differences in the UI indices. Thus, *A. trichomanes* had the highest UI of lipids (1.373), whereas it was somewhat lower in *A. nidus* and *P. bifurcatum* (0.927 and 1.140, respectively). A distinctive feature of the composition of lipid FAs of all studied species was the presence of a fairly large variety of very-long-chain FAs (VLCFAs) (Ivanova *et al.*, 2009). For *A. nidus*, these were represented by 11 types of FAs (seven saturated FAs and one mono-, di-, tri-, and tetraene FAs), in *A. trichomanes* – by seven types (three saturated FAs and four unsaturated FAs), and in *P. bifurcatum* – by five types of FAs (two saturated FAs and one di-, tri-, tetraene FA). For the lipids of epiphytic ferns *A. nidus* and *P. bifurcatum*, individual saturated VLCFAs (20:0, 24:0, and 26:0) were the major ones, as mentioned before. However, this was not observed in the terrestrial fern. Therefore, for *A. trichomanes,* $\sum$VLCFA will be only 4.3% of all FAMEs, which is 2.5 and almost five times less than that for *P. bifurcatum* (10.8% of all FAMEs) and *A. nidus* (21.1% of all FAMEs).

Most saturated VLCFAs, except for 20:0, 24:0 and 26:0 for some fern species, as well as all unsaturated VLCFAs belonged to minor FAs. It should be noted that the FA that is characteristic of most seed-free vascular plants – arachidonic (20:4n-6) was present in all studied ferns. The greatest diversity of VLCFAs was found in *A. nidus*: 20:0, gondoic (20:1n-9), 11-*cis*,14-*cis*-eicosadienoic (20:2n-6), 8-*cis*,11-*cis*,14-*cis*-eicosatrienoic (20:3n-6), 20:4n-6,

TABLE 1. Lipid fatty acid composition (mass % of the amount of FAMEs) and absolute content of fatty acid (μmol of esterified FAs/g wet weight or dry weight) of the *Platycerium bifurcatum*, *Asplenium nidus*, and *Asplenium trichomanes* leaves. Values are presented as means ± SEM. Different letters indicate a significant difference between the means ($p < 0.05$). One-way ANOVA, followed by Tukey's HSD test was performed separately for each individual FA.

Life form		**Epiphyte**		**Terrestrial**
Reference number	**FA**	***Platycerium bifurcatum***	***Asplenium nidus***	***Asplenium trichomanes***
1	12:0	-	$0.25^b \pm 0.024$	$0.01^a \pm 0.002$
2	13:0	-	0.02 ± 0.002	-
3	14:0	$1.34^b \pm 0.117$	$1.09^b \pm 0.121$	$0.62^a \pm 0.054$
4	15:0	$0.66^b \pm 0.053$	$0.70^b \pm 0.069$	$0.44^a \pm 0.032$
5	16:0	$28.40^b \pm 2.649$	$32.06^b \pm 3.853$	$18.71^a \pm 2.182$
6	16:1n-9	-	$0.63^a \pm 0.077$	$1.24^b \pm 0.202$
7	16:1n-7	-	$0.67^a \pm 0.071$	$0.65^a \pm 0.072$
8	16:1n-5	-	-	0.93 ± 0.112
9	16:2n-6	$0.99^c \pm 0.102$	$0.03^a \pm 0.006$	$0.65^b \pm 0.069$
10	16:3n-3	-	-	0.12 ± 0.014
11	17:1n-7	-	$0.04^a \pm 0.010$	$0.10^b \pm 0.014$
12	18:0	$7.18^c \pm 1.127$	$3.92^b \pm 0.874$	$2.11^a \pm 0.423$
13	18:1n-11	-	1.32 ± 0.119	-
14	18:1n-9	$15.60^b \pm 2.338$	$10.43^a \pm 1.720$	$26.98^c \pm 3.876$
15	18:1n-7	$0.22^a \pm 0.034$	-	$0.76^b \pm 0.024$
16	18:2n-5	-	$0.66^a \pm 0.157$	$3.65^b \pm 0.329$
17	18:2n-6	$20.06^a \pm 2.206$	$18.13^a \pm 2.900$	$31.35^b \pm 3.763$
18	19:0	-	0.13 ± 0.010	-
19	18:3n-3	$14.70^b \pm 1.756$	$8.81^a \pm 0.881$	$7.37^a \pm 0.910$
20	20:0	$5.35^c \pm 0.691$	$1.55^b \pm 0.162$	$0.27^a \pm 0.024$
21	20:1n-9	-	$0.03^a \pm 0.110$	$0.12^b \pm 0.015$
22	20:2n-6	$0.82^b \pm 0.066$	$0.75^b \pm 0.068$	$0.20^a \pm 0.024$
23	20:3n-6	$1.06^b \pm 0.215$	$1.31^b \pm 0.157$	$0.40^a \pm 0.045$
24	20:4n-6	$1.78^a \pm 0.301$	$2.50^{ab} \pm 0.459$	$2.79^b \pm 0.474$
25	22:0	$1.84^b \pm 0.277$	$2.29^b \pm 0.357$	$0.40^a \pm 0.038$
26	23:0	-	0.37 ± 0.040	-
27	24:0	-	$6.20^b \pm 0.745$	$0.12^a \pm 0.013$
28	25:0	-	0.52 ± 0.070	-
29	26:0	-	5.24 ± 0.734	-
30	28:0	-	0.36 ± 0.064	-
FA mass, μmol/g ww		9.926 ± 0.561	7.921 ± 0.570	67.114 ± 4.363
FA mass, μmol/g dw		86.013 ± 6.013	54.376 ± 4.385	272.268 ± 18.459

behenic (22:0), tricosanoic (23:0), 24:0, pentacosanoic (25:0), 26:0, and montanic (28:0) acids (Table 1).

The difference between the epiphytic ferns *P. bifurcatum* and *A. nidus* and the terrestrial fern *A. trichomanes* is more evident when FAs groups are analyzed depending on the number of double bonds (Fig. 1). So, in the epiphytic ferns *P. bifurcatum* and *A. nidus*, more than 50% of the total amount of FAMEs were saturated FAs, whereas this class of FAs only made up 20% in the terrestrial fern, with most of the unsaturated FAs being mono- and diene acids, which in total made up about 65% of all FAMEs.

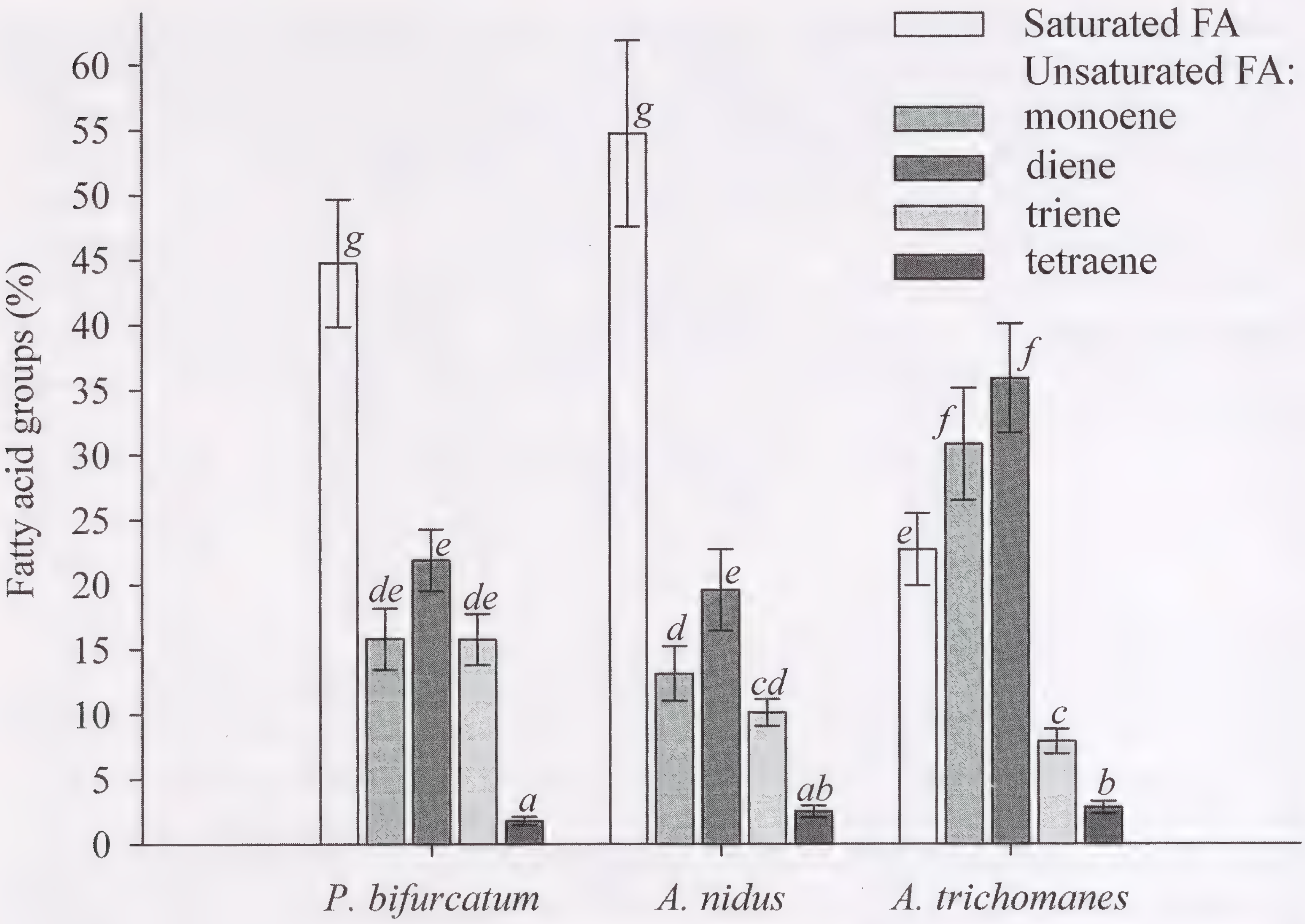

FIG. 1. Saturated and unsaturated (monoene, diene, triene, and tetraene) fatty acids composition of the *Platycerium bifurcatum*, *Asplenium nidus,* and *Asplenium trichomanes* leaves. Values are presented as means ± SEM. Different letters indicate a significant difference between the means ($p < 0.05$). One-way ANOVA, followed by Tukey's HSD test was performed separately for FA groups.

All the features of the composition of lipid FAs of the three studied species are reflected by the SC values. For epiphytes *P. bifurcatum* and *A. nidus*, SC values are 0.81 and 1.21, respectively, and for *A. trichomanes* SC is several times lower (0.29).

A strong significant positive correlation was found between the FAs content in two epiphytic fern species (Fig. 2A). A weaker but significant positive correlation was observed between the FAs content in two *Asplenium* species (Fig. 2C). Moreover, there was a strong correlation between the content of FA groups (%) in *P. bifurcatum* and *A. nidus* (Fig. 2B), whereas there was no correlation between the content of FA groups (%) in two *Asplenium* species (Fig. 2D).

Striking differences in the absolute amount of FAMEs were observed between the studied species. For epiphytic ferns it was 9.926 and 7.921 μmol/g wet weight (ww) (*P. bifurcatum* and *A. nidus*, respectively), whereas for *A. trichomanes* this value was almost 7-8 times higher (Table 1). The differences in the amount of FAMEs between the epiphytic and terrestrial species were slightly less strking when expressed on a dry weight (dw) basis, but in *A. trichomanes*, the mass of FAMEs remained 3-5 times higher than the mass of FAMEs in the epiphytic ferns under study (Table 1).

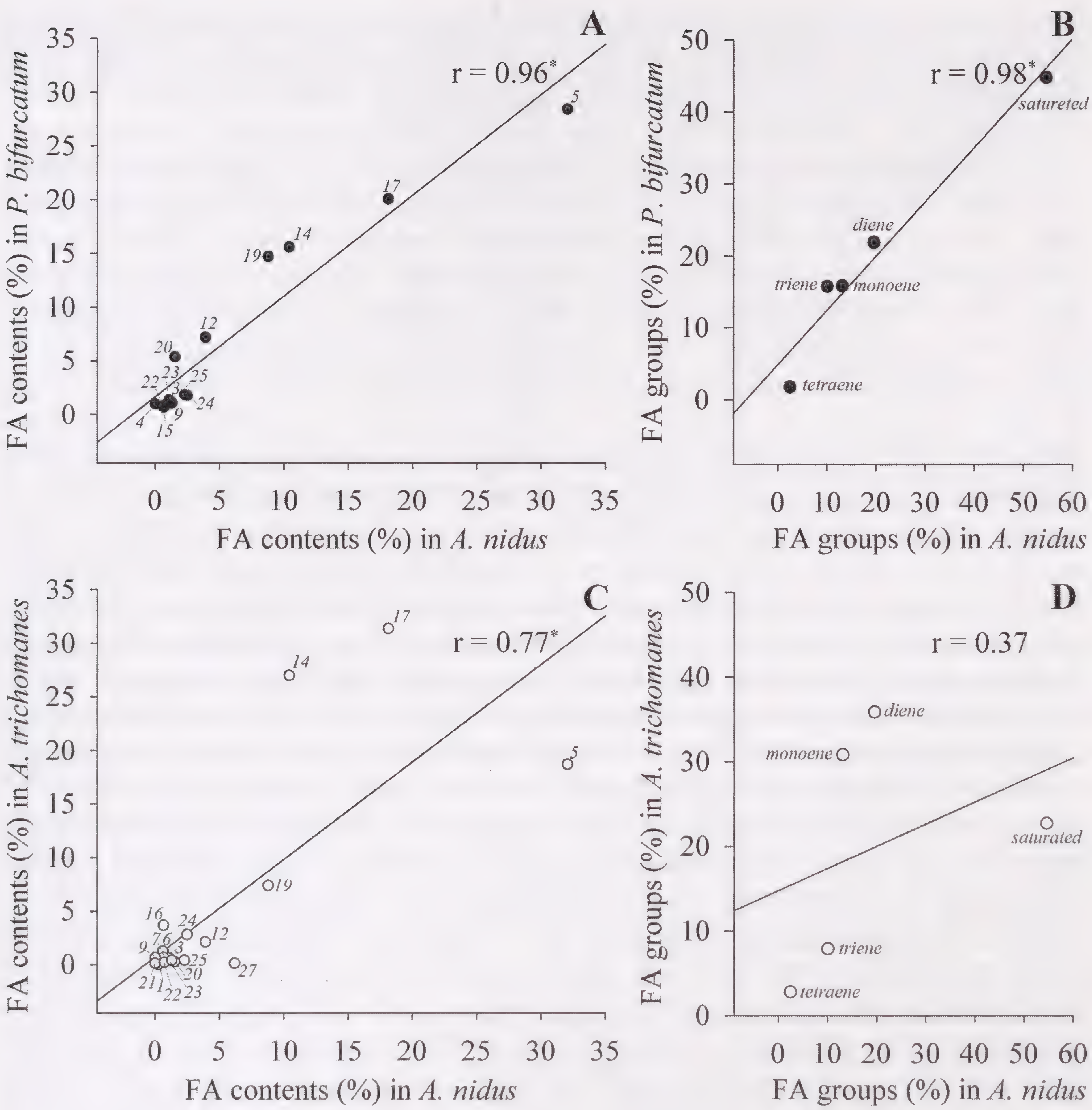

FIG. 2. Correlation between the content of individual fatty acids in *Platycerium bifurcatum* and *Asplenium nidus* (A), in *Asplenium nidus* and *Asplenium trichomanes* (C) and between the FA groups (specified depending on the number of double bonds) in *Platycerium bifurcatum* and *Asplenium nidus* (B), in *Asplenium nidus* and *Asplenium trichomanes* (D). Reference numbers for the individual FAs are shown in Table 1. Given are the regression lines and the Pearson correlation coefficients (r) (* significant at $p < 0.05$).

In *P. bifurcatum* and *A. nidus*, the ODR and LDR values, as well as the ratios 2/1 and 2/3, were higher than those of *A. trichomanes* (Table 2). In contrast, the SDR and the 2/0 ratio were markedly higher in *A. trichomanes* (Table 2).

DISCUSSION

A comparative analysis of the literature and our data on the FAs content in ferns revealed both characteristic features of all ferns and distinctive features

TABLE 2. Desaturation ratios in the *Platycerium bifurcatum*, *Asplenium nidus*, and *Asplenium trichomanes* leaves (relative units). Values are presented as means ± SEM. Different letters indicate a significant difference between the means ($p < 0.05$). One-way ANOVA, followed by Tukey's HSD test, was performed separately for each parameter.

	Platycerium bifurcatum	*Asplenium nidus*	*Asplenium trichomanes*
SDR	$0.685^{a} \pm 0.048$	$0.727^{a} \pm 0.065$	$0.928^{b} \pm 0.080$
ODR	$0.690^{ab} \pm 0.058$	$0.721^{b} \pm 0.048$	$0.589^{a} \pm 0.047$
LDR	$0.423^{b} \pm 0.041$	$0.327^{b} \pm 0.039$	$0.190^{a} \pm 0.015$
2/0	$2.796^{a} \pm 0.242$	$4.620^{b} \pm 0.508$	$14.871^{c} \pm 1.464$
2/1	$1.286^{a} \pm 0.135$	$1.739^{b} \pm 0.171$	$1.162^{a} \pm 0.093$
2/3	$1.365^{a} \pm 0.163$	$2.057^{b} \pm 0.256$	$4.255^{c} \pm 0.553$

of the fern species under study. Thus, algae (Sinetova *et al.,* 2020) and most higher spore-producing plants (Beike *et al.*, 2014), including ferns (Sato and Furuya, 1984), are characterized by the presence of 20:4n-6 acid, which is not found in seed plant tissues (Ivanova *et al.*, 2019; Voronkov *et al.*, 2020). We likewise found this acid to be a component of all three fern species. It should be noted that it is usually present in ferns at both gametophytic (Nekrasov, Shelikhan, and Svetashev, 2009) and sporophytic stages (DeLong *et al.*, 2011), but is absent from fern spores (Gemmrich, 1977). There is also evidence in the literature that some ferns do not contain 20:4n-6 (Brouwer *et al.*, 2016), but, if the latter is present, eicosapentaenoic acid (20:5n-3) is always also found in the tissues (Jamieson and Reid, 1975; Nekrasov, Shelikhan, and Svetashev, 2009; DeLong *et al.*, 2011; Nekrasov *et al.*, 2019). However, 20:5n-3 was never detected in our study (Fig. S1–S3, supplementary material). It is known that 20:4n-6 is synthesized from 18:2n-6, and 20:5n-3 is synthesized from 18:3n-3 using the enzymes Δ6- and Δ5-desaturases and Δ6-elongase (Sayanova and Napier, 2004). Thus, it can be assumed that due to the predominance of ω-6 substrate, the biosynthetic pathway of 20:5n-3 is most likely to be suppressed. However, FA synthesis pathways in ferns are currently extremely poorly studied, and therefore the absence of 20:5n-3 acid species in the lipids of the studied species could also be explained by metabolic peculiarities.

Our results show that VLCFA content in the lipids of the sori of the epiphytic ferns *P. bifurcatum* and *A. nidus* was several times higher than that in the leaves of the terrestrial fern *A. trichomanes*. The analysis of the literature indicates that the average VLCFA values in lipids of tissues of various ferns range from 10% (Nekrasov *et al.*, 2019) to 20% (Jamieson and Reid, 1975; DeLong *et al.*, 2011). Currently, VLCFAs are credited with many functions in plant life. It has been reliably shown that they are an important component in the formation of plant tissues, controlling cell proliferation, participating in the regulation of cytokinin synthesis (Nobusawa *et al.*, 2013) and polar auxin transport (Roudier *et al.*, 2010). They increasingly appear to play an important signaling role (Bach and Faure, 2010), and information on their participation in the response of plants to the penetration of pathogens is especially remarkable (Raffaele, Leger, and Roby, 2009). In some of our work,

we also pointed to the role of VLCFAs as one of the factors of passive immunity of plants to mycoses (Voronkov *et al.*, 2020; Voronkov, Kumachova, and Ivanova, 2020). However, for epiphytes – plants that live on other plants and are constantly exposed to interactions with microorganisms, high levels of VLCFAs can be of special importance. It is understood that the penetration of any pathogenic organism (bacteria or fungus) induces a complex organizational process, which includes the synthesis of VLCFAs, sphingolipids, and cuticular compounds, and the changes in plasma membrane microdomain organization. Therefore, pathogen growth is differentially affected by the onset of the hypersensitive response, according to their invasion strategy (Raffaele, Leger, and Roby, 2009). Thus, VLCFAs can be involved in differentiated responses of plants to the penetration of a variety of pathogens. This is undoubtedly very important for epiphytic ferns, often living on the decaying remains of leaf litter and other organics. Therefore, we conclude that the high content of VLCFAs in the lipids of *P. bifurcatum* and *A. nidus* may be related to the peculiarities of their life form.

It is known that saturated FAs typically make up about 25% of the total lipid FAs in ferns (Jamieson and Reid, 1975; DeLong *et al.*, 2011; Nekrasov *et al.*, 2019). Approximately the same level of saturated acids was observed in *A. trichomanes*, and these data are clearly displayed by a low SC. Conversely, the amount of saturated FAs in lipids of epiphytic ferns is much higher, slightly exceeding 50% of all FAMEs. The main contribution to the high SC belongs to 16:0, as well as, to a slightly lesser extent, to 18:0, 20:0, and 22:0 FAs. Palmitic acid is known to be a primary higher FA synthesized in the cell, whereas nearly all other FAs of natural lipids are the products of its further modification caused by elongation, desaturation, or insertion of various functional groups, such as methyl, hydroxy, oxo, and epoxy (Sidorov *et al.*, 2014). As a saturated FA, 16:0 is used by the cell for regulating its functional state by shifting the membrane fluidity under adverse environmental conditions. It is noted that 16:0 predominates in high-polar lipids that may be compared to annular lipids and are indispensable for the operation of numerous enzymatic systems (Zhukov, 2015). Indeed, in the epiphytes *P. bifurcatum* and *A. nidus*, higher levels of the activity of ω6- and ω9-desaturases have been found compared to the terrestrial fern *A. trichomanes* (Table 2). Hypothetically, this may indicate a higher potential of the plant for the formation of unsaturated FAs if this is necessary (Cartea *et al.*, 1998; Brown, Slabas, and Rafferty, 2009). It should be noted that epiphytic ferns, despite the high content of saturated FAs, also have a rather high UI. This is probably due to the greater number of unsaturated VLCFAs. However, the UI value of *A. trichomanes* is still noticeably higher, which, we assume, can indicate its greater cold tolerance (Mironov *et al.*, 2012), since it grows in both tropical and temperate regions.

The lipids of *P. bifurcatum* and *A. nidus* differ markedly from the ones of *A. trichomanes* in the absolute content of FAMEs. In the epiphytes, the mass of FAs is significantly lower than in the terrestrial fern. This may be related to the more complex structure of *A. trichomanes* leaves. A decrease in the differences

in the weight of FAs when calculated on dw basis indicates that the leaves of epiphytic ferns contain a greater amount of water, which is typical for angiosperm epiphytes, as they tend to accumulate intermittently incoming moisture in their tissues (Silvera and Lasso, 2016; Zotz, 2016).

Unfortunately, to date, the features of the FAs composition of fern lipids have been studied very poorly. We were unable to find any data on the composition of FAs in epiphytic ferns. However, we can search for similar differences in FAs profile between epiphytic and terrestrial seed plants, comparing one group of seed plants that occupies an ecological niche similar to epiphytic ferns, *e.g.*, orchids. Thus, in the work of Holman and Nichols (1972), a high content of saturated FAs was noted. This was also characteristic of the studied epiphytic ferns *P. bifurcatum* and *A. nidus* (Table 1). Therefore, it may be suggested that high content of saturated FAs is a common characteristic of epiphytic plants. Bearing in mind the fact that in epiphytic fungi associated with algal crusts, high content of 16:0 and 18:0 was also noted (Ellis, Geuns, and Zarnowski, 2002), it can be suggested that a high SC in epiphytic ferns may be due to the need for intercellular host-fungal interactions. As mentioned above, VLCFAs may also be involved in establishing these interactions.

In conclusion, the features of the total lipid FAs composition that we discovered are closer in unrelated epiphytic species *P. bifurcatum* and *A. nidus* than in related *A. nidus* and *A. trichomanes*. Their evolutionary distribution to different ecological groups clearly supports the hypothesis that the habitat greatly influences the FAs profile in these species. Unfortunately, ferns, in comparison with angiosperms, are extremely poorly studied in this regard. Our work is only a small contribution to understanding the physiology of these amazing ancient plants, and it certainly needs to be continued.

Acknowledgments

ASV and TVI have contributed equally to this work.

This work was supported by the Ministry of Science and Higher Education of the Russian Federation (Project № 0106-2019-0008).

Literature Cited

Andama, E., C. M. Michira, and G. B. Luilo. 2003. Studies on epiphytic ferns as potential indicators of forest disturbances. XII World Forestry Congress, 0129-B1. Quebec, Canada.

Bach, L., and J.-D. Faure. 2010. Role of very-long-chain fatty acids in plant development, when chain length does matter. Comptes Rendus Biologies 333:361–370.

Beike, A. K., C. Jaeger, F. Zink, E. L. Decker, and R. Reski. 2014. High contents of very long-chain polyunsaturated fatty acids in different moss species. Plant Cell Reports 33:245–254.

Brouwer, P., A. van der Werf, H. Schluepmann, G.-J. Reichart, and K. G. J. Nierop. 2016. Lipid yield and composition of *Azolla filiculoides* and the implications for biodiesel production. Bioenergy Research 9:369–377.

Brown, A. P., A. R. Slabas, and J. B. Rafferty. 2009. Fatty acid biosynthesis in plants – metabolic pathways, structure and organization. Pp. 11–34, *in* H. Wada and N. Murata (eds.), *Lipids in Photosynthesis: Essential and Regulatory Functions*. Springer, Netherlands.

Cartea, M. E., M. Migdal, A. M. Galle, G. Pelletier, and P. Guerche. 1998. Comparison of sense and antisense methodologies for modifying the fatty acid composition of *Arabidopsis thaliana* oilseed. Plant Science 136:181–194.

Christenhusz, M. M., J., M. Fay, and J.W. Byng. 2018. *The Global Flora: Special Edition: GLOVAP Nomenclature Part 1.* Plant Gateway Ltd., Bradford.

Cody, W. J. 1968. *Asplenium trichomanes* new to Newfoundland. American Fern Journal 58:179–180.

DeLong, J. M., D. M. Hodges, R. K. Prange, C. F. Forney, P. M. A. Toivenon, M. C. Bishop, M. L. Elliot, and M. A. Jordan. 2011. The unique fatty acid and antioxidant composition of ostrich fern (*Matteuccia struthiopteris*) fiddleheads. Canadian Journal of Plant Science 91:919–930.

DeLong, J. M., D. M. Hodges, R. K. Prange, C. F. Forney, L. Fan, M. C. Bishop, M. L. Elliot, M. A. Jordan, and C. Doucette. 2013. The influence of cold water storage on fatty acids, antioxidant content and activity, and microbial load in ostrich fern (*Matteuccia struthiopteris*) fiddleheads. Canadian Journal of Plant Science 93:683–697.

Ellis, R. J., J. M. C. Geuns, and R. Zarnowski. 2002. Fatty acid composition from an epiphytic strain of *Fusarium oxysporum* associated with algal crusts. Acta Microbiologica Polonica 51:391–394.

Gemmrich, A. K. 1977. Fatty acid composition of fern spore lipids. Phytochemistry 16:1044–1046.

Holman, R. T. and P. C. Nichols. 1972. Characterization of the lipids of some orchids. Phytochemistry 11:333–337.

Hoshizaki, B. J. and M. G. Price. 1990. *Platycerium* update. American Fern Journal 80:53–69.

Ivanova, T. V., A. S. Voronkov, E. I. Kuznetsova, T. Kh. Kumachova, V. K. Zhirov, and V. D. Tsydendambaev. 2019. Lipid fatty acids from the pericarp of *Cydonia oblonga* Mill. and *Mespilus germanica* L. are involved in plant adaptation to altitudinal zonality. Doklady Biochemistry and Biophysics 486:229–233.

Ivanova, T. V., A. S. Voronkov, T. Kh. Kumakhova, and V. D. Tsydendambaev. 2020. Distinguishing features of fatty acid content and composition in total lipids of *Malus orientalis* Uglitzk. pericarp. Russian Journal of Plant Physiology 67:463–471.

Ivanova, T. V., N. A. Myasoedov, V. P. Pchelkin, V. D. Tsydendambaev, and A. G. Vereshchagin. 2009. Increased content of very-long-chain fatty acids in the lipids of halophyte vegetative organs. Russian Journal of Plant Physiology 56:787–794.

Jamieson, G. R. and E. H. Reid. 1975. The fatty acid composition of fern lipids. Phytochemistry 14:2229–2232.

Martin, C. E. 2009. Comparative photosynthetic capacity of abaxial and adaxial leaf sides as related to exposure in two epiphytic ferns in a subtropical rainforest in Northeastern Taiwan. American Fern Journal 99:145–154.

Metzgar, J. S. 2016. Clarifying the taxonomy of Alaskan *Asplenium trichomanes* populations. American Fern Journal 106:227–229.

Mironov, K. S., R. A. Sidorov, M. S.Trofimova, V. S. Bedbenov, V. D. Tsydendambaev, S. I. Allakhverdiev, and D. A. Los. 2012. Light-dependent cold-induced fatty acid unsaturation, changes in membrane fluidity, and alterations in gene expression in *Synechocystis.* Biochimica et Biophysica Acta (BBA) – Bioenergetics 1817:1352–1359.

Nath, K., M. K. Bhattacharya, A. Sen, S. Kar. 2013. Antibacterial activity of frond extract of *Asplenium Nidus* L., a threatened ethno-medicinal fern of North East India. International Journal of Pharmacognosy and Phytochemistry 28:1169–1172.

Nekrasov, E. V., L. A. Shelikhan, and V. I. Svetashev. 2009. Fatty acid composition of gametophytes of *Matteuccia struthiopteris* (L.) Tod. (Onocleaceae, Polypodiophyta). Botanica Pacifica 8:63–66.

Nekrasov, E. V., V. I. Svetashev, O. V. Khrapko, and M. V. Vyssotski. 2019. Variability of fatty acid profiles in ferns: relation to fern taxonomy and seasonal development. Phytochemistry 162:47–55.

Nobusawa, T., Y. Okushima, N. Nagata, M. Kojima, H. Sakakibara, and M. Umeda. 2013. Synthesis of very-long-chain fatty acids in the epidermis controls plant organ growth by restricting cell proliferation. PLoS Biology 11:e1001531.

Pemberton, R. W. 2003. The common staghorn fern, *Platycerium bifurcatum,* naturalizes in southern Florida. American Fern Journal 93:203–206.

Raffaele, S., A. Leger, and D. Roby. 2009. Very long chain fatty acid and lipid signaling in the response of plants to pathogens. Plant Signaling and Behavior 4:94–99.

Roudier, F., L. Gissot, F. Beaudoin, R. Haslam, L. Michaelson, J. Marion, D. Molino, A. Lima, L. Bach, H. Morin, F. Tellier, J.-C. Palauqui, *et al.* 2010. Very-long-chain fatty acids are involved in polar auxin transport and developmental patterning in *Arabidopsis.* The Plant Cell 22:364–375.

Sato, N. and M. Furuya. 1984. The composition of lipids and fatty acids determined at various stages of haploid and diploid generations in the fern *Adiantum capillus-veneris.* Physiologia Plantarum 62:139–147.

Sayanova, O. V, J. A. Napier. 2004. Eicosapentaenoic acid: biosynthetic routes and the potential forsynthesis in transgenic plants. Phytochemistry 65:147–158.

Sidorov, R. A., A. V. Zhukov, V. P. Pchelkin, and V. D. Tsydendambaev. 2014. Palmitic acid in higher plant lipids. Pp. 125–144, *in* L. F. Porto (ed.), *Palmitic Acid: Occurrence, Biochemistry and Health Effects.* NOVA Publishers, New York.

Silvera, K. and E. Lasso. 2016. Ecophysiology and crassulacean acid metabolism of tropical epiphytes. Pp. 25–43, *in* G. Goldstein and L. S. Santiago (eds.), *Tropical Tree Physiology: Adaptations and Responses in a Changing Environment.* Springer International Publishing, Switzerland.

Sinetova, M. A., R. A. Sidorov, A. Yu. Starikov, A. S. Voronkov, A. S. Medvedeva, Z. V. Krivova, M. S. Pakholkova, D. V. Bachin, V.S. Bedbenov, D.A. Gabrielyan, B.K. Zayadan, K. Bolatkhan, *et al.* 2020. Assessment of the biotechnological potential of cyanobacterial and microalgal strains from the culture collection of the Institute of Plant Physiology. Applied Biochemistry and Microbiology 56:36–50.

Voronkov, A. S., T. Kh. Kumachova, and T. V. Ivanova. 2020. Plant passive immunity: micromorphological and biochemical features of the Maloideae (Rosaceae) external tissues. Pp. 1–16, *in* S. Borek (eds.), *Current Research Trends in Biological Science. Volume 1.* Book Publisher International, London.

Voronkov, A. S., T. V. Ivanova, E. I. Kuznetsova, and T. Kh. Kumachova. 2019. Adaptations of *Malus domestica* Borkh. (Rosaceae) fruits grown at different altitudes. Russian Journal of Plant Physiology 66:922–931.

Voronkov, A. S., T. V. Ivanova, T. K. Kumachova, A. D. Kozhevnikova, and V. D. Tsydendambaev. 2020. Polyunsaturated and very-long-chain fatty acids are involved in the adaptation of Maloideae (Rosaceae) to combined stress in the mountains. Chemistry and Biodiversity 17:e1900588.

Voronkov, A., T. Ivanova, and T. Kumachova. 2020. Micromorphological and biochemical features of *Malus* fruit*: Malus domestica* Borkh. and its parent species—*Malus orientalis* Uglitzk. Brazilian Journal of Botany 43:21–28.

Zhukov, A.V. 2015. Palmitic acid and its role in the structure and functions of plant cell membranes. Russian Journal of Plant Physiology 62:706–713.

Zotz, G. 2016. *Plants on Plants – the Biology of Vascular Epiphytes.* Springer International Publishing, Switzerland.

American Fern Journal 111(2):129–146 (2021)
Published on 7 June 2021

Population Genetics of Species in the Genera *Botrychium* and *Botrypus* (Ophioglossaceae)

Evelyn Webb Williams
Adaptive Restoration LLC., 8864 Offerdahl Road, Mount Horeb, WI, 53572, USA

Abstract.—The population genetics of ferns, which results from initiation of individuals in a new location (often via long-distance dispersal) plus a wide range of mating systems, merit continued study. In the case of species in the subfamily Botrychioideae (specifically the genera *Botrychium* and *Botrypus*), previous work using allozyme and isozyme techniques revealed low genetic diversity and weak population genetic structure. This lack of genetic differentiation between populations is in spite of underground fertilization in the genus resulting in high levels of inbreeding and primarily fixed heterozygosity in tetraploids. In the present study, Amplified Fragment-Length Polymorphisms (AFLPs) were used to examine population genetics and structure of three species in the genus *Botrychium* and one species in the genus *Botrypus*. Measures of population genetic diversity were generally low, with the highest measures in the relatively common *Botrypus virginianus*. Across all species, measures of population differentiation were low and most genetic variation was contained within populations. Bayesian analysis of population structure using the program STRUCTURE corroborated these findings, with inferred genetic clusters that generally did not correspond to geographic collecting locations. These results agree with previous studies, with low genetic diversity within and among populations likely due to self-fertilization that limits outcrossing and long-distance spore dispersal that results in genetically similar populations.

Key Words.—AFLPs, *Botrychium angustisegmentum, Botrychium matricariifolium, Botrychium pallidum, Botrypus virginianus*

Multiple factors impact genetic diversity and population differentiation in fern species. Long-distance spore dispersal plays an important role in colonizing new populations in fragmented habitats (De Groot *et al.*, 2012), which further impacts population genetic structure. The resulting amount of genetic diversity found within and among populations is worth continued study, especially since different mating systems also impact genetic structure. Ferns in the genus *Botrychium* (Ophioglossaceae) present a particularly interesting case study of the impact of long-distance dispersal, given their underground mating system that results predominately in self-fertilization.

Botrychium species are found world-wide (Johnson-Groh and Lee, 2002) although individual plants are quite small (typically less than 15 cm), making discovery of them notable wherever they are spotted. Species distinctions are notoriously cryptic (Paris, Wagner, and Wagner, 1989), and over half of *Botrychium* species are allotetraploids (Hauk, 1995; Farrar, 1998; Hauk and Haufler, 1999; Dauphin, Grant, and Mráz, 2016; Dauphin *et al.*, 2018). Previous work has teased apart these allotetraploid relationships in the genus using allozyme markers as well as chloroplast and nuclear DNA sequences (Hauk,

email address: ewwilli@gmail.com

Parks, and Chase, 2003; Hauk, Kennedy, and Hawke, 2012; Williams and Waller, 2012; Dauphin, Vieu, and Grant, 2014; Dauphin, Grant, and Mráz, 2016; Dauphin, 2017; Farrar and Gilman, 2017; Dauphin *et al.*, 2018). There is also evidence that allotetraploids are formed from recurring and distinct hybridizations of the same parental species (Williams, Farrar, and Henson, 2016; Dauphin *et al.*, 2017), often leading to a wide range of confusing morphology in species such as the common allotetraploid *Botrychium matricariifolium*.

Populations of *Botrychium* are ephemeral (Johnson-Groh and Lee, 2002; Williams and Waller, 2015) and tend to be in disturbed habitats with herbaceous vegetation that supports *Botrychium* via mycorrhizal associations. These include old roads and trails, shifting sand dunes, tundra, and Alpine meadows. Species are hypothesized to be mycoheterotrophs, forming associations with *Glomerus* species (Winther and Friedman, 2007), among others. Spores do not germinate without these associations and sporophytes can spend several years underground before sending up an above-ground photosynthetic structure (Johnson-Groh *et al.*, 2002). This long generation time likely limits the impact of genetic drift on population differentiation. Fertilization via bisexual gametophytes is underground (Johnson-Groh *et al.*, 2002), likely limiting gene flow between individuals. In addition to keeping genetic diversity low, underground self-fertilization results in diploids that are homozygous and polyploids with fixed heterozygosity. Rare outcrossing would only occur when soil moisture conditions allowed sperm to swim to another gametophyte, and has been estimated at 10% (Farrar, 2011). Spore dispersal is the only method of gene movement between populations, which is relatively rare given that, as has been demonstrated in *Botrypus virginianus* (L.) Michx., a related, taller species (up to half a meter), less than 10% of spores travelled beyond 5 meters (Peck, Peck, and Farrar, 1990). Although rare, long-distance spore dispersal undoubtedly occurs, enabling *Botrychium* species to colonize new habitats. Infrequent long distance dispersal, underground fertilization, and long generation time likely result in low genetic diversity and little population structure in *Botrychium* populations.

Previous research has used isozymes and ISSRs to study the population genetics of species in the genus and related genera (Table 1: McCauley, Whittier, and Reilly, 1985; Soltis and Soltis, 1986; Watano and Sahashi, 1992; McMaster, 1994; Hauk and Haufler, 1999; Camacho and Liston, 2001; Barker and Hauk, 2003; Chung *et al.*, 2010, 2013; Dauphin, 2017). In general, the number of alleles in isozyme studies was low, regardless of ploidy level. Estimates of heterozygosity were also low, again regardless of ploidy level and in spite of fixed heterozygosity reported in the genus (Hauk and Haufler, 1999). In related genera, measures were relatively low and AMOVA results found most variation was within populations, not among. Although few studies calculated measures of population differentiation, Dauphin (2017) found low levels of pairwise F_{ST} in *Botrychium lunaria*. Taken together, these results indicate that indeed genetic variation and population differentiation is low.

Table 1. Population genetic metrics of species in the Ophioglossaceae family

Species	Ploidy	Technique[1]	Reference	# loci	alleles per locus	% poly-morphic	FST[2]	H[3]	Notes
Botrychium angustisegmentum	diploid	AFLPs	This study	207	-	37.36	Φ_{PT}=0.034	0.11	Mantel test not significant, AMOVA found 97% within
Botrychium ascendens	tetraploid	isozymes	Hauk and Haufler (1999)	6	1.33	33.33	-	0.169	
Botrychium crenulatum	diploid	isozymes	Hauk and Haufler (1999)	6	1	0	-	0	
Botrychium echo	tetraploid	isozymes	Hauk and Haufler (1999)	6	1.67	66.67	-	0.343	
Botrychium hesperium	tetraploid	isozymes	Hauk and Haufler (1999)	6	1.5	50	-	0.253	
Botrychium lanceolatum	diploid	isozymes	Hauk and Haufler (1999)	6	1.07	21.4	-	0.086	
Botrychium lunaria	diploid	isozymes	Hauk and Haufler (1999)	6	1.11	11.9	-	0.07	Now *B. neolunaria*
Botrychium lunaria	diploid	SNPs	Dauphin (2017)	513	1.33	100	0.002-0.005	0.232	
Botrychium matricariifolium	tetraploid	AFLPs	This study	207	-	43.32	ΦPT=0.028	0.14	Mantel test found weak but significant correlation, AMOVA found 97% within
Botrychium matricariifolium	tetraploid	isozymes	Hauk and Haufler (1999)	6	1.67	50	-	0.271	
Botrychium minganense	tetraploid	isozymes	Hauk and Haufler (1999)	6	1.35	45.45	-	0.233	
Botrychium pallidum	diploid	AFLPs	This study	156	-	52.24	ΦPT=0.125	0.17	Mantel test found weak but significant correlation, AMOVA found 87% within

Table 1. Continued.

Species	Ploidy	Technique[1]	Reference	# loci	alleles per locus	% poly-morphic	FST[2]	H[3]	Notes
Botrychium pedunculosum	tetraploid	isozymes	Hauk and Haufler (1999)	6	1.33	33.33	-	0.089	
Botrychium pinnatum	tetraploid	isozymes	Hauk and Haufler (1999)	6	1.42	41.66	-	0.218	
Botrychium pumicola	diploid	isozymes	Hauk and Haufler (1999)	6	1	0	-	0	
Botrychium pumicola	diploid	ISSRs	Camacho and Liston (2001)	15	-	34 - 48	-	0.1027–0.1622	
Botrychium simplex	diploid	isozymes	Hauk and Haufler (1999)	6	1.03	3.3	-	0.017	
Botrychium spathulatum	tetraploid	isozymes	Hauk and Haufler (1999)	6	1.17	16.67	-	0.089	
Botrypus virginianus (Botrychium s.l.)	tetraploid	AFLPs	This study	340	-	77.25	ΦPT=0.164	0.25	Mantel test not significant, AMOVA found 84% within
Botrypus virginianus (Botrychium s.l.)	tetraploid	isozymes	Soltis and Soltis (1986)	18	1.19	16.1	0.09	0.036	GST=0.0289–0.1647
Sceptridium dissectum (Botrychium s.l.)	unknown	isozymes	McCauley et al. (1985)	5	-	-	0.09	-	
Sceptridium dissectum (Botrychium s.l.)	unknown	ISSRs	Barker and Hauk (2003)	69	-	94	0.085	-	AMOVA found 96.62% within
Sceptridium robustum (Botrychium s.l.)	diploid	isozymes	Watano and Sahashi (1992)	9	2	55.6	-	0.193	
Sceptridium nipponicum (Botrychium s.l.)	diploid	isozymes	Watano and Sahashi (1992)	9	1.44	33.3	-	0.116	
Sceptridium ternatum (Botrychium s.l.)	diploid	isozymes	Chung et al. (2010)	22	1.23	22.7	0.414	0.026	Mantel test not significant, GST =0.299
Sceptridium ternatum (Botrychium s.l.)	diploid	isozymes	Watano and Sahashi (1992)	9	2.11	55.6	-	0.216	AMOVA found 81% within, GST=0.19

Table 1. Continued.

Species	Ploidy	Technique[1]	Reference	# loci	alleles per locus	% poly-morphic	FST^2	H^3	Notes
Sceptridium triangularifolium (Botrychium s.l.)	diploid	isozymes	Watano and Sahashi (1992)	9	1	0	-	0	
Mankyua chejuense	diploid	isozymes	Chung et al. (2010)	30	1.13	10	0.245	0.007	Mantel test not significant, GST =0.272
Ophioglossum pusillum	unknown	isozymes	McMaster (1994)	26	1	0	-	0	All loci monomorphic and homozygous
Ophioglossum vulgatum	diploid	isozymes	Chung et al. (2013)	21	1.43	38.1	0.733	0.11	Mantel test found weak but significant correlation

Notes: 1 - Isozymes include allozymes, 2- Φ_{PT} is a comparable measure of population differentiation to FST calculated with binary data, 3 - Mean or expected heterozygosity

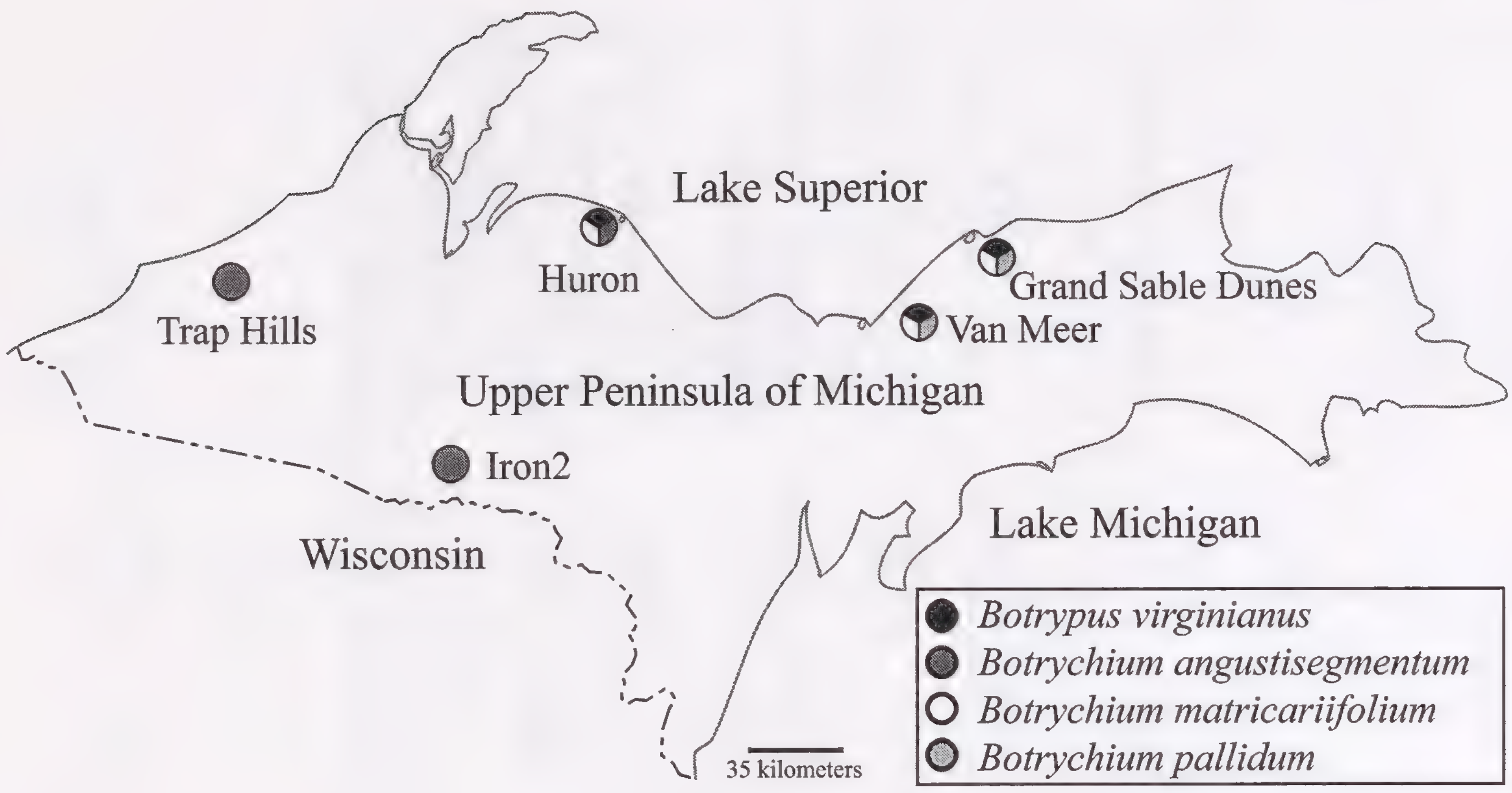

Fig. 1. Collection sites in the Upper Peninsula. Additional information found in Table 2. For reference, the Grand Sable Dunes site is at roughly 46.667 N and -86.022 W.

In this study, I examined the population genetics of three species of *Botrychium* and one species in the genus *Botrypus* (included with *Botrychium* in subfamily Botrychioideae; PPG I, 2016) from the Upper Peninsula of Michigan, USA. I included two diploid species, *Botrychium pallidum* W.H. Wagner and *Botrychium angustisegmentum* (Pease & A.H. Moore) Fernald (*Botrychium lanceolatum angustisegmentum* subsp. *angustisegmentum* (Pease & A.H. Moore) R.T. Clausen), the allotetraploid *Botrychium matricariifolium* (Döll) A. Braun ex W.D.J. Koch, and the widespread species *Botrypus virginianus*. A previous study using AFLPs found that the three *Botrychium* species were separate lineages (Williams, Farrar, and Henson, 2016) and provided support for the hypothesis that *B. matricariifolium* is the allotetraploid offspring of *B. pallidum* and *B. angustisegmentum*. Based on their life history traits and previous findings on genetic diversity in the genus, I expected to find low genetic diversity and population differentiation. I also expected that allotetraploids would have higher measures of genetic diversity as a consequence of fixed heterozygosity, as reported by Hauk and Haufler (1999).

Materials and Methods

Collections.—I sampled the four target species from populations across the Upper Peninsula of Michigan (Fig. 1; Table 2). In general, I aimed for 20 individuals and three populations, but this was not always possible. I used three populations of *B. matricariifolium* with 36 total individuals, three populations of *B. angustisegmentum* with 34 total individuals, two populations of *B. pallidum* with 15 total individuals, and three populations of *Bo. virginianus* with 64 total individuals. Species often grow in sympatry, allowing me to collect multiple species from each location. I stored samples in

Table 2. Sampling information

Species	Population	Location	# samples	Collection #	Lab #
Botrypus virginianus	Huron	Huron Mountain Club, Marquette County, Michigan, USA	19	EW1079	E312
Botrypus virginianus	Van Meer	Alger County, Michigan, USA	21	EW1070	E326
Botrypus virginianus	Grand Sable Dunes	Grand Sable Dunes, Alger County, Michigan, USA	24	EW995	E240
Botrychium matricariifolium	Huron	Huron Mountain Club, Marquette County, Michigan, USA	9	EW936	E105
Botrychium matricariifolium	Van Meer	Alger County, Michigan, USA	12	EW178	E018
Botrychium matricariifolium	Grand Sable Dunes	Grand Sable Dunes, Alger County, Michigan, USA	15	EW204	E019
Botrychium angustisegmentum	Grand Sable Dunes	Grand Sable Dunes, Alger County, Michigan, USA	13	EW945	E355
Botrychium angustisegmentum	Iron2	Iron County, Michigan, USA	15	EW372	E364
Botrychium angustisegmentum	Iron1	Iron County, Michigan, USA	6	EW949	E359
Botrychium pallidum	Van Meer	Alger County, Michigan, USA	9	EW4	E202
Botrychium pallidum	Grand Sable Dunes	Grand Sable Dunes, Alger County, Michigan, USA	6	EW313	E033

All vouchers deposited at MICH. Specific locations available from the author. Lab number corresponds to DNA extraction used.

silica gel and extracted DNA using Qiagen DNeasy Plant Mini kits (Qiagen, Valencia, California, USA).

AFLPs.—I generated Amplified Fragment Length Polymorphisms (AFLPs; Vos *et al.*, 1995) from a library of genomic DNA digested with the restriction enzymes EcoR1 and MseI following Williams and Waller (2012). I used four primer pairs for *Botrychium* and three for *Bo. virginianus* (E+AGC and M+CTC [not used for *B. pallidum*], M+CTTGC, M+CCAG, and M+CCCG [not used for *Bo. virginianus*]). A ThermoFisher 3730 Genetic Analyzer at the Biotechnology Center at the University of Wisconsin – Madison was used to sequence the samples. To analyze the DNA fragments I employed the program GeneMarker (SoftGenetics LLC, 2005), creating panels and scoring fragments by hand using conservative criteria following Holland *et al.* (2008): intensity over 100, band sizes greater than 100, symmetric peaks and small bin sizes. To standardize data across runs I used ten replicates within each run and examined chromatograms to score alleles that amplified through all runs. I scored the

three *Botrychium* species together, however, one primer pair did not amplify for three (20%) of the *B. pallidum* individuals, so those data are not included. This resulted in 207 loci for *B. matricariifolium* and *B. angustisegmentum* and 156 loci for *B. pallidum*. I scored *Bo. virginianus* separately which resulted in 340 loci.

Population genetics.—I used GenAlEx v6.51b2 (Peakall and Smouse, 2006; Peakall and Smouse, 2012) to calculate diversity statistics (number of alleles, effective number of alleles, Shannon genetic information index, percent polymorphic loci, observed and expected heterozygosity, Φ_{PT}, AMOVA). For the AMOVA test, the null hypothesis is that Φ_{PT} is not statistically different from zero. I also used GenAlEx to run Mantel tests of geographic and genetic distance with 999 permutations, based on the null hypothesis that the correlation between distances is not significantly different from random. Finally, I used Principal Coordinates Analysis (PCoA) to visual genetic distance between individuals and populations.

I used the program STRUCTURE (Pritchard, Stephens, and Donnelly, 2000) to look for patterns of genetic structure. I followed the procedure in Evanno *et al.* (2005) for coding AFLPs and performed runs of 1,000,000 generations with 100,000 generations burn-in using an admixture model and 20 runs per K (K = 1 – 6). I used the method described in Evanno *et al.* (2005) to estimate the optimal value of K, or genetic clusters in the data, as implemented in STRUCTURE HARVESTER (Earl and vonHoldt, 2012). However, as these results may be biased towards a result of $K = 2$ (Meirmans, 2015; Janes *et al.*, 2017), I also examined the likelihood scores and STRUCTURE plots in light of the existing geographic distance between species, the population genetic diversity statistics, and the AMOVA results.

RESULTS

Gene diversity, expressed as the percent polymorphic loci (Table 3) was highest for *Bo. virginianus* and lowest for *B. angustisegmentum*. This pattern of high diversity for *Bo. virginianus* held for the other measures, which may also be because *Bo. virginianus* had more loci (340 vs. 207 and 156). Φ_{PT} values, which are comparable to F_{ST} values but specialized for binary co-dominant data, were low (0.028 [*B. matricariifolium*] – 0.164 [*Bo. virginianus*]), indicating little differentiation between populations. These results agree with the AMOVA results which showed that each species had more variation within populations (84- 97%, all significant, $P < 0.007$) than among populations, *i.e.*, each population possessed nearly the entire compliment of genetic variation found in all the populations. Despite this, two species had low but significant correlations between genetic and geographic distance using Mantel tests; *B. pallidum* ($R^2 = 0.083$, $n = 15$, $p = 0.007$) and *B. matricariifolium* ($R^2 = 0.023$, $n = 36$, $p = 0.04$). There was no significant correlation for *B. angustisegmentum* ($R^2 = 0.0006$, $n = 34$, $p = 0.35$) or *Bo. virginianus* ($R^2 = 0.0001$, $n = 64$, $p = 0.3$).

TABLE 3. Population genetic metrics

Species	n	# of popu-lations	# of loci	% poly-morphic	Na	Ne	I	He	Φ_{PT}	AMOVA p-value	Source of variation (among, within)	Mantel test R^2, p-value
Botrychium matricariifolium	36	3	207	43.32±2%	1.11±0.04	1.2±0.01	0.21±0.01	0.14±0.01	0.028	0.007	3, 97%	0.02, 0.043
Botrychium angustisegmentum	34	3	207	37.36±0.6%	0.98±0.04	1.2±0.01	0.17±0.01	0.11±0.01	0.034	0.004	3, 97%	0.0006, 0.3
Botrychium pallidum	15	2	156	52.24±0.3%	1.2±0.05	1.3±0.02	0.25±0.02	0.17±0.01	0.125	0.002	13, 87%	0.08, 0.007
Botrypus virginianus	64	3	340	77.25±5%	1.7±0.02	1.4±0.01	0.38±0.01	0.25±0.01	0.164	0.001	16, 84%	0.001, 0.3

The PCoA plot and STRUCTURE results for each species show little population differentiation. The results for $K = 2$, 3, and 4 are shown. The *B. angustisegmentum* STRUCTURE results indicated $K = 2$ was the optimal value (Fig. 2), though individuals from both clusters were found in all populations, with a slight differentiation of the Trap Hills population. The value of $K = 1$ also has a high likelihood. The *B. pallidum* STRUCTURE results (Fig. 3) indicated $K = 3$ was optimal. One population, Grand Sable Dunes, had individuals from each of the three clusters, while the Van Meer population was mainly made up of one genetic cluster. The optimal value for *B. matricariifolium* (Fig. 4) indicated by likelihood and STRUCTURE Harvester was $K = 2$, though $K = 1$ and $K = 3$ values had similar likelihoods. The Huron population was slightly different from the other two populations, but all populations had individuals from each cluster. The results for *Bo. virginianus* (Fig. 5) showed evidence for clustering, with the majority of individuals from the Van Meer site clustering away from the other two populations. The STRUCTURE results showed that $K = 4$ has the highest likelihood, though the STRUCTURE Harvester indicated $K = 2$ was the optimal value.

DISCUSSION

In general, these results agree with previous work on population genetics in the genus *Botrychium*. All species contained low inter-population differentiation, with most genetic variation found within populations using AMOVA. Reduced inter-population differentiation was reflected in the STRUCTURE results. Optimal values of K ranged from 2 to 4, depending on the method used, but did not show strong correspondence with sampling locations. The visualization of genetic distances using PCoA also did not show strong clustering of individuals by geography. Although two species did have significant correlations between genetic and geographic distance, the R^2 values were low (*B. matricariifolium;* 0.02 and *B. pallidum;* 0.08).

The majority of previous studies used isozymes or allozymes which may be under selection, making direct comparisons difficult as AFLPs are random markers targeting coding and non-coding regions. However, previous work found similar trends of relatively low polymorphic loci, low F_{ST}, and high fractions of variation occurring within populations (McCauley, Whittier, and Reilly, 1985; Soltis and Soltis, 1986; Watano and Sahashi, 1992; Hauk and Haufler, 1999; Camacho and Liston, 2001; Barker and Hauk, 2003; Dauphin, 2017).

A study of *Botrychium pumicola*, a western U.S. diploid species, using ISSRs (Camacho and Liston, 2001) assessed three populations, similar to the sampling done here. They also found low population differentiation (G_{ST} = 0.115) with genetic differences uncorrelated with geographic distance. They attributed this to high rates of gene flow due to long-distance spore dispersal. Alternatively, the three populations sampled could be relicts from a larger wide-spread population which contracted following climatic changes. Dauphin (2017) proposed a similar explanation for their study of *Botrychium*

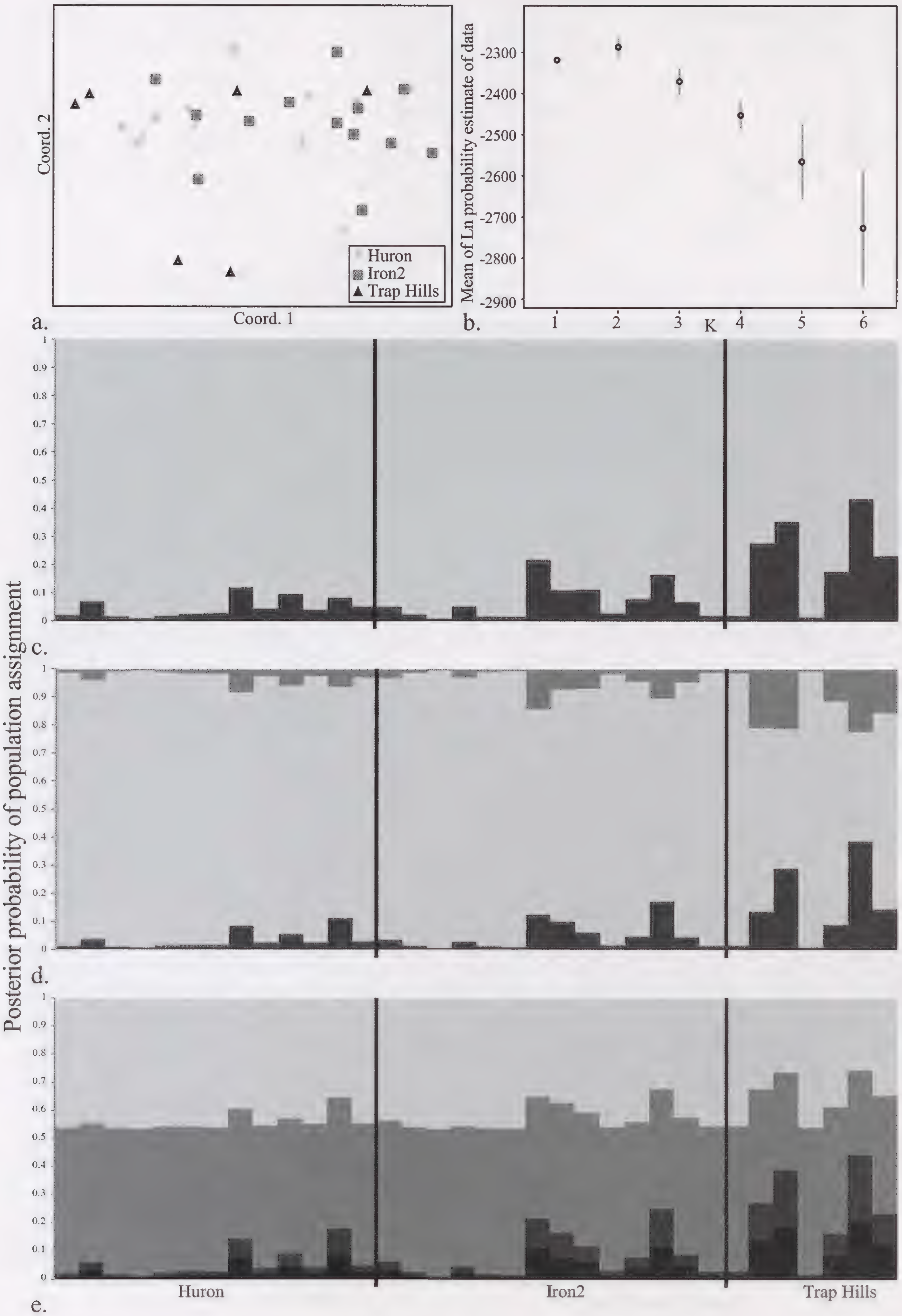

FIG. 2. *Botrychium angustisegmentum* from three populations. A. PCoA B. STRUCTURE likelihood results. C. *K*=2, the optimal value indicated by STRUCTURE Harvester and likelihood D. *K*=3 E. *K*=4

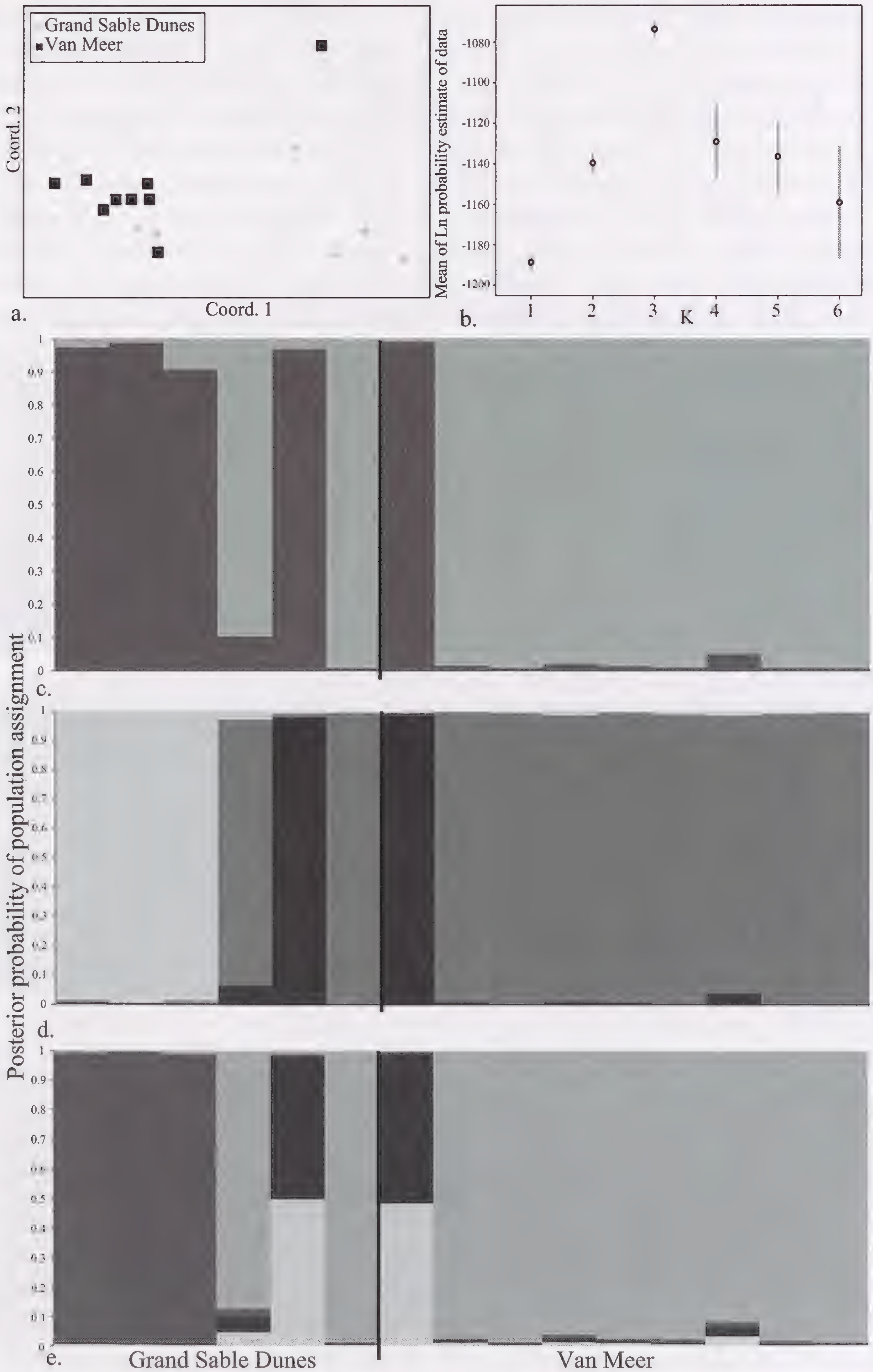

FIG. 3. *Botrychium pallidum* from two populations. A. PCoA B. STRUCTURE likelihood results. C. K=2 D. K=3, the optimal value indicated by STRUCTURE Harvester and likelihood E. K=4

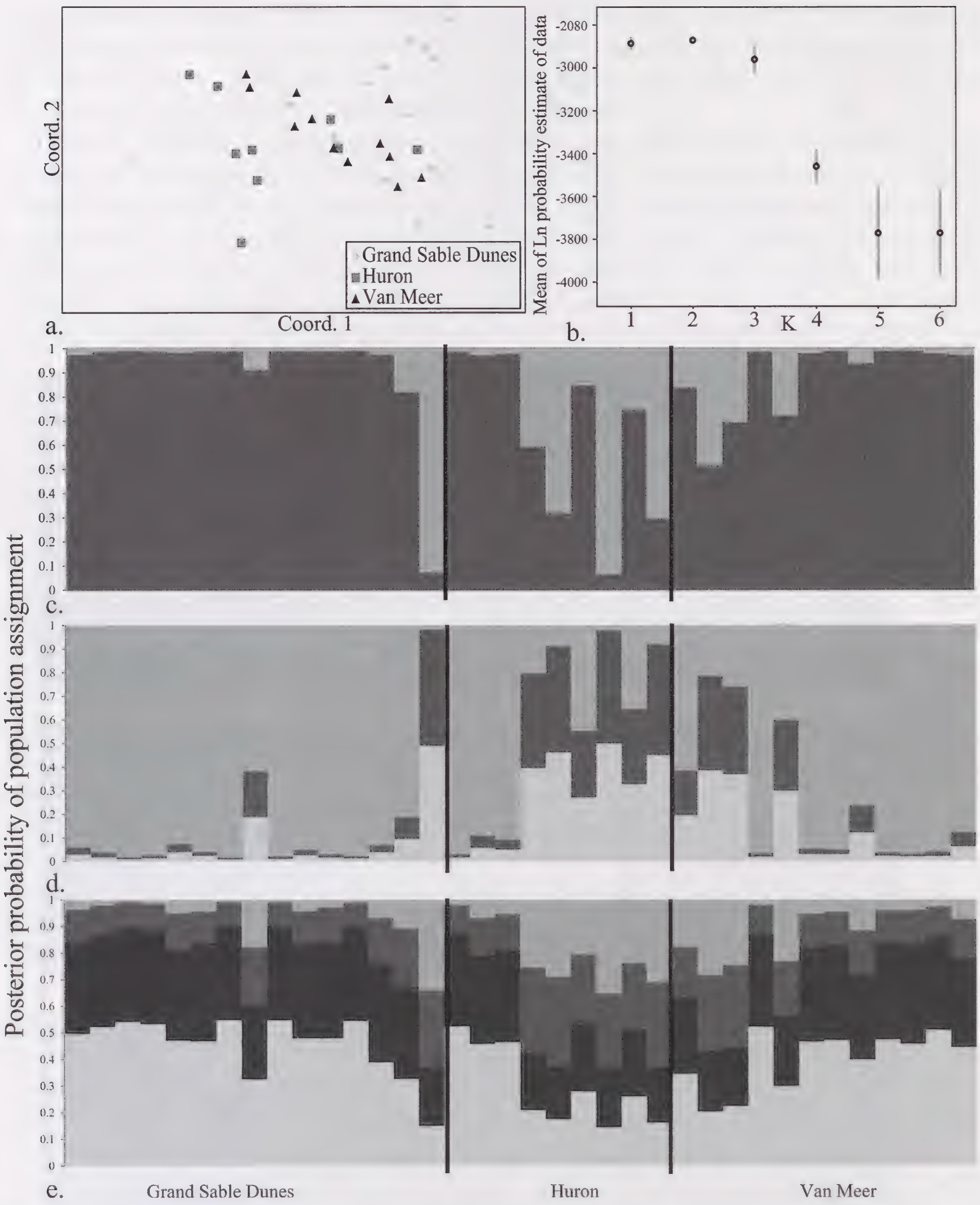

FIG. 4. *Botrychium matricariifolium* from three populations. A. PCoA B. STRUCTURE likelihood results. C. *K*=2, the optimal value indicated by STRUCTURE Harvester D. *K*=3 E. *K*=4

lunaria in the Swiss Alps using SNPs. The four populations studied (well-sampled with 45+ individuals per population) had low population differentiation (pairwise F_{ST} =0.002 – 0.005). They note that populations may have been recently derived from a large variable population, as population differentiation appears recent, perhaps following colonization after glaciation.

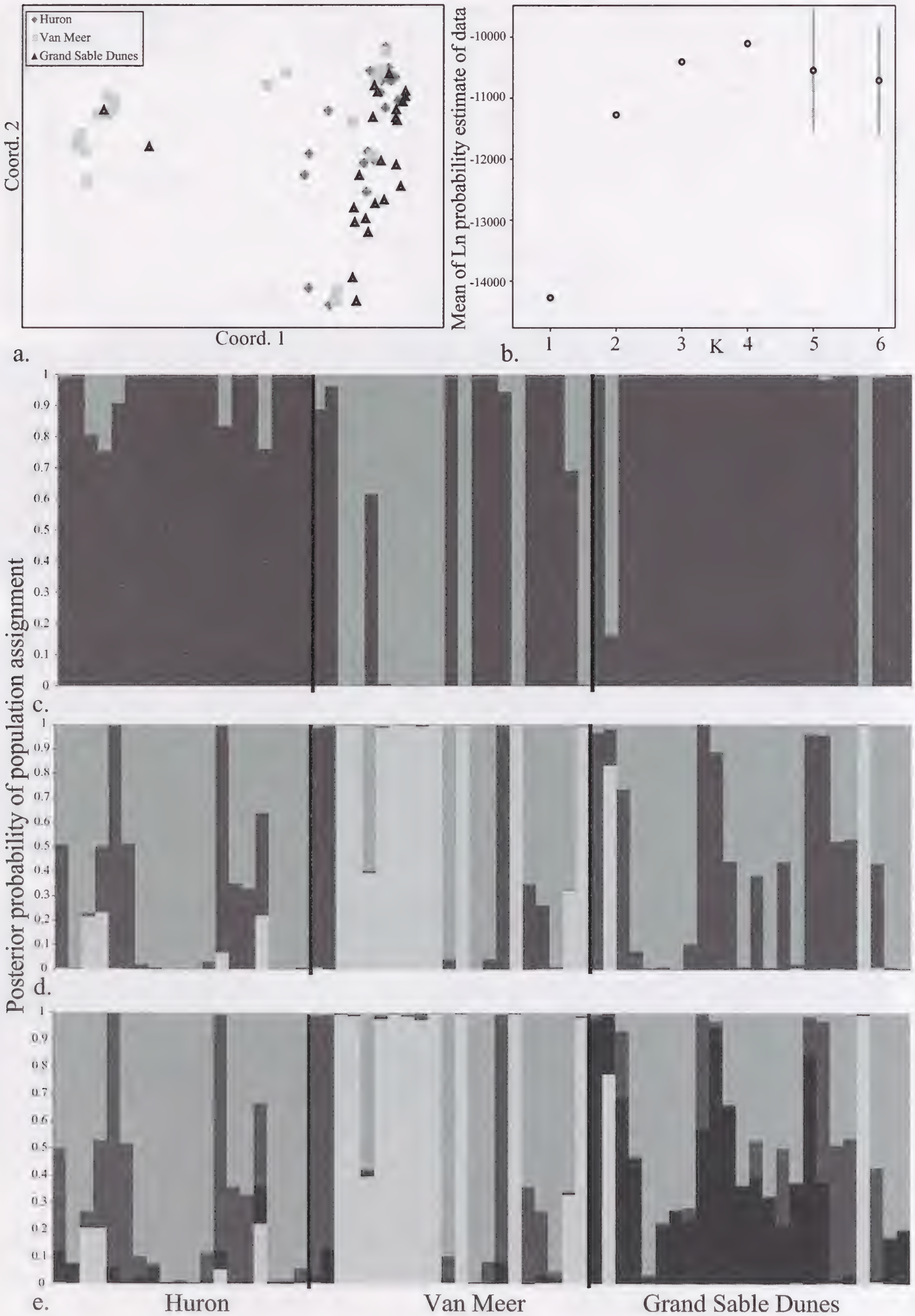

FIG. 5. *Botrypus virginianus* from three populations. A. PCoA B. STRUCTURE likelihood results. C. K=2, the optimal value indicated by STRUCTURE Harvester D. K=3 E. K=4, the optimal value indicated by likelihood.

It is possible that a similar scenario occurred across the Upper Peninsula of Michigan, where glaciers retreated ~10,000 years ago. Re-colonization of glaciated areas, plus gene flow through rare but effective long-distance dispersal, could result in the patterns seen here.

Indeed, studies in *Sceptridium dissectum,* the sister genus to *Botrychium*, obtained similar results. Work by McCauley *et al.* (1985) and Barker and Hauk (2003) reported low F_{ST} values –0.085 and 0.09 – using isozymes and ISSRs, respectively. McCauley *et al.* (1985) used isozymes to evaluate the genetic structure of three *S. dissectum* populations. Based on two isozyme loci they found $F_{ST} = 0.09$ and $F_{IS} = 0.951$, one of the highest F_{IS} values reported at that time. Using this value they estimated that *S. dissectum* outcrosses only 5% of the time and is highly inbred. Watano and Sahashi (1992) used isozymes to examine four *Sceptridium* species and found that all were highly inbred. In addition, 81% of genetic diversity was within populations vs. 19% among populations for *Sceptridium ternatum.* These results suggest that high selfing rates allow for genetic structure resembling clonal plant populations. Similarly, Chung (2010) found evidence for high inbreeding in *S. ternatum* along with low genetic diversity. When Barker and Hauk (2003) used ISSRs to examine *S. dissectum* they found F_{ST} to be low as well (0.085) with 91% of the variation occurring within populations. Barker and Hauk (2003) hypothesized that in *Sceptridium* recolonization of glaciated areas occurred too recently for populations to have had time to diverge.

In general, I found that *Bo. virginianus* had higher levels of genetic diversity, exhibiting the highest percent polymorphic loci, number of effective alleles, and expected heterozygosity. *Botrypus virginianus* also had the highest amount of population differentiation, and the highest percentage of genetic variation found among populations. However, these values were not dramatically higher or lower compared to *Botrychium* species, and in general, genetic differences among populations were negligible. For example, the measure of population differentiation (Φ_{PT}) was 0.164 for *Bo. virginianus*, and 0.034 to 0.125 for the species of *Botrychium.* The higher number of loci, a missing primer pair, and more balanced sampling for *Bo. virginianus* also means that it is difficult to directly compare results. In their survey of five fern species using isozymes Soltis, Soltis, and Holsinger (1988) found *Botrypus virginianus* had the lowest rate of gene flow estimated using *Nm.* They hypothesized this could reflect gametophytic selfing given that the populations had low F_{ST} values and high F_{IS} values (Soltis and Soltis, 1986). The high levels of inbreeding were attributed to below ground gametophytes, but this lack of differentiation between populations was surprising given significant inbreeding. They determined this pattern could be due to high spore dispersal, rapid recolonization with little subsequent genetic differentiation (due to inbreeding), or both (Soltis, Soltis, and Holsinger, 1988; Soltis and Soltis, 1990).

In terms of differences in ploidy level, my species sampling is likely not sufficient to make robust comparisons. In their study of 16 *Botrychium* species, Hauk and Haufler (1999) found that most diploid species had low allelic

diversity, with fewer than two genotypes in each population. They also found higher levels of heterozygosity and percent polymorphic loci in tetraploids compared to diploids. The present study contained only one tetraploid, *B. matricariifolium,* to compare with the two diploid species. In general, *B. matricariifolium* had intermediate measures of genetic diversity, with diploid *B. pallidum* having more polymorphic loci despite having fewer loci overall and low sampling numbers. It is not clear why the results in this study differ from those of Hauk and Haufler, but including additional polyploids and diploids for comparison would be valuable in the future.

Previous work on *Botrychium* and related species indicates that long-distance dispersal, though likely rare, plays an important role in colonization and structuring populations. Once a spore reaches a site, it will likely require many years for the underground gametophyte to produce an above-ground sporophyte (Johnson-Groh *et al.*, 2002). Although I did not calculate measures of inbreeding here, previous research has generally found high levels of inbreeding in *Botrychium s.l.* Underground gametophytic fertilization probably results in inbreeding and fixed heterozygosity. It is likely that underground mating is rare and that few offspring are produced at each site, with most individuals at a site originating from spores arriving via long- distance dispersal. A long generation time, combined with underground self-fertilization and long-distance spore movement likely generated the low population differentiation observed among the species included here.

This study yields additional information on the population genetics of *Botrychium* species, but is hindered by low sample sizes in terms of individuals and populations. In addition, although AFLPs require less initial knowledge as the primers are not species-specific, they are dominant markers. Co-dominant markers would not only provide information about heterozygosity and inbreeding, but could also be used to examine hybridization and allotetraploid origins in the genus. Future datasets using highly variable markers such as microsatellites or next-generation sequencing techniques like RADSeq will be useful for expanding the patterns seen here.

Acknowledgements

The author thanks two anonymous reviewers for their comments which substantially improved the paper; D. Waller for review of previous drafts; and L. Loope, B. Leutscher, and S. Trull for help with permits. This research was supported by the Clarence R. & Florence N. Hanes Foundation, the Huron Mountain Wildlife Foundation, the Department of Botany John J. Davis Grant, the Michigan Rare Plant Fund, and the UW-Madison Vilas Travel Award.

Literature Cited

Barker, M. S., and W. D. Hauk. 2003. An evaluation of *Sceptridium dissectum* (Ophioglossaceae) with ISSR markers: implications for *Sceptridium* systematics. American Fern Journal 93:1-19.

Camacho, F. J., and A. Liston. 2001. Population structure and genetic diversity of *Botrychium pumicola* (Ophioglossaceae) based on inter-simple sequence repeats (ISSR). American Journal of Botany 88:1065-1070.

CHUNG, M. Y., J. LOPEZ-PUJOL, J. M. CHUNG, M. O. MOON, AND M. G. CHUNG. 2013. Genetic diversity in the homosporous fern *Ophioglossum vulgatum* (Ophioglossaceae) from South Korea: inference of mating system and population history. Journal of Heredity 104:263-272.

CHUNG, M. Y., J. D. NASON, B.-Y. SUN, M.-O. MOON, J. M. CHUNG, C.-W. PARK, AND M. G. CHUNG. 2010. Extremely low levels of genetic variation in the critically endangered monotypic fern genus *Mankyua chejuense* (Ophioglossaceae) from Korea: implications for conservation. Biochemical Systematics and Ecology 38:888-896.

DAUPHIN, B. 2017. Evolution of moonwort ferns (*Botrychium*, Ophioglossaceae) on local to global scales. Ph.D., Université de Neuchâtel, Switzerland.

DAUPHIN, B., J. VIEU, AND J. R. GRANT. 2014. Molecular phylogenetics supports widespread cryptic species in moonworts (*Botrychium* s.s., Ophioglossaceae). American Journal of Botany 101:128-140.

DAUPHIN, B., J. GRANT, AND P. MRÁZ. 2016. Ploidy level and genome size variation in the homosporous ferns *Botrychium s.l.* (Ophioglossaceae). Plant Systematics and Evolution 302:575–584.

DAUPHIN, B., D. R. FARRAR, A. MACCAGNI, AND J. R. GRANT. 2017. A worldwide molecular phylogeny provides new insight on cryptic diversity within the moonworts *(Botrychium s. s.*, Ophioglossaceae). Systematic Botany 42:620-639.

DAUPHIN, B., J. R. GRANT, D. R. FARRAR, AND C. J. ROTHFELS. 2018. Rapid allopolyploid radiation of moonwort ferns (*Botrychium*; Ophioglossaceae) revealed by PacBio sequencing of homologous and homeologous nuclear regions. Molecular Phylogenetics and Evolution 120:342-353.

DE GROOT, G. A., H. J. DURING, S. W. ANSELL, H. SCHNEIDER, P. BREMER, E. R. WUBS, J. W. MAAS, H. KORPELAINEN, AND R. J. H. ERKENS. 2012. Diverse spore rains and limited local exchange shape fern genetic diversity in a recently created habitat colonized by long-distance dispersal. Annals of Botany 109:965-978.

EARL, D. A., AND B. M. VONHOLDT. 2012. STRUCTURE HARVESTER: a website and program for visualizing STRUCTURE output and implementing the Evanno method. Conservation Genetics Resources 4:359-361.

EVANNO, G., S. REGNAUT, AND J. GOUDET. 2005. Detecting the number of clusters of individuals using the software STRUCTURE: a simulation study. Molecular Ecology 14:2611-2620.

FARRAR, D. R. 1998. Population genetics of moonwort *Botrychiums. In* N. Berlin, P. Miller, J. Borovansky, U. S. Seal, and O. Byers [eds.], Population and Habitat Viability Assessment (PHVA) for the Goblin Fern (*Botrychium mormo*), 109-113. Conservation Biology Specialist Group, Apple Valley, MN.

FARRAR, D. R. 2011. Moonwort (*Botrychium*) Systematics Website www.public.iastate.edu/~herbarium/botrychium.html [accessed August 2015].

FARRAR, D. R., AND A. V. GILMAN. 2017. Relationships in the *Botrychium campestre* (Ophioglossaceae) complex. Brittonia 69:265-275.

HAUK, W. D. 1995. A molecular assessment of relationships among cryptic species of *Botrychium* subgenus *Botrychium* (Ophioglossaceae). American Fern Journal 85:375-394.

HAUK, W. D., AND C. H. HAUFLER. 1999. Isozyme variability among cryptic species of *Botrychium* subgenus *Botrychium* (Ophioglossaceae). American Journal of Botany 86:614-633.

HAUK, W. D., C. R. PARKS, AND M. W. CHASE. 2003. Phylogenetic studies of Ophioglossaceae: evidence from *rbcL* and *trnL-F* plastid DNA sequences and morphology. Molecular Phylogenetics and Evolution 28:131-151.

HAUK, W. D., L. KENNEDY, AND H. M. HAWKE. 2012. A phylogenetic investigation of *Botrychium* s.s. (Ophioglossaceae): evidence from three plastid DNA sequence data sets. Systematic Botany 37:320-330.

HOLLAND, B. R., A. C. CLARKE, AND H. M. MEUDT. 2008. Optimizing automated AFLP scoring parameters to improve phylogenetic resolution. Systematic Biology 57:347-366.

JANES, J. K., J. M. MILLER, J. R. DUPUIS, R. M. MALENFANT, J. C. GORRELL, C. I. CULLINGHAM, AND R. L. ANDREW. 2017. The K = 2 conundrum. Molecular Ecology 26:3594-3602.

JOHNSON-GROH, C., AND J. M. LEE. 2002. Phenology and demography of two species of *Botrychium* (Ophioglossaceae). American Journal of Botany 89:1624-1633.

Johnson-Groh, C., C. Riedel, L. Schoessler, and K. Skogen. 2002. Belowground distribution and abundance of *Botrychium* gametophytes and juvenile sporophytes. American Fern Journal 92:80-92.

McCauley, D. E., D. P. Whittier, and L. M. Reilly. 1985. Inbreeding and the rate of self- fertilization in a grape fern, *Botrychium dissectum*. American Journal of Botany 72:1978- 1981.

McMaster, R. T. 1994. Ecology, reproductive biology, and population genetics of *Ophioglossum vulgatum* (Ophioglossaceae). Rhodora 96:259-286.

Meirmans, P. G. 2015. Seven common mistakes in population genetics and how to avoid them. Molecular Ecology 24:3223-3231.

Paris, C. A., F. S. Wagner, and W. H. Wagner. 1989. Cryptic species, species delimitation, and taxonomic practice in the homosporous ferns. American Fern Journal 79:46-54.

Peakall, R., and P. E. Smouse. 2006. GenAlEx 6: genetic analysis in Excel. Population genetic software for teaching and research. Molecular Ecology Notes 6:288-295.

Peakall, R., and P. Smouse. 2012. GenAlEx 6.5: Genetic analysis in Excel. Population genetic software for teaching and research - an update. Bioinformatics 10.1093/bioinformatics/bts460 10.1093/bioinformatics/bts460.

Peck, J. H., C. J. Peck, and D. R. Farrar. 1990. Influences of life-history attributes on formation of local and distant fern populations. American Fern Journal 80:126-142.

PPG I. 2016. A community-derived classification for extant lycophytes and ferns. Journal of Systematics and Evolution 54:563-603.

Pritchard, J. K., M. Stephens, and P. Donnelly. 2000. Inference of population structure using multilocus genotype data. Genetics 155:945-959.

Soltis, D. E., and P. S. Soltis. 1986. Electrophoretic evidence for inbreeding in the fern *Botrychium virginianum* (Ophioglossaceae). American Journal of Botany 73:588-592.

Soltis, P. S., and D. E. Soltis. 1990. Genetic variation within and among populations of ferns. American Fern Journal 80:161-172.

Soltis, P. S., D. E. Soltis, and K. E. Holsinger. 1988. Estimates of intragametophytic selfing and interpopulational gene flow in homosporous ferns. American Journal of Botany 75:1765-1770.

Vos, P., R. Hogers, M. Bleeker, M. Reijans, T. Vandelee, M. Hornes, A. Frijters, J. Pot, J. Peleman, and M. Kuiper. 1995. AFLP - a new technique for DNA fingerprinting. Nucleic Acids Research 23:4407- 4414.

Watano, Y., and N. Sahashi. 1992. Predominant inbreeding and its genetic consequences in a homosporous fern genus, *Sceptridium* (Ophioglossaceae). Systematic Botany 17:486-502.

Williams, E. W., and D. M. Waller. 2012. Phylogenetic placement of species within the genus *Botrychium* (Ophioglossaceae) based on chloroplast sequences, AFLPs, and flow cytometry. International Journal of Plant Sciences 173:516-531.

Williams, E. W., and D. M. Waller. 2015. Tracking morphological change and demographic dynamics in ephemeral *Botrychium* s.s. (Ophioglossaceae) populations. The Journal of the Torrey Botanical Society 142:152-165.

Williams, E. W., D. R. Farrar, and D. Henson. 2016. Cryptic speciation in allotetraploids: Lessons from the *Botrychium matricariifolium* complex. American Journal of Botany 103:740-753.

Winther, J. L., and W. E. Friedman. 2007. Arbuscular mycorrhizal symbionts in *Botrychium* (Ophioglossaceae). American Journal of Botany 94:1248-1255.

American Fern Journal 111(2):147–149 (2021)
Published on 7 June 2021

Shorter Note

A New Combination for a *Bolbitis* Species Commonly Grown in Aquaria.—A curious mixture of species occurs under the name *Bolbitis heteroclita* (C.Presl) Ching (Lomariopsidaceae). These species, which are commonly cultivated, were considered forms by Hennipman (Monograph of the Fern Genus *Bolbitis* (Lomariopsidaceae). Leiden University Press. 1977. 332pp.). The "forms" differ greatly among themselves, and each maintains its distinctiveness in cultivation, even on the same growing media (pers. obs.). The forms can be readily distinguished by lamina shape and division (Fig. 1, Table 1).

The largest form, when submersed or when emersed and still young, resembles poison ivy (*Toxicodendron radicans*). In the horticultural trade, this form is called *B. heteroclita* or sometimes *B. heteroclita cuspidata*. It is native to most of southeastern Asia and the East Indies.

A second form is smaller and often called "mini-*Bolbitis*" or "*Bolbitis heteroclita difformis*." It resembles a *Davallia* and is sometimes sold as "*Davallia* spec." It was first described as *Edanyoa difformis* by Copeland (Philippine Journal of Science 81: 22, t. 17. 1952.), and the type collection (University of Michigan collection #1191294) bears an annotation (undated) by Hennipman as *Bolbitis heteroclita*. In his monograph, Hennipman states that various dwarf and juvenile forms of *B. heteroclita* resemble *Edanyoa*. The only other herbarium specimen I found collected from the wild is in the Rijksherbarium, Leiden (specimen number L3516213). Both specimens are from Negros Oriental, Philippines. Interestingly, the entry for *B. heteroclita* in the "Field Guide to the Pteridophytes of Chiang Mai, Thailand" (John Rey C. Colado *et al.*; published online at http://issuu.com/naniegonzales/docs/fieldguide_pteridophytes) shows *B. difformis*, not *B. heteroclita*, and makes the dubious claim that it grows all over southeast Asia (which claim undoubtedly attains to *B. heteroclita*, not *B. difformis*). However, *B. difformis* has been grown in and out of aquaria for years and appears to be constant in its shape and form. Originating in the Philippines (and possibly other countries of southeastern Asia), it was apparently grown as a potted plant for many years before being introduced into the aquarium trade. No definite date of introduction could be found, but an article published in 2009 noted both species as new to the aquarium trade (Christel Kasselman, *Bolbitis heteroclita* "*cuspidata*" und *B. heteroclita* "*difformis*". Zwei neue Farne für die Aquaristik,"in D. Aqua. u. Terr. Z. (Datz) 12/2009: 46-50). Thus, these species have been in the aquarium trade at least since then. The article also stated that the original aquarium trade material of both this and *B. inconstans* (Copel.) Ching came from the Botanical Garden Berlin-Dahlem courtesy of Tropica, a commercial horticulture firm. Many websites claim that *difformis* is a variety of the African species *B. heudelotii*, which is obviously false. *Bolbitis difformis* is known for being difficult to grow as a submersed plant, and for taking months to establish itself after being cultivated in an aquarium, not liking

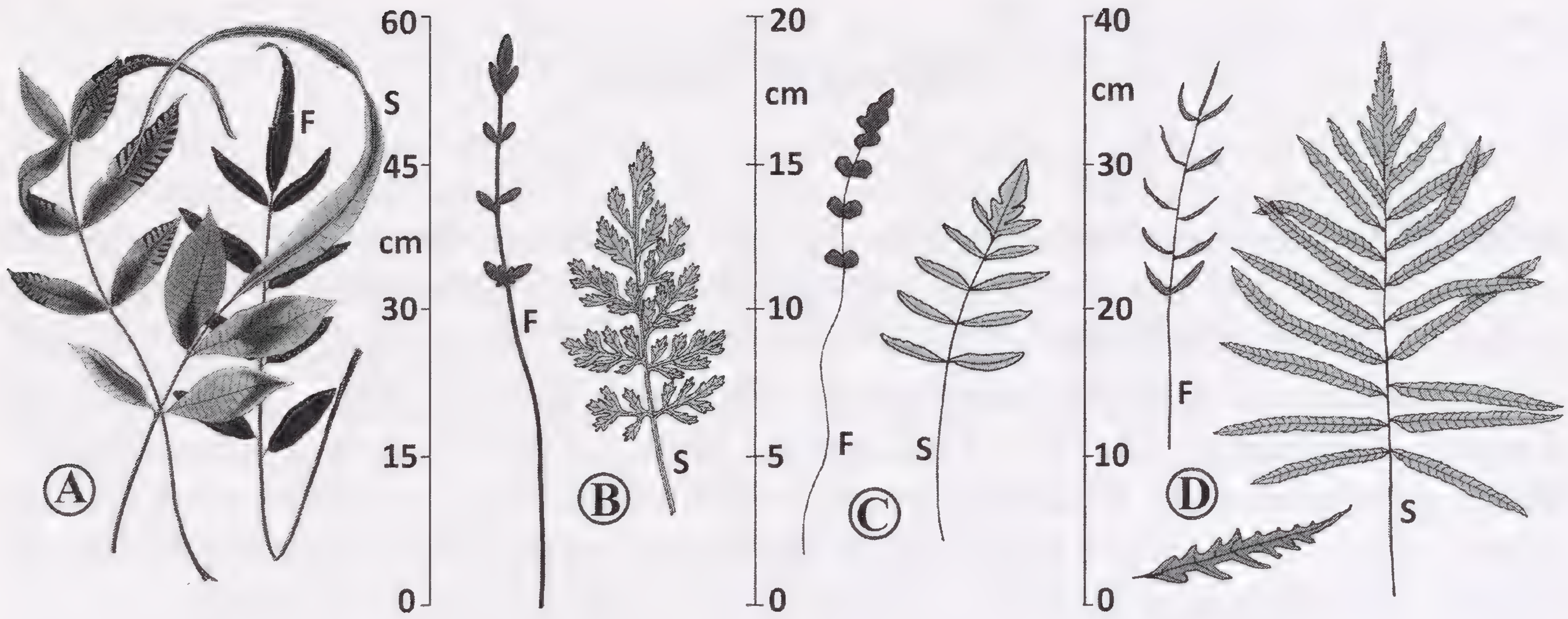

FIG. 1. A. *Bolbitis heteroclita*, from Hooker, W.J., Icones Filicum Vol. 1, plate 23, 1831. B. *B. difformis*, C. *B. inconstans*, and D. *B. heudelotii*, drawings by the author. F=fertile leaf; S=sterile leaf. *B. heteroclita* also shows an intermediate. Drawings by the author are composites of herbarium specimens except for the sterile leaf of *B. difformis*, which was drawn from a composite of on-line images. B and C are the same scale.

buried roots but doing best on driftwood or other elevated substrate with a significant water flow rate. It grows easily, however, as an emersed potted plant.

The third and last form is smaller and depauperate, being referred to in the trade as "*B. heteroclita cuspidata*" and sometimes as "micro-*Bolbitis*." In the Kasselman article cited above, it was called *Gymnopteris inconstans* Copeland (Perkins, Fragmenta Florae Philippinae 177. 1905.), a name that appears on the type (U.S. National Museum specimen number 438099) along with an annotation of *B. heteroclita* '*cuspidata*' by Hennipman. It is not the plant named in the horticultural trade as *B. heteroclita cuspidata*, but rather it is micro-*Bolbitis*. It is also difficult to grow submersed.

TABLE 1. Comparison of morphological characteristics differentiating the *Bolbitis* species.

Species	Sterile Leaf Dissection	Sterile Leaf Pinnules	Sterile Leaf Pinnae Apices	Sterile Leaf Length	Fertile Leaves
B. heteroclita	Once-pinnate	Short-stalked	Long-attenuate on terminal, otherwise acuminate	Up to 80 cm	Once-pinnate
B. difformis	Twice-pinnate pinnatifid	Winged stalks	Cuneate	Up to 15 cm	Pinnatifid, markedly taller
B. inconstans	Once-pinnate	Sessile	Cuneate to blunt	Up to 15 cm	Pinnatifid, markedly taller
B. heudelotii	Once-pinnate or pinnate-pinnatifid	Sessile	Cuneate-lanceolate	Up to 50 cm	Pinnate, lower pinnae stalked

All three forms, whether grown submersed or emersed, maintain their distinctiveness. A striking difference is size: *Bolbitis heteroclita* may have leaves more than 80 cm long, whereas the other two typically have leaves less than 15 cm long. After examining on-line images of herbarium specimens, I am satisfied that these three entities are separate species, with markedly different leaf dissection, textures, and sizes. It is remarkable that they have been considered as representing the same species for so long.

For comparison, *Bolbitis heudelotii* (Bory) Ching, an African species, is included in Table 1. It is by far the most popular species of *Bolbitis* grown by aquarium enthusiasts, and is easily the most adaptable to a submersed existence. This is probably because it is pre-adapted to submersion, as it grows natively as a rheophyte. The species has been in the aquarium trade considerably longer than the other two discussed here. As can be seen, *B. inconstans* resembles *B. heudelotii* far more closely than it resembles *B. heteroclita* (Fig. 1).

The three main species discussed herein are distinct by several characters (Table 1). They do not intergrade, except for some juvenile and depauperate forms of *B. heteroclita* that resemble *B. inconstans*. Because of their distinctness, each of the three entities should be recognized at the rank of species. The name that should be applied to the plant in Fig. 1A is *B. heteroclita*, and for the plant in Figure 1C, *B. inconstans* (Copel.) Ching in C. Chr., Index Fil. Suppl. Ter., 48. 1934. For the plant in Figure 1B, a new combination is required: *Bolbitis difformis* (Copel.) Knouse, comb. nov. Basionym," *Edanyoa difformis* Copel., Philippine Journal of Science 81:22, tab. 17. 1952.—John A. Knouse, PO Box 1196, Athens, OH 45701; email: knousejohn@gmail.com

American Fern Journal 111(2):150–156 (2021)
Published on 7 June 2021

Shorter Note

The Taxonomic Distribution of Chlorophyllous Spores in Ferns: An Update.— Most fern species have achlorophyllous, non-green spores. These spores lack chloroplasts when mature and are thus of any color but green. There is, however, a considerable number of species with chlorophyllous or green spores, which at maturity do contain chloroplasts and are therefore visibly green. Recently, Sundue, Vasco, and Moran (International Journal of Plant Sciences 9:1110–1119. 2011) described a third spore type in *Elaphoglossum* (Dryopteridaceae), *Lomariopsis* (Lomariopsidaceae), and *Pleopeltis* (Polypodiaceae), which they called cryptochlorophyllous. These spores contain chlorophyll but appear non-green to the eye due to thick cell walls or other pigments so that chlorophyll fluorescence or other analyses are necessary to detect the chloroplasts. Currently, chlorophyllous spores are considered to be characteristic for all species in the families Hymenophyllaceae, Equisetaceae, Osmundaceae, and Onocleaceae, as well as in the genus *Loxogramme* (Polypodiaceae), and in particular clades of some families, such as the grammitid ferns in Polypodiaceae (Lloyd and Klekowski, Biotropica 2:129–137. 1970; Sundue, Vasco, and Moran. 2011), which represent around 10% of all fern species worldwide. In addition, there are reports of individual species with chlorophyllous spores in genera typically assumed to be achlorophyllous, such as *Lomaria nuda* Willd. (Blechnaceae), *Platycerium wallichii* Hook. (Polypodiaceae), and *Pleopeltis wiesbaurii* (Sodiro) Lellinger, among others (Lloyd and Klekowski, 1970).

One of the most relevant ecological implications of chlorophyllous spores is their shorter life span compared to non-chlorophyllous spores (Lloyd and Klekowski, 1970), with longevity as short as a few days in *Vandenboschia maxima* (Bl.) Copel. and *Hymenophyllum javanicum* Spreng. (Hymenophyllaceae) (Stokey, Botanical Gazette 101:759–790. 1940), and a few weeks for some species of the grammitid group (Lloyd and Klekowski, 1970). Several researchers have tried to preserve chlorophyllous spores in spore banks (*e.g.*, Pence, Fern Gazette 19:309–319. 2014; Pence, American Fern Journal 90:119–126. 2000; Ballesteros *et al.*, CryoLetters 32:89–98. 2011), which has turned out to be highly challenging, especially if there are long delays in bringing the material to the laboratory (Barnicoat *et al.*, In Vitro Cellular & Developmental Biology-Plant 47:37–45. 2011). This observation is surprising considering that species with short-lived chlorophyllous spores belonging to Hymenophyllaceae and the grammitid group are overrepresented on oceanic islands (Dassler and Farrar, Brittonia 53:352–369. 2001; Moran and Smith, Brittonia 53:304–351. 2001), which suggests that they are able to survive to the long-distance dispersal before they reach a place to germinate. On the other hand, there are reports on spores of some species of *Elaphoglossum* remaining viable after years of being storage at 5°C (Chiou, Farrar, and Ranker, Canadian Journal of Botany 76:1967-1977. 1998; D. R. Farrar, pers. comm.), and observations on

spores of *Matteuccia struthiopteris* (L.) Todaro without significant loss of germination between leaves collected in December and overwintering leaves collected in March (Farrar, American Fern Journal 66:49-52. 1976). Despite the potential importance of life span differences between chlorophyllous and achlorophyllous spores for fern reproduction and long-distance dispersal, the ecological consequences of this trait are not fully understood. Traditionally, information on the presence of chlorophyll in spores has been extrapolated from few observations to entire families and genera, but a reliable data set documenting the presence of chlorophyll in fern spores is needed to advance phylogenetic, ecological, and biogeographical analyses, and conservation management. To fill this gap, we conducted a systematic review of the pertinent literature on fern spores using Web of Science® and Google Scholar searching for each of the 329 genera belonging to the class Polypodiopsida listed in PPG I (Journal of Systematics and Evolution 54:563–603. 2016) plus "spores" as keywords (*e.g.*, "*Hymenophyllum*" "spores"), between November 2019 and July 2020. For genera with more than 100 results on Google Scholar, we used the tool "Custom range" and filtered the results every 20 years, ranging from 1900 to 2020. This allowed us to optimize the search results summarizing the most relevant articles on the first pages and prevented us from missing studies randomly sorted by the search engine. Species names were standardized using the website WorldFerns (Hassler and Smith, https://worldplants.webarchiv.kit.edu/ferns/. 2019). We only considered studies in which spores were effectively observed by the authors. Such studies had information on spore size, texture, chemical content, or photographs. Studies describing spore color based on previous studies were excluded.

When reporting chlorophyll presence in fern spores, there are three problems: 1) chlorophyll may lose its greenness over time, 2) achlorophyllous spores can turn green just before germinating - a false indication of chlorophyll presence, and 3) a greenish tinge of the spore walls may lead to confusing classifications. Further, we found contradictory information on chlorophyll content for two newly described species of *Didymoglossum* (Hymenophyllaceae): Senterre *et al.* (Phytotaxa 292:201–217. 2017) reported yellow spores, although the genus has long been known for its chlorophyllous spores in all North and Central America (Farrar, *Flora of North America*. Oxford University Press, New York. 1993; D. R. Farrar, pers. comm.). This could indicate that some species may deviate in this trait from the rest of the genus or, alternatively, be related to the degradation of chlorophyll. This would be in line with observations of Mostacero (American Fern Journal 103:53–56. 2013), who described color changes in chlorophyllous spores from green to whitish to yellow over time in voucher specimens of *Ceradenia gameriana* (Vareschi) Mostacero (Polypodiaceae). We made similar observations with chlorophyllous spores of *Osmunda regalis* L. (Osmundaceae) and *Todea barbara* (L.) Moore (Osmundaceae): these turned yellow, and finally white within a few months of storage at room temperature. This observation could also explain reports of achlorophyllous spores in *Abrodictyum polystromaticum* (Bierh.) comb. ined. (Hymenophyllaceae) made by Bierhorst (American Journal of

Botany 64:1225–1234. 1977), or reports of achlorophyllous spores in five *Loxogramme* species (Das and Dixit, Bulletin of the Botanical Survey of India 38:64–95. 1996; Singh and Panigrahi, Bulletin of the Botanical Survey of India 27:252–254. 1985; Nayar, Grana Palynologica 4:388–392. 1963), while all other congenerics are reportedly chlorophyllous (Hennipman, Veldhoen, Kramer, and Price, *The Families and Genera of Vascular Plants. Vol I: Pteridophytes and Gymnosperms.* Springer, Berlin. 1990). In these cases, most of the spores were described as yellow or golden yellow.

There are also reports suggesting that there may be numerous species with chlorophyllous spores in groups that are generally considered achlorophyllous. Nayar and Devi (Grana Palynologica 8:185–206. 1968; Grana Palynologica 7:568–600. 1967; Grana Palynologica 5:80–120. 1964; Grana Palynologica 5:222–246. 1964; Grana Palynologica 5:342–395. 1964) described spores containing chloroplasts or green plastids in almost 70 species, including members of 42 genera typically characterized by achlorophyllous spores. At least two species studied by Nayar and Devi were classified as cryptochlorophyllous by Sundue, Vasco, and Moran, 2011, and Tseng *et al.* (Journal of Plant Research 130:407–416. 2017). Even when the fluorescence analyses help to confirm the chlorophyll presence in an allegedly achlorophyllous species, the age of the spores should be considered. Most achlorophyllous spores turn green before germination due to the development of the first chloroplasts of the young prothalli (Raghavan, *Developmental Biology of Fern Gametophytes.* Cambridge University Press. 1989), and in some cases, this is even taken as the first sign of germination (Praptosuwiryo, Biodiversitas 18:175–182. 2017). The ambiguity of some spore color descriptions in the literature emphasizes the importance of noting the developmental state in which the spores were observed. Some descriptions found in this review (*e.g.*, Zhang and He, Systematic Botany 36:854–86. 2011; He and Zhang, Novon: A Journal for Botanical Nomenclature 22:160–165. 2012; He and Zhang, Novon: A Journal for Botanical Nomenclature 25:153–157. 2017) are good examples. These studies include comments on the age of the spores during observation, and some even include a description of the color of both young and mature spores. Another finding is that some spores are described as green but in a reference to the color of the perispore or exospore pigmentation and not as an indication of chlorophyll presence, as in the descriptions of *Notholaena galapagensis* Weath. & Svenson ex Svenson (Pteridaceae), *Cheilanthes sarmientoi* Ponce (Pteridaceae), and *Monachosorum subdigitatum* (Bl.) Kuhn (Dennstaedtiaceae) (See Appendix I for a complete list of species and their colors).

Bearing these challenges in mind, our survey yielded 443 studies with reliable descriptions of color or chlorophyll content of the spores of 2637 fern taxa belonging to 299 genera and 45 families (Table 1), supported with at least one reference (See Appendix I). Our data thus cover about one quarter of all fern species and 91% of all genera. Currently, we lack information for this trait for only 27 genera (Appendix I), but these are all small taxa, often with restricted geographical distribution. Coverage of the genera was uneven with data on

TABLE 1. Alphabetical list of fern families indicating numbers of species with information on achlorophyllous spores (AC), chlorophyllous spores (C), and cryptochloropyllous spores (CC). (+) includes species with contradictory or ambiguous descriptions. Also given are total species number per family, and percentage of species with information on spore color (% Described). Subspecies and varieties are excluded. For a complete species list see Appendix 1.

Family	ac	c	cc	+	Total richness	% Described
Anemiaceae	10				115	9
Aspleniaceae	113				748	15
Athyriaceae	51				758	7
Blechnaceae	73	1	1		264	28
Cibotiaceae	4				12	33
Culcitaceae	2				2	100
Cyatheaceae	60		1		679	9
Cystodiaceae	1				1	100
Cystopteridaceae	21				40	53
Dennstaedtiaceae	64			1	235	28
Desmophlebiaceae					2	0
Dicksoniaceae	8				37	22
Didymochlaenaceae	1				1	100
Diplaziopsidaceae	4				4	100
Dipteridaceae	4				10	40
Dryopteridaceae	287	9	11	3	2125	15
Equisetaceae		12			16	75
Gleicheniaceae	21				146	14
Hemidictyaceae	1				1	100
Hymenophyllaceae		136		3	614	23
Hypodematiaceae	2				18	11
Lindsaeaceae	72				239	30
Lomariopsidaceae	7	3	7		60	28
Lonchitidaceae	2				2	100
Loxsomataceae	2				2	100
Lygodiaceae	11				29	38
Marattiaceae	17				129	13
Marsileaceae	33				55	60
Matoniaceae					2	0
Metaxyaceae	1				6	17
Nephrolepidaceae	6				28	21
Oleandraceae	10				27	37
Onocleaceae		4			5	80
Ophioglossaceae	30				119	25
Osmundaceae		12		1	23	57
Plagiogyriaceae	5				12	42
Polypodiaceae	474	15	9	9	956	53
Psilotaceae	6				18	33
Pteridaceae	473	1	1	3	1312	36
Rhachidosoraceae					8	0
Saccolomataceae	3				21	14
Salviniaceae	2				17	12
Schizaeaceae	4				33	12
Subf.Grammitioideae	1	248		2	829	30
Tectariaceae	33				324	10
Thelypteridaceae	134			1	1203	11
Thyrsopteridaceae	1				1	100
Woodsiaceae	11				55	20

TABLE 2. Alphabetical list of fern genera indicating numbers of species with information on achlorophyllous spores (AC), chlorophyllous spores (C), and cryptochloropyllous spores (CC). (+) includes species with contradictory or ambiguous descriptions. Also given are total species number per family, and percentage of species with information on spore color (% Described). Subspecies and varieties are excluded. For a complete species list see Appendix 1. Family abbreviations: BLE (Blechnaceae), CYA (Cyatheaceae), DRY (Dryopteridaceae), EQU (Equisetaceae), GRA (Subfamily Grammitidoideae), HYM (Hymenophyllaceae), LOM (Lomariopsidaceae), ONO (Onocleaceae), OSM (Osmundaceae), POL (Polypodiaceae), and PTE (Pteridaceae).

Genus	Family	ac	c	cc	+	Total richness	% Described
Abrodictyum	HYM		7		1	41	20
Acrosorus	GRA		2			9	22
Adenophorus	GRA		10			10	100
Aglaomorpha	POL	22	1			33	70
Alansmia	GRA		8			27	30
Alsophila	CYA	24		1		275	9
Antrophyum	PTE	2		1		32	9
Archigrammitis	GRA		1			6	17
Ascogrammitis	GRA		13			17	76
Callistopteris	GRA		1			6	17
Calymmodon	GRA	1	7			55	15
Cephalomanes	HYM		1			9	11
Ceradenia	GRA		15			77	19
Chrysogrammitis	GRA		3			3	100
Claytosmunda	OSM		1			1	100
Cochlidium	GRA		8			17	47
Crepidomanes	HYM		13			61	21
Ctenopterella	GRA		4			19	21
Dasygrammitis	GRA		5			8	63
Didymoglossum	HYM		14		2	55	29
Elaphoglossum	DRY	42	9	11	3	729	9
Enterosora	GRA		8			28	29
Equisetum	EQU		12			16	75
Galactodenia	GRA		3		2	5	100
Grammitis	GRA		13			30	43
Hymenophyllum	HYM		70			326	21
Lellingeria	GRA		14			51	27
Leptochilus	POL	12		2		32	44
Leptopteris	OSM		2			7	29
Leucotrichum	GRA		5			6	83
Lomaphlebia	GRA		1			2	50
Lomaria	BLE		1	1		6	33
Lomariopsis	LOM	5	3	7		50	30
Loxogramme	POL	1	8		5	37	38
Luisma	GRA		1			1	100
Matteuccia	ONO		1			1	100
Melpomene	GRA		10			29	34
Micropolypodium	GRA		2			3	67
Moranopteris	GRA		13			30	43
Mycopteris	GRA		11			18	61
Notogrammitis	GRA		11			12	92
Onoclea	ONO		1			1	100
Onocleopsis	ONO		1			1	100

TABLE 2. Continued.

Genus	Family	ac	c	cc	+	Total richness	% Described
Oreogrammitis	GRA		36			198	18
Osmunda	OSM		4		1	8	63
Osmundastrum	OSM		1			1	100
Pentarhizidium	ONO		1			2	50
Platycerium	POL	15	1	1		17	100
Plenasium	OSM		3			4	75
Pleopeltis	POL	45	4	5	3	92	62
Pleurosoriopsis	POL		1			1	100
Polyphlebium	HYM		7			18	39
Polytaenium	PTE	5	1			13	46
Prosaptia	GRA		11			67	16
Scleroglossum	GRA		5			11	45
Stenogrammitis	GRA		13			25	52
Terpsichore	GRA		6			15	40
Todea	OSM		1			2	50
Tomophyllum	GRA		6			36	17
Tricholepidium	POL	2		1		5	60
Trichomanes	HYM		13			73	18
Vandenboschia	HYM		10			25	40
Xiphopterella	GRA		3			14	21

spore color for all species in 59 mostly small genera, whereas in 57 genera, descriptions of spore color were available for less than 10% of their members.

Overall, 2068 species (81%) of all species with data on spore color were classified as achlorophyllous, whereas 441 species (17%) had chlorophyllous, and 30 (1%) cryptochlorophyllous spores. For 11 species (*e.g.*, *Didymoglossum beccarianum* (Ces.) Senterre & Rouhan, *Loxogramme subecostata* (Hook.) C. Chr.), there were conflicting reports on chlorophyll content. Our survey indicates chlorophyll to be present in most species of those genera and groups that have long been known to be chlorophyllous (TABLE 2), but we also identify a number of exceptions. Even if some of these discrepancies may be due to the methodological issues outlined above, it seems well established that there can be variation in chlorophyll content within a genus – although most species of a genus have spores either strictly chlorophyllous or achlorophyllous. The different ways in which spore color and chlorophyll content are currently described and sampled hamper progress and future studies should be standardized to facilitate the use and classification of this trait for synthetic analyses. Finally, we suggest that authors incorporate spore age in their descriptions. We hope that this survey provides a basis for future well-documented reports on spore color.

APPENDIX I: https://doi.org/10.25625/EDJ2E3

Acknowledgments

We appreciate the comments of the editor Christopher Haufler and associate editor Klaus Mehltreter. The paper also benefited from comments by Donald R. Farrar and an anonymous reviewer. This work was funded by the National Agency for Research and Development (ANID)/ Scholarship Program/ DOCTORADO BECAS CHILE/2018 – 72190330.—Daniela Mellado-Mansilla[1,2*], Gerhard Zotz[2,3], Holger Kreft[1], Michael Sundue[4], Michael Kessler[5]. * d.mellado.mansilla@gmail.com. [1]Department of Biodiversity, Macroecology and Biogeography, Faculty of Forest Sciences and Forest Ecology, University of Göttingen, Göttingen, Germany. [2]Institute for Biology and Environmental Sciences, AG Functional Ecology, University Oldenburg, Oldenburg, Germany. [3]Smithsonian Tropical Research Institute, Panama. [4]The Pringle Herbarium, Department of Plant Biology, University of Vermont, Burlington, USA. [5]Department of Systematic and Evolutionary Botany, University of Zürich, Zürich, Switzerland.

American Fern Journal 111(2):157–158 (2021)
Published on 7 June 2021

John Arthur Knouse 1953–2021

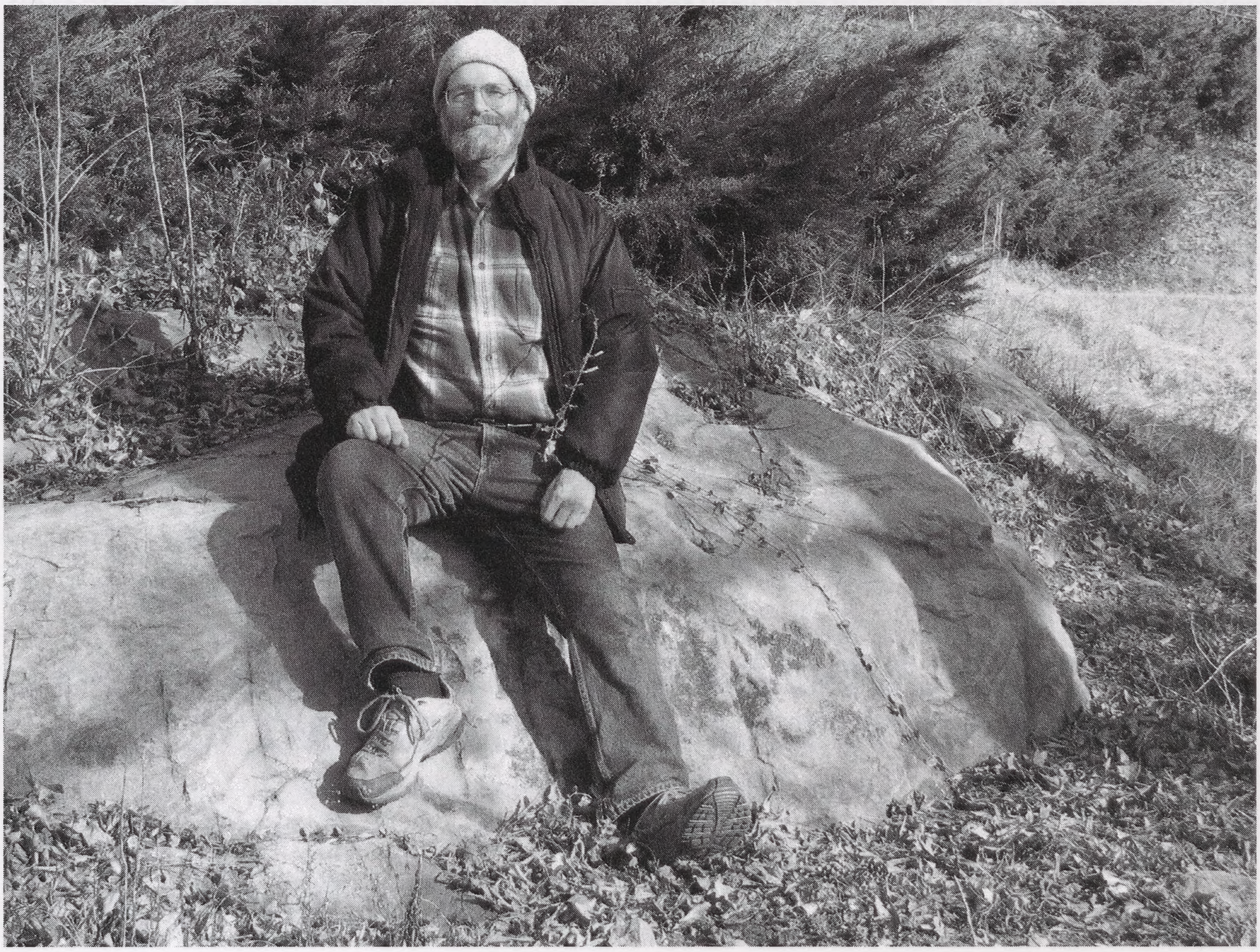

On January 9, 2021 John Arthur Knouse passed away at the age of 67 after a long battle with congestive heart failure.

John was born June 22, 1953 in Grand Rapids, Michigan and grew up traveling the country but always considered Kansas City, Missouri to be his hometown. He studied at Juniata College (PA) and received his BS from University of Louisville (KY). John lived in Louisville, KY for 20 years where he (among other endeavors) worked at Metro Parks, Jefferson County Memorial Forest, and was a member of both the Paddlewheel Alliance and Good Neighbor Food Co-op. John spent the last 24 years of his life in Athens, Ohio, where he continued to dedicate himself to sustainability and community engagement and ran several entrepreneurial ventures including Earthrise Ovens. A few more of his pursuits in Athens included working for Athens Parks and Recreation, leading numerous volunteer efforts to combat invasive species, and doing everything he could to encourage people to vote including working the polls every year.

John shared his love of nature with anyone who would listen and devoted his life to building trails, studying ferns, and enhancing the preservation and appreciation of green spaces wherever he could. As a child, he baked his own

whole wheat bread when it wouldn't have otherwise been available and as a young man sewed his own reusable grocery bags before it had occurred to most of the world to avoid using plastic. He taught his daughters that "every dollar you spend is a vote towards the kind of world that you want to live in," and loved taking people hiking and introducing them to every plant along the trail as if he were introducing old friends.

John wrote science fiction stories, composed music, and moonlighted as a political cartoonist. He was a renaissance man who studied biology, genealogy, cartography, and geology. John was passionate and uncompromising until his final days.

Contributed by Vivian Knouse.

INFORMATION FOR AUTHORS

Authors are encouraged to submit manuscripts pertinent to the study of ferns and lycophytes for publication in the *American Fern Journal*. Manuscripts should be submitted to http://www.editorialmanager.com/afj/. Acceptance of papers for publication depends on merit as judged by two or more referees. Authors are encouraged to contribute toward publishing costs; however, the payment or non-payment of page charges will affect neither the acceptability of manuscripts nor the date of publication. Mandatory fees will be charged for color figures in print and/or in electronic versions of published papers.

Information for authors, including detailed requirements for formatting manuscripts can be found online at: https://www.amerfernsoc.org/american-fern-journal/.

FOR INFORMATION REGARDING AVAILABLE PUBLICATIONS, VISIT THE AMERICAN FERN SOCIETY'S WEBSITE: http://amerfernsoc.org/

The "American Fern Journal" (ISSN 0002-8444) is an illustrated quarterly devoted to the general study of ferns. It is owned by the American Fern Society, and published at The American Fern Society, c/o 926 W. Campus Drive, MC 0406, Blacksburg, VA 24061-1040. Periodicals postage paid at Blacksburg, VA, and additional entry.

Claims for missing issues, made 6 months (domestic) to 12 months (foreign) after the date of issue, and orders for back issues should be addressed to Dr. George Yatskievych, Plant Resources Center, University of Texas at Austin, Main Bldg, Rm 127, 110 Inner Campus Dr, Stop F0404, Austin, TX 78712-1711; e-mail: george.yatskievych@austin.utexas.edu

Changes of address, dues, and applications for membership should be sent to the Membership Secretary.

General inquiries concerning ferns should be addressed to the Secretary.

Back volumes are available for most years as printed issues. Please contact the Back Issues Curator for prices and availability. Digital versions of back issues three years or older are available free online through the Biodiversity Heritage Library: http://www.biodiversitylibrary.org/bibliography/43943#/summary

Subscriptions Rates per Volume for electronic access:

Student/Non-academic membership	$20
Academic membership	$40
Lifetime membership	$600
Libraries, Herbaria, & Commercial Organizations	$60

Print access to the journal is available for an additional $20/year

POSTMASTER: Send address changes to American Fern Journal, c/o Sally Chambers, Botany Department, Marie Selby Botanical Gardens, 1534 Mound St., Sarasota FL 34236.

AMERICAN
FERN JOURNAL

VOLUME 111 NUMBER 2 APRIL-JUNE 2021

COVER CAPTION: *Bolbitis heteroclita*, from Hooker, W.J., Icones Filicum Vol. 1, plate 23, 1831. See Knouse pp. 147-149.